



Progetto S2 - Schede di rendicontazione scientifica delle singole Unità di Ricerca

Task 4:

Caratterizzazione delle principali strutture sismogenetiche e calcolo della probabilità di loro attivazione

Responsabile: Laura Peruzza (OGS)

UR 4.1 - Akinci	INGV-RM1
UR 4.2 - Di Giovambattista	INGV-CNT
UR 4.3 - Cinti	INGV-RM1
UR 4.4 - Garavaglia	PoliMI
UR 4.5 - Godano	Uni2NA
UR 4.6 - Mantovani	UniSI
UR 4.7 - Murru	INGV-RM1
UR 4.8 - Peruzza	OGS
UR 4.9 - Rotondi	IMATI-CNR



UR 4.1 - Coordinatore: Aybige Akinci, INGV, sezione ROMA-I

Introduction

This report presents probabilities for the occurrence of the individual sources in the central Apennines and the Calabria's for the 30-year period 2006-2036. We have calculated conditional probabilities of occurrence for each seismogenic source in central Italy and Calabria using the Brownian passage time distribution.

In this study, we used the individual sources as defined in the Database of Italy's Seismogenic Sources (DISS3.0.2) based on Geological/Geophysical data (GGs). In the database, GG's are the best-known sources: the fault segments are presented according to their kinematic such as geometry and structure and dynamic properties such as timing, rupture length and displacements (such as, max. magnitude, length, width, min./max. depth and min./max. slip rate(s), min./max. recurrence time) and all necessary literature regarding to those parameters. There are 66 sources in this category, in the magnitude range between 5.3 and 7.0: the biggest events are the 30 Dec 1456, Frosolone; 28 Dec. 1908, Messina and 13 Jan. 1915, Fucino earthquakes, for 18 sources the long-term slip rate is given by individual data. The rest is given by a slip rate uncertainty such as 0.1-1.0mm/yr. The date of the last event is not given for 12 sources. In the database, the geometric parameters of the individual sources are often controlled by empirical regression relationships, and only few cases of multiple events with dating are reported. Therefore, it is important to characterize the uncertainty in the recurrence rates as well as the probability of occurrence together with its aperiodicity, α parameter, on the fault segments. In this report, we have shown the effect of uncertain occurrence models together with uncertain slip rates, maximum magnitudes (and hence, recurrence intervals) contribute to the uncertainty of the probability of occurrence on the individual GG sources.

Earthquake source model: Magnitudes slip rates and the recurrence rates

The total seismic moment release for a fault source is sometimes partitioned between two different magnitude-frequency recurrence models, the *Characteristic* or maximum magnitude model (CH hereafter) which considers all moment release is associated with a single maximum magnitude and *Gutenberg-Richter* (GR hereafter) that considers earthquakes with a range of magnitudes between the minimum and maximum magnitude. Together, these models are meant to incorporate our uncertainty about the manner of earthquake activity for a particular fault. The geological and historical individual sources defined in DISS follow "*the basic assumption that each seismogenic source tends to generate repeatedly and exclusively its largest allowed earthquake, that is the assumption of "characteristic" behavior (in the sense of Schwartz and Coppersmith, 1984) for what concerns fault location, geometry and size.*" (Valensise&Pantosti, 2001, p. 802). Therefore, in this study the long-term seismic potential of a fault segment has been modeled by the characteristic earthquake model. We then define the return time associated to the characteristic event using the technique known as the conservation of the seismic moment rate on the fault segment given by Field et al., (1999);

$$\text{RateCH} = \mu \cdot L \cdot W \cdot SR / 10^{c^*Mw+d} \quad (1)$$

where, μ = shear modulus, L = fault length, W = fault width, calculated using the fault depth and the dip, SR = slip rate, $c=1.5$ and $d=9.05$ are from the moment-magnitude

relation ($\log M_o = c * M_w + d$), and M_w = characteristic or maximum magnitude obtained from the empirical relationships calibrated on type/style of the fault mechanism (Wells and Coppersmith, 1994) by using the rupture area RA given by $L * W$, given by:

$$\begin{aligned} M_w &= 3.93 + 1.02 \log(RA) \text{ Normal} \\ M_w &= 4.33 + 0.90 \log(RA) \text{ Reverse} \\ M_w &= 3.98 + 1.02 \log(RA) \text{ Strike} \end{aligned} \quad (2)$$

Table-1 gives the necessary information related with the fault geometry (length, L , width, W) and its seismic behavior (slip rates, SR , maximum magnitude, M_{max}) as defined in database the DISS.3.0.2. Using the equation (1) and the fault parameters given in Table-1, we calculated the recurrence times from min./max. slip rates of each individual source. We compared these values with those are given in the database which are mostly fixed at 700 yrs as a min. return time (Figure 1). As it is seen clearly in Figure 1, variability of the return times is quite large. As most of the sources have been characterized by a regional "reasonable" slip rate varying from 0.1 to 1.0 mm/yr, the recurrence times may vary from hundreds to thousands of years as well.

How to quantify slip rates and maximum magnitudes along with their uncertainties for all fault sources?

Slip rate, magnitude (hence return time) uncertainty

In order to estimate how much the uncertainty on the value of slip rates can influence on the calculation of the probability of occurrence of an event on a fault segment, it is necessary to define a distribution of probability for this parameter. The definition of such distribution is particularly problematic for the faults to which has been assigned a slip rate variable from 0.1 to 1.0mm/yr. In order to reduce the uncertainty on the slip parameter we decide to use an approach based on the Bayes Law. This statistical procedure which endeavors to estimate parameters of an underlying distribution based on the observed distribution. A "prior distribution" is derived from the geological limits on the studied region regarding to geotechnical and paleoseismological observation (Personal communication, R. Basili, UR 1.0). Likelihood is obtained from a penalty function which is the misfit between the cumulative number of events per year versus magnitude observed historically and the predicted rates calculated from equation (1) for slip rates between 0.1 and 2.5 mm/yr (Figure 2). Therefore, we examine the difference between expected earthquake rates inferred from the historical earthquake catalog (CPTI04, Working Group 2004) and the geologic data that was used to develop the seismic source model for the study region. As it is seen in Figure 2, considering the min. slip rates on the faults (0.1mm/yr), the model does not supply a cumulative number of events per year in agreement with the historical catalog.

Our lognormal likelihood function (for log cumulative rate), peaks near 0.77 (Figure 3). Therefore, we estimate the lognormal density to have a mean at log (0.77) and a log standard deviation about 0.28. Then the product of the *a priori* distribution (*magenta color*) and the *likelihood* (*red color*) defines the distribution *a posterior* (*green color*) which represents the uncertainty on the slip rates for the faults (Figure 3) and given by follow function and/or equation;

$$y = \left(\frac{0,535}{x} \right) \left(\exp \left(-0,5 \left(\frac{\ln x - \ln (0,575)}{0,165 \ln 10} \right)^2 \right) \right) \quad (3)$$

Using this function (posteriori of the slip rates) we estimate the uncertainties on the probability of occurrence of a characteristic event to the variability of the slip rates through a Monte Carlo type procedure.

We also assessed the uncertainty of some other parameters involved in the determination of maximum magnitude and earthquake recurrence. We describe the uncertainties on width and length, hence max. magnitude eq.(2), as a normal distribution: defined by mean values, correspond to those of DISS3.0.2 (Table 1) and standard deviation is the 20% changed on those mean values.

Overall uncertainty

We approached the uncertainty analysis in a stochastic manner that we feel is more amenable to critical review. The uncertainties are determined by a 1000 simulation while randomly varying the input parameters during each run. We then presented the uncertainties by selecting the larger difference between the 50th and 18th percentiles and the 84th and 50th percentiles. This represents a 68% confidence band that is a value that can be added/subtracted to the median to compute 68% confidence limits of a distribution. If the simulated values have a normal distribution, the 68% confidence band is an estimator of one standard deviation. Varying the length and the width together simultaneously in each run, we obtained magnitudes which has a standard deviation between 0.1 and 0.3 at each single fault segment. Figure 4 and Figure 5 shows the magnitudes and the recurrence times at each individual fault (from Table 1) together with their calculated uncertainties as a ±1 standard deviation. The uncertainties on the occurrence probability are obtained separately for each single aperiodicity/alpha value of 0.3, 0.5 and 0.7 (see following section for details).

Calculating earthquake probabilities for the Central Apennines and Calabria's Occurrence probability models

In contrast to the Poisson model, a time-dependent renewal process model is based on the assumption that after one earthquake on a fault segment, another earthquake on that segment is unlikely until sufficient time has elapsed to build sufficient stress for another rupture (Lindh, 1983; Sykes and Nishenko, 1984; Nishenko and Buland, 1987; Ellsworth, 1995; Ogata, 1999). Various statistical models have been proposed for the computation of the probability density function for earthquake recurrence, such as Gaussian, log-normal, Weibull, Gamma and Brownian. Among those, the log-normal distribution is the most commonly used in engineering practice. In this study we use the Brownian Passage Time (BPT) probability model that is based on a simple physical model of the earthquake cycle and yields values that are very similar to the log-normal probability distribution except at elapsed times greater than the average recurrence interval. This model has many desirable statistical properties that make it a suitable candidate for describing the statistics of earthquake recurrence (Matthews et al., 2002).

Both log-normal and BPT models require a minimum of two parameters, and require, as well, knowledge of the time of the most recent rupture. One parameter is the mean recurrence interval, μ , and the other describes the variability of recurrence intervals and can be related to the variance of the distribution. This variability of recurrence intervals is described as the aperiodicity, α , which is related to the mean divided by the standard deviation. In the BPT model, the failure condition of the fault is described by a state

variable that rises from a ground state to the failure state during the earthquake cycle (Matthews et al., 2002; Ellsworth et al., 1999; Kagan and Knopoff, 1987).

The probability density for the BPT model is given by:

$$f_{BPT}(t) = \sqrt{(\mu/2\pi\alpha^2 t^3)} \exp[-(t-\mu)^2 / 2\alpha^2 \mu t] \quad (4)$$

where t is time. The behavior of a BPT model depends strongly on the value of α . For smaller values of α , $f_{BPT}(t)$ is more periodic and is strongly peaked and remains close to zero longer. For larger values, the “delay” or “dead time” becomes shorter, $f_{BPT}(t)$ becomes increasingly Poisson-like, and its mode decreases. The hazard function in the quasi-stationary state increases with decreasing values of α and becomes Poisson-like with increasing values that approach 1.0.

Probabilities of occurrence for the next 30 year (2006)

We calculated conditional probabilities of occurrence for each seismogenic source in central Italy using the Poisson model (Time-independent, Figure 6) and the Brownian passage time distribution (Time-dependent model, Figure 7). BPT distribution uses an *aperiodicity* parameter; α, \square which describes how regularly or irregularly characteristic earthquakes are expected to occur on any time-dependent fault. This parameter is ordinarily derived from the coefficient of variation of *actual observed recurrence time intervals on individual faults* and can be reinforced with *geological evidence* (Ellsworth et al., 1999; Cramer et al., 2000). The paleoseismic and seismological data are sparse and/or not available for most of seismogenic sources in Central Italy and Calabria (except like Irpinia, Fucino and may be few more). Since we do not have experimental data of repeated earthquakes on the individual faults we have used values which those are similar to the coefficient of variation of 0.5 ± 0.2 used by Working Group on Regional Earthquake Likelihood Model (RELM) of the Southern California Earthquake Center (SCEC, 1994).

An illustration of how the α value affects time-dependent results is given in Figure 7. Increase of aperiodicity increases probabilities if early in the cycle, and lower probabilities if later in the cycle. Generally, the conditional probability for α equal to 0.5 and 0.7 is closer to the fixed Poisson probability than the conditional probability for a α of 0.3. Also the conditional probability for a α equal to 0.7 and 0.5 rises above the Poisson probability level earlier in the recurrence cycle than the conditional probability for a α of 0.3. In general, the smaller the \square , the more the rise in probability of occurrence above the Poisson level occurs near the average recurrence time.

Twelve of the 66 faults do not have the elapsed time, and the last earthquakes on these faults are assumed to have occurred in 700 AD and have a lapse time of 1306 (Table 1). For these twelve faults the elapsed times mostly exceed the average calculated recurrence interval so that they have the high probability of occurrence.

In the Poisson model the hazard is not sensitive to the recency of rupture on the faults. Generally, but not always, time-dependence raises the probabilities except for those faults that have had earthquakes recently (e.g. the Fuciuno, Colliano, Ripobottoni, San Giuliano di Puglia, San Greco Magno, A.Cinque Miglia, Colfiorito South and North, Gubbio South, Sellano). If the elapsed time is near or greater than the average recurrence time, probability of occurrence increases with decreasing alpha. At values of elapsed time near 60 percent of the average recurrence time, the probability of occurrence can first increase and then decrease with decreasing alpha. The hazard function obtained using α of 0.7

increases sooner after an earthquake compared to the hazard function using α of 0.3 and 0.5; accordingly its probability is closer to the fixed Poisson.

In the study region, most of the sources have negligible probabilities less than around 10%. Thirteen sources actually have a conditional probability of a characteristic earthquake in the next 30 years greater than 30%. Those probabilities are associated with their overall uncertainty regarding to alpha values of 0.3, 0.5 and 0.7; max. magnitudes; recurrence rates as well as slip rates and presented by one standard deviation. Those segments are given as follow together with their ID code, name, max. magnitude, date of the last event and calculated occurrence probability;

- 1-) Ascoli Satriano (ITGG082), M=6.0, 17 Jul. 1361, (29,4%)
- 2-) Aspromonte NW (ITGG042), M=5.3, 06 Feb 1783, (53,3%)
- 3-) Bisceglie (ITGG083), M=4.7, 11 May 1560, (35,7%)
- 4-) Carpino (ITGG089), M=5,8, No previous event, (47,2%)
- 5-) Monte Sant' Angelo (ITGG020), M=6.4, No previous event, (25,4%)
- 6-) San Giovanni Rotondo (ITGG021), M=6.1, No previous event, (26,6%)
- 7-) Scilla offshore (ITGG041), M=5.3, 16 Nov. 1894, (17,3%)
- 8-) Anghiari (ITGG064), M=5.8, No previous event, (34,1%)
- 9-) Bastia (ITGG060), M=5,4, 12 Feb. 1854, (28,6%)
- 10-) Conero offshore (ITGG029), M=5.9, 23 Dec. 1690, (30,8 %)
- 11-) Gubbio North (ITGG038), M=6.0, No previous event, (28,8%)
- 12-) Pesaro San Bartolo (ITGG032), M=5,8, No previous event, (19,8%)
- 13-) Selci Lama (ITGG065), M=5.5, 30 Sept. 1789, (24,3%)

Finally, we mapped the conditional probabilities in the next 30 years (2006-2036) for the Central Italy and Calabria (Figure 8). Height of the bars corresponds to the maximum probability of occurrence with the associated errors comes from overall uncertainty processes, colors correspond to the magnitudes of each segment. These maps enhance the contribution of moderate events having relatively short return times, with respect to the sources of large events, which are supposed to have a mean return time usually much longer than the time elapsed since the last event.

In general, the time-dependent models may be applicable in a few areas because we know little about the recurrence rates for the majority of seismic sources. However, for few faults for which we think we have adequate information on time-dependent behavior, a time-dependent model may be better at identifying the short-term risks for economic loss assessment.

References

- Ellsworth, W.L., 1995. Characteristic earthquakes and long-term earthquake forecasts: implications of central California seismicity, in Cheng, F.Y., and Sheu, M.S., eds., Urban Disaster Mitigation: the Role of Science and Technology, Elsevier, p. 1-14.
- Ellsworth, W.L., Matthews, M.V., Nadeau, R.M., Nishenko, S.P., Reasenberg, P.A., and Simpson, R.W., 1999. A physically-based earthquake recurrence model for estimation of long-term earthquake probabilities: U. S. Geological Survey, OFR 99-522, 23 p.
- Field, E. H., D. D. Johnson, and J. F. Dolan; 1999: A mutually consistent seismic-hazard source model for Southern California. Bull. Seism. Soc. Am., **89**, 559-578.
- SCEC Phase II, (1994). Seismic Hazards in Southern California: Probable Earthquakes, 1994 to 2024 (Phase II): Southern California Earthquake Center, Report.
- Lindh, A.G., (1983). Preliminary assessment of long-term probabilities for large earthquakes along selected segments of the San Andreas fault system in California: U.S. Geological Survey Open-File Report 83-63, 15 p.
- Matthews, M. V., W. L. Ellsworth, and P. A. Reasenberg (2002), A Brownian model for recurrent earthquakes, Bull. Seismol. Soc. Am., **92**, 2233– 2250.
- Nishenko, S.P., and Buland, R., (1987). A Generic Recurrence Interval Distribution for Earthquake Forecasting , v. 77, p. 1382-1399.
- Ogata, Y., (1999). Estimating the hazard of rupture using uncertain occurrence times of Paleoearthquakes: Journal of Geophysical Research, B, Solid Earth and Planets, v. 104, no. 8, p. 17,995-18,014.
- Kagan, Y.Y., and Knopoff, L., (1987). Random stress and earthquake statistics; time dependence: Geophys. J. R. Astr. Soc., v. 88, p. 723-731.
- Cramer, C. H., Petersen M.D., Cao, T., Toppozada, T. R. and Reichle, M., (2000). A Time-Dependent Probabilistic Seismic-Hazard Model for California Bull. Seism. Soc. Am., v. 90; no. 1; p. 1-21.
- Working Group CPTI, 2004. Catalogo Parametrico dei Terremoti Italiani, versione 2004 (CPTI04). INGV, Bologna, Italy. <http://emidius.mi.ingv.it/CPTI/>
- Valensise G. and Pantosti D. (eds.), 2001. Database of potential sources for earthquakes larger than M 5.5 in Italy, version 2.0, Ann. Geofis., suppl. to vol. 44, 797-964.
- Wells D. and Coppersmith, 1994. New empirical relationships among Magnitude, Rupture Length, Rupture Width, Rupture Area and Surface Displacement. Bull. Seism. Soc. Am., **84**, 974-1002.

Table -1 DISS3.0.2 geological/geophysical sources: identification code (ID) and name presented together with the geometrical and kinematic parameters used in this study. Red color indicates the sources has more than 10% of probability of occurrence (25 event) with no previous event associated (taken as 1306) (11 event) blue color same as the reds and associated with one previous event (14 event).

ID	FAULT NAME	L	W	SR MIN	SR MAX	TREC MIN	TREC MAX	LAPSE TIME	M max	TREC est.
ITGG008	Agri Valley	23	13,5	0,1	1	740	7400	149	6,5	1226
ITGG092	Arriano Irpino	30	14,9	0,1	1	2000	20000	550	6,9	1262
ITGG082	Ascoli Satriano	12,6	8,4	0,1	1	700	4200	745	6	666
ITGG042	Aspremonte Northeast	10	7,5	0,1	1	700	2700	112	5,8	472
ITGG040	Aspremonte Northwest	5	4,5	0,1	1	700	1600	223	5,3	276
ITGG043	Aspromonte East	12,5	8,8	0,1	1	700	3700	99	6	622
ITGG088	Bisaccia	29,4	16	0,4	0,6	950	9500	82	6,7	1685
ITGG083	Bisceglie	8,6	6,3	0,1	1	700	2900	446	4,7	462
ITGG004	Boiano Basin	24	13,8	0,1	1	970	9700	201	6,6	1695
ITGG089	Carpino	8,9	7,5	0,01	1	700	3000	1306	5,8	538
ITGG009	Castrovilliari	15,6	10,3	0,2	0,6	833	2500	1306	6,2	1039
ITGG080	Cerinola	18,6	11,3	0,1	1	700	6000	275	6,3	945
ITGG077	Colliano	28	15	0,4	0,6	1680	3140	26	6,2	1762
ITGG095	Frosolone	36	14,9	0,1	1	2500	25000	550	7	1816
ITGG012	Gioia Tauro Basin	25	15	0,1	1	860	8600	223	6,6	1450
ITGG081	Melfi	17,2	11	0,1	1	700	6600	155	6,3	916
ITGG010	Melondro-Pergola	17,9	11,3	0,1	1	570	5700	149	6,5	1051
ITGG023	Mercuri Basin	22	12,7	0,1	1	700	5800	1306	6,4	1002
ITGG013	Messina Straits	31,4	15	0,93	2	700	1500	98	7	1602
ITGG020	Monte Sant'Angelo	20	12	0,5	1,2	700	1340	1306	6,4	815
ITGG044	Nicotera Rosarno	12,5	8,8	0,1	1	700	3700	78	6	731
ITGG079	Pecopagano	15	10	0,4	0,6	1680	3140	26	6,8	626
ITGG084	Potenza	7,9	6,2	0,1	1	700	2600	16	5,7	514
ITGG053	Ripobottoni	9,4	8	0,1	1	700	1800	4	5,7	469
ITGG021	San Giovanni Rotondo	11	12	0,1	1	700	4300	1306	6,1	756
ITGG052	San Giuliano di Puglia	10,5	8	0,1	1	700	2000	4	5,8	585
ITGG022	San Marco Lamis	10	12	0,1	1	700	4800	131	6,1	832
ITGG054	San Severo	34	15	0,1	1	900	9000	379	6,8	1554
ITGG005	Tammaro Basin	25	14,3	0,1	1	900	9000	318	6,6	1111
ITGG011	Upper Mesina Basin	22	13,5	0,1	1	1090	10900	223	6,6	1876
ITGG078	SGMagno	9	15	0,4	0,6	1680	3140	26	6,2	737
ITGG041	Scilla offshore	5	4,5	0,1	1	700	1600	112	5,3	280
ITGG006	Uffita Valley	26	14,7	0,1	1	840	8400	374	6,6	1390
ITGG026	Amatrice	14	9,5	0,22	0,4	1075	1954	367	6,1	1323
ITGG064	Anghiari	9,1	7	0,1	1	700	3500	1306	5,8	554
ITGG003	Aremo.-Cinque Miglia	20	12,2	0,1	0,6	1100	6600	1306	6,4	2031
ITGG028	Barrea	10	7,5	0,1	1	700	2700	22	5,8	473
ITGG060	Bastia	6,2	4	0,1	1	700	2000	152	5,4	255
ITGG047	Cagli	17,2	7,5	0,1	1	700	5000	225	6,2	775
ITGG049	Camerino	8	6	0,1	1	700	4000	207	5,8	494
ITGG025	Campotosto	14	9,5	0,3	0,4	1075	1433	1306	6,1	1206
ITGG017	Colfiorito North	12	7,5	0,1	1	700	3700	9	6	558
ITGG018	Colfiorito South	9	6	0,1	1	700	3800	9	5,7	462
ITGG029	Conero offshore	9,4	6	0,1	1	700	4000	316	5,9	445
ITGG048	Fabriano	13	9	0,1	1	700	5500	265	6,2	603
ITGG031	Fano Ardizio	12	8	0,24	0,36	1666	2500	1306	6,1	1303
ITGG061	Foligno	10,2	6	0,1	1	700	3500	174	5,8	512

ITGG002	Fucino Basin	28	15,4	1,2	1,7	1400	2600	91	6,7	697
ITGG038	Gubbio North	7,5	4	0,1	1	700	1700	1306	6	716
ITGG037	Gubbio South	7,5	4	0,1	1	700	1700	22	6	674
ITGG024	Mondolfo	8,9	5,9	0,24	0,36	700	833	82	5,4	846
ITGG063	Monterchi	9,1	7	0,1	1	700	3500	89	5,8	554
ITGG015	Montereale Basin	23,4	13,6	0,1	1	720	7200	303	6,5	1251
ITGG016	Norcia Basin	25	14,3	0,1	0,6	2000	10000	303	6,5	1961
ITGG070	Offida	7,9	7,4	0,1	1	700	4000	63	5,9	427
ITGG001	Ovindoli-Pezza	27	15	0,7	1,2	1300	3000	1306	6,6	1225
ITGG032	Pesaro San Bartolo	8	6	0,24	0,36	1166	1750	1306	5,8	651
ITGG055	Sarnano	9,5	7,5	0,1	1	700	5000	133	6	498
ITGG065	Selci Lama	7,5	4,2	0,1	1	700	2500	217	5,5	401
ITGG019	Sellano	6	6	0,1	1	700	2100	9	5,6	348
ITGG030	Senigallia	12	6,9	0,24	0,36	1111	1666	76	5,9	1066
ITGG027	Sulmona Basin	20	12,2	0,6	0,7	942	1100	691	6,4	971
ITGG094	Tocco da Casauria	12	8	0,1	1	700	4500	550	6	735
ITGG062	Trevi	7	4,5	0,1	1	700	2500	128	5,5	396
ITGG059	Velletri	7,2	6	0,1	1	700	3000	200	5,6	411

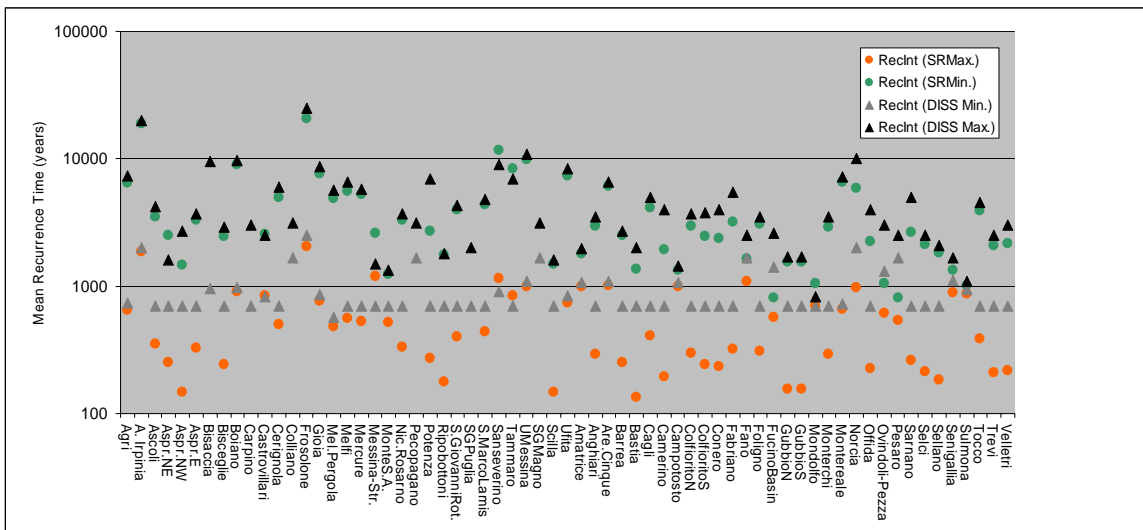
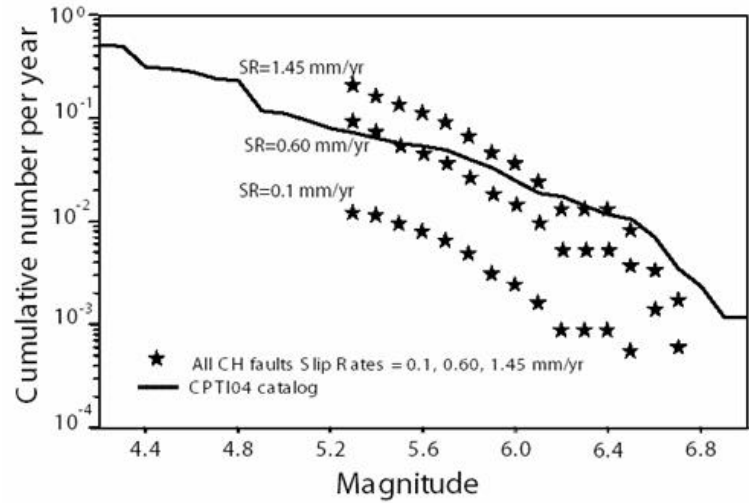


Figure 1 - Recurrence times for the geological/geophysical sources: RecInt (DISS Min. and Max.) as reported in database 3.0.2 and RecInt (SR Min. and Max.) obtained from equation (1) using min and max. slip rate is given in the database.



Figures 2 - The cumulative number of events per year versus magnitude observed historically in the Central Apennines (thick line) and the predicted rates from the characteristic faults/earthquakes, CH (star symbols). The recurrence rates are calculated using the slip rates from the 0.1 to the 1.45 mm/yr on the all faults.

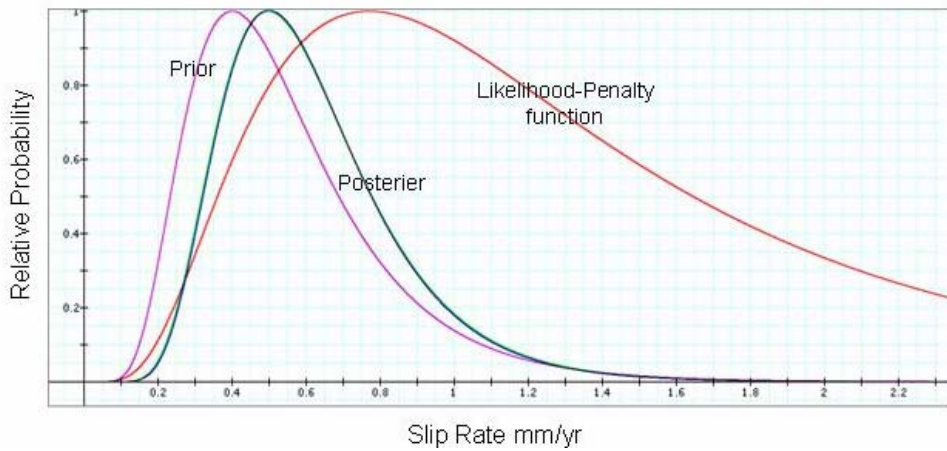


Figure 3 - Functions defined using an approach based on Bayes Law. A priori function is calculated from geologic data. Likelihood/penalty function is defined considering the misfit between the cumulative number of events per year in the CPTI04 and the rates previewed from the characteristic earthquake model with a slip rates variable between 0.1 and 2.5 mm/yr on each fault (distribution log-normal with equal maximum to log (a 0.77) and equal standard deviation to 0.28). The function a posteriori is given from the product of the a priori distribution and the likelihood as given by eq. (3).

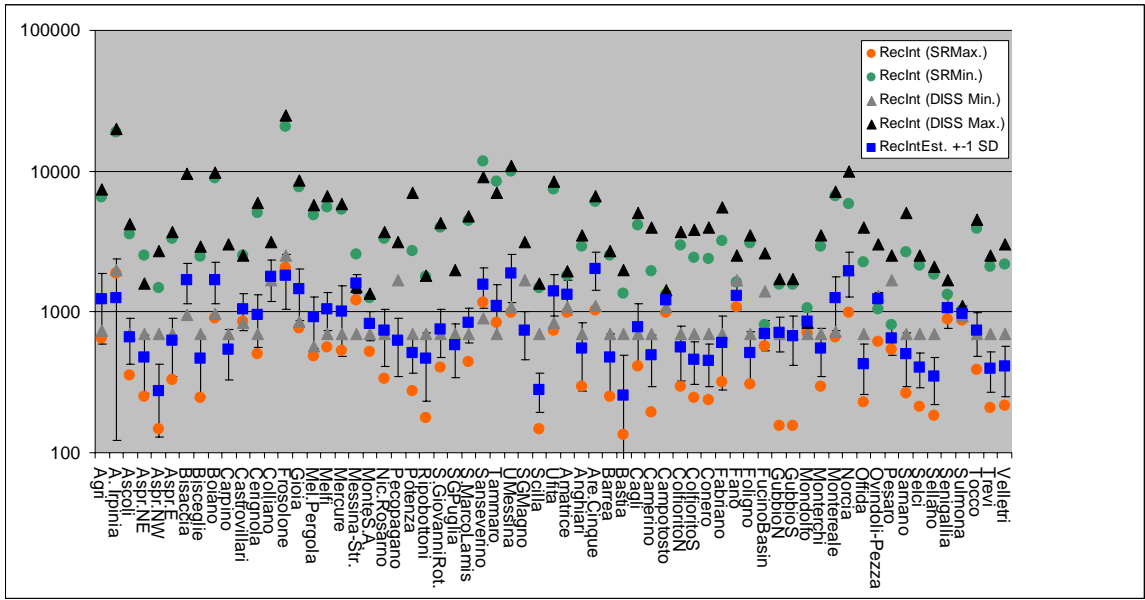


Figure 4 - Recurrence times for the geological/geophysical sources: RecInt (DISS Min. and Max.) as reported in database and RecInt (SR Min. and Max.) obtained from equation (1) using min and max. slip rates are given in the database, Mean RecInt Est. is calculated using equation (1) fixing the slip rate, 0.57mm/yr from aposterior distribution. Uncertainties are computed using aposterior slip rate distribution through a Monte Carlo simulation. Errors are represented as ± 1 standard deviation or within 68% confidence limits.

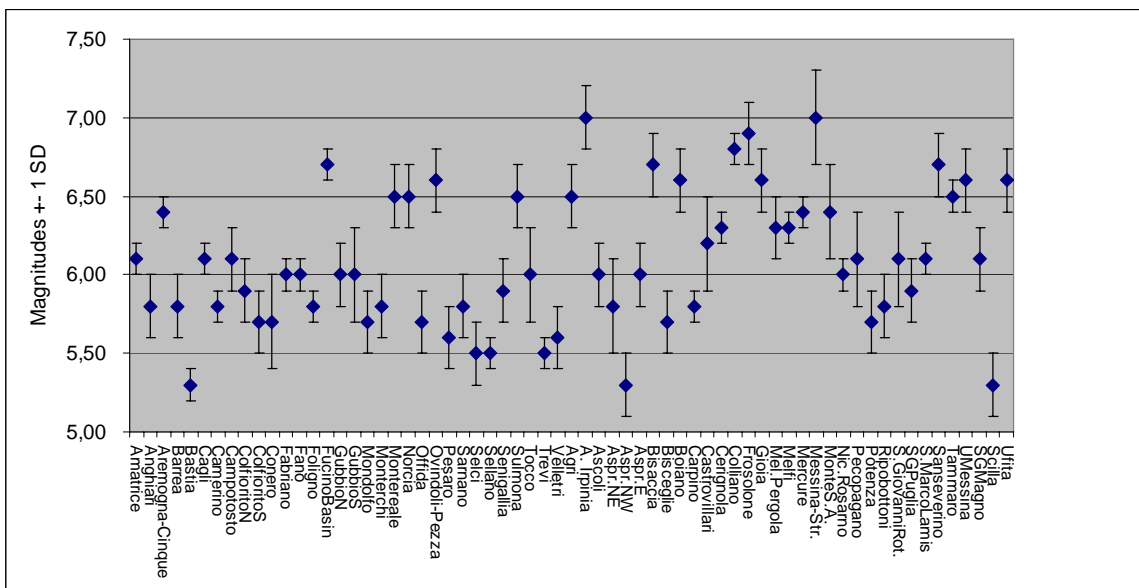


Figure 5 - Uncertainties in the magnitude of the characteristic event (M_{\max}) for the geologica/geophysical sources: blue dots correspond to one from DISS3.0.2. Bars are the one standard deviation computed using Monte Carlo approach under the assumption that the length and the width of GG sources vary 20% of their presented values and have normal statistical distribution.

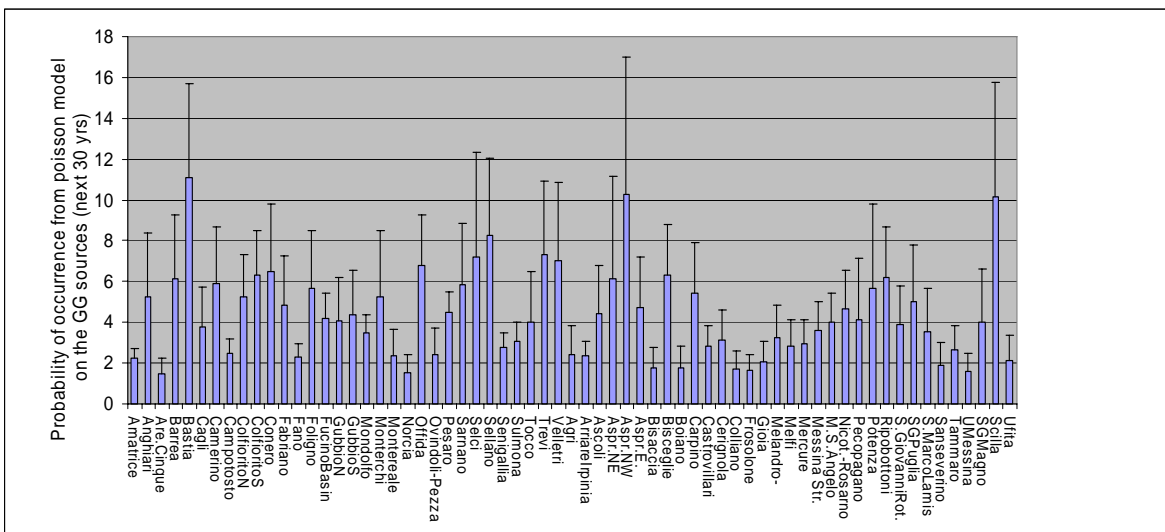


Figure 6 - Probability of occurrence from Poisson time-independent model of the maximum event in the next 30 years, on the individual structures together with the one standard deviation.

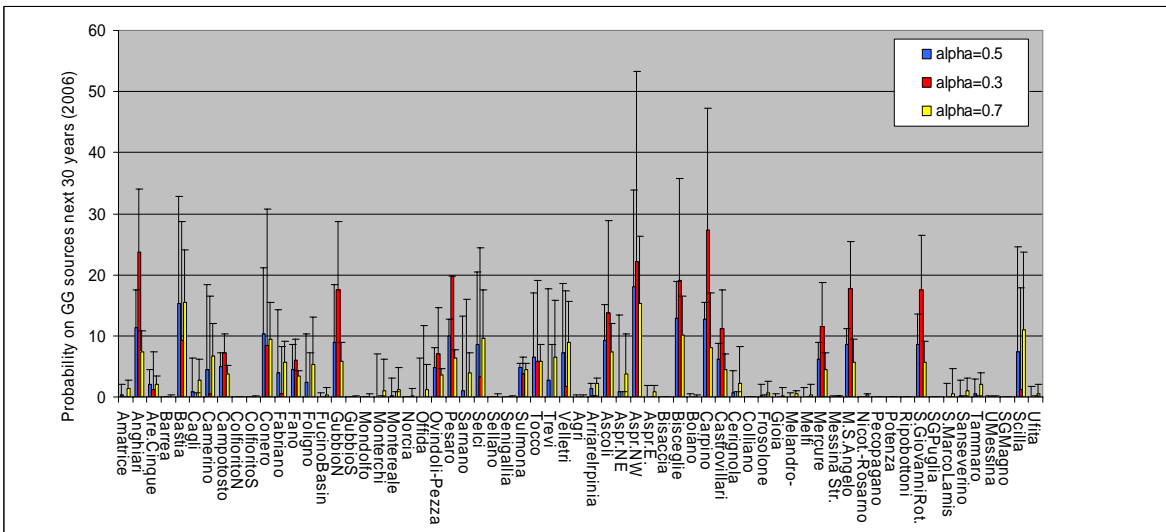


Figure 7 - Probability of occurrence of the maximum event for DISS geological sources in the next 30 years from 2006, given the mean recurrence and elapsed time (Table 1) using BPT, aperiodicity values are the same for each sources as $\alpha=0.3, 0.5$ and 0.7 . Error bars correspond to one standard deviation is obtained from overall uncertainty analysis (see text in details). The date of the last event when not available is fixed at 1306. Most of the sources exhibit a probability less than 20%.

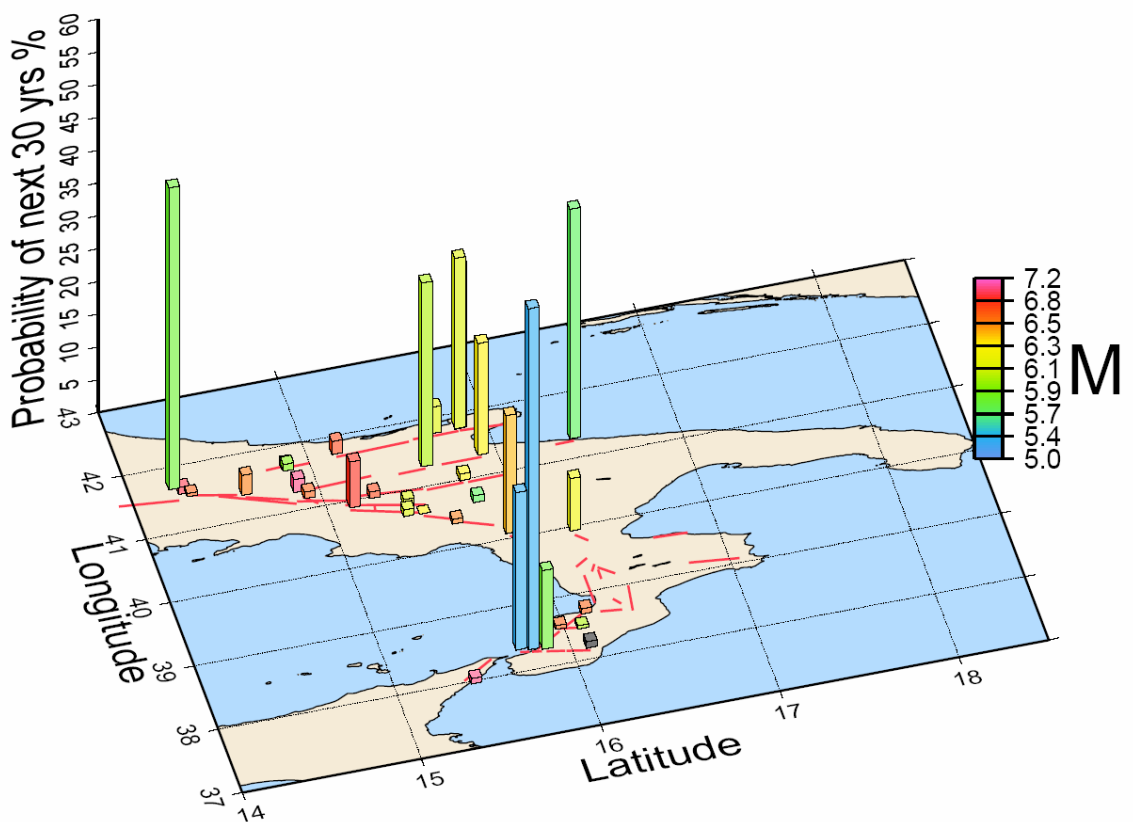
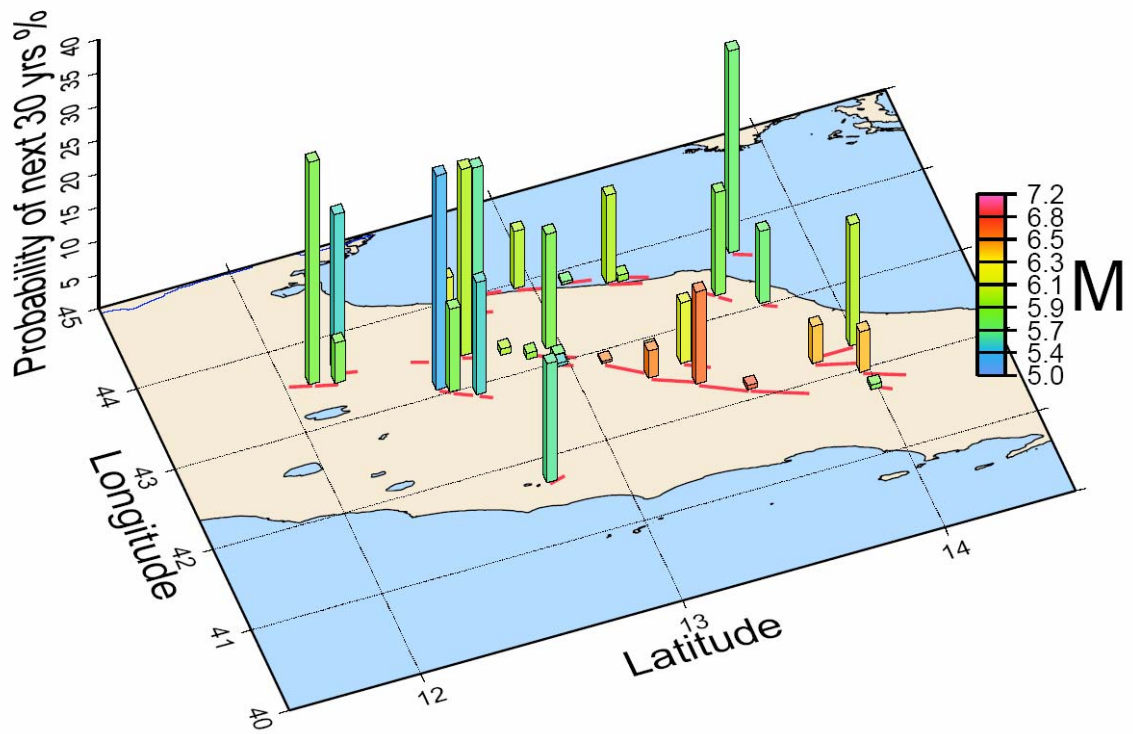


Figure 8 - Maximum Probability of occurrence in the 30 years calculated with BPT model for the fault segments of the central Apennines and Calabria (errors are associated into the probabilities). Height of the bars corresponds to the maximum probability of occurrence with the associated errors; colors correspond to the magnitude of each segment.



UR 4.2 - Coordinatore: Rita Di Giovambattista (INGV)

La ricerca condotta nell’ambito di questo progetto fa parte di una più grande indagine del processo fisico che evidenzia un’accelerazione del rilascio dell’energia prima di alcuni forti terremoti. La partecipazione al progetto ha consentito di affrontare le tematiche in studio mediante una ricerca collaborativa tra responsabili di progetti pilota condotti in diversi paesi e promuovendo sinergie tra Unità di Ricerca del progetto.

E’ stato osservato in diverse aree tettoniche del globo che i forti eventi sono a volte preceduti da un sistematico incremento nel livello della sismicità di background in vaste aree entro una certa distanza dall’evento principale (*accelerating moment release “AMR”*) o (*Time-to-failure*) (California [Bowman et al., 1998; Bowman and King, 2001; Knopoff et al., 1996; Sammis et al., 2004], Turchia ed Egeo [Karakaisis; Papazachos], New Zealand [Robinson, 2000], Central United States [Brehm and Braile, 1998], Alaska [Bufo et al., 1994;], Cina [Jiang and Zhongliang, 2006]).

Bowman e King, 2001 hanno documentato l’occorrenza dell’AMR per tutti i forti terremoti ($M \geq 6.5$) della California meridionale verificatisi dal 1950. L’AMR è stato osservato anche nel caso del tristemente famoso terremoto di Sumatra, che con una magnitudo di 8,9 ed essendo considerato il più forte evento dal 1965 ha attirato l’attenzione di molti esperti del settore (Mignan et al., 2006). La maggior parte di tali osservazioni sono state ottenute con un’analisi a posteriori della sismicità, conoscendo quindi la localizzazione del forte evento che è utilizzata come centro dell’area sulla quale l’AMR viene ricercato e la sua magnitudo. Le evidenze incoraggianti e le conoscenze raggiunte nella comprensione e modellazione statistica del metodo hanno consentito di includere il modello AMR o alcune sue generalizzazioni tra quelli selezionati da vari organismi di ricerca internazionali al fine di una loro rigorosa validazione scientifica. Nel 2005 il working group “Regional Earthquake Likelihood Models (RELM) del Southern California Earthquake Center (SCEC) ha finanziato uno studio con l’obiettivo di valutare un estimatore regionale di probabilità di terremoto basato sul modello Amr. L’unica applicazione del modello AMR alla sismicità italiana è stata condotta dai ricercatori partecipanti a questo progetto. L’attività di ricerca è stata condotta prendendo come riferimento il seguente schema:

1. Analisi retrospettiva dei forti eventi $M > 5.5$ avvenuti in Italia dal 1985 ad oggi per calcolare i parametri del modello “Accelerating Moment Release (AMR)”, nei casi in cui i dati permettano una buona stima della variazione del rilascio dell’energia rispetto alla sismicità di fondo.
2. Valutazione di come le diverse aree sismogenetiche italiane seguano l’andamento temporale del modello AMR.
3. Validazione statistica del metodo nelle aree campioni in esame.

In particolare sono stati esaminati tutti i forti terremoti avvenuti sul territorio italiano per i quali esiste una buona completezza del catalogo. I risultati sembrano promettenti in quanto l’analisi retrospettiva ha mostrato che 8 di 11 terremoti sono stati preceduti da un significativo incremento dell’AMR. Nel caso di alcuni terremoti verificatisi nel 1980 la scarsa completezza delle registrazioni potrebbe aver mascherato l’AMR. Inoltre l’AMR sembra mostrare una apparente dipendenza dai meccanismi focali degli eventi in studio risultando maggiormente evidenziato per i forti terremoti appenninici con meccanismi normali mentre non è così evidente per terremoti appartenenti ad altri domini sismotettonici, come il terremoto di Potenza del 1990 o il terremoto del Molise del 2002. Una prima fase del lavoro è stata dedicata alla stima dei parametri del modello sulla base di un’analisi retrospettiva di alcuni forti terremoti ben monitorati. Successivamente sono

stati analizzati vari aspetti che riguardano l'applicazione pratica del modello e le possibili simulazioni per stimare l'affidabilità di una sua applicazione. Alcuni aspetti dell'AMR non sono stati ancora chiariti a causa della limitata casistica sinora disponibile, essenzialmente dovuta alla mancanza di dati. In particolare non è stato ancora chiarito se la durata del periodo nel quale si osserva l'AMR è in qualche modo dipendente dalla magnitudo dell'evento in preparazione o è piuttosto condizionata dalle caratteristiche tettoniche dell'area. Per contribuire alla comprensione di tali aspetti, sono stati utilizzati dati prodotti mediante esperimenti di laboratorio sulla fatturazione delle rocce e sono stati formulati nuovi modelli fisico-numerici che possano adeguatamente descrivere il fenomeno dell'AMR. L'applicazione sistematica dell'AMR alla sismicità italiana, ha messo in evidenza che nel caso di alcune sequenze sismiche particolarmente energetiche come la sequenza del Matese del 1997 (Milano et al., 2005, 2006), la sequenza di Isernia del 2001 ed altre ancora, l'AMR porterebbe a stimare una magnitudo di molto superiore rispetto a quella osservata. Studi globali hanno evidenziato che le sequenze sono generalmente caratteristiche di mezzi eterogenei e si verificano nelle regioni dove dominano tensioni orizzontali o sono spesso osservate in aree vulcaniche o in presenza di fluidi.

Studi sismotettonici mirati all'analisi delle sequenze italiane per le quali l'AMR fornisce una sovrastima della magnitudo aspettata hanno evidenziato che tali sequenze tendono a collocarsi ai bordi delle faglie dei forti eventi storici, ed in aree di transizione tra domini simotettonici nelle quali il campo di stress locale è diverso da quello regionale. L'integrazione dell'informazione derivante da studi sismotettonici condotti in collaborazione con le altre UR del progetto potrebbe quindi fornire un vincolo sull'utilizzo dell'AMR che proprio per la sua formulazione non può distinguere se un'incremento della sismicità sia dovuto ad un'attivazione di foreshocks o all'attività di una sequenza sismica.

Un parametro cruciale del modello AMR è la dimensione dell'area sulla quale si deve osservare l'AMR. L'area dove i patterns premonitori possono essere osservati è stata dapprima stimata da alcuni autori che hanno ipotizzato una dipendenza dell'area di preparazione di un forte terremoto dalla magnitudo dell'evento in preparazione. La relazione sperimentale ipotizzata è del tipo

$$\log(R) = CM + D$$

con R raggio dell'area in preparazione e M la magnitudo del forte evento in preparazione. Alcuni autori hanno suggerito i seguenti coefficienti, proposti mediante l'analisi di terremoti della California e di altre importanti zone sismogenetiche

C=0.44 (Bowman et al. 1998), 12 EQS occurring in California
C=0.75 (Brehm and Braile 1998), 19 EQS from the New Madrid zone
C=0.36 (Jaumé and Sykes 1999).

Abbiamo condotto un Best Fitting lineare combinando entrambe i dataset di Bowman et al., 1998 e di Brehm And Braile, 1998 ed abbiamo trovato il seguente valore

$$C=0.37 \pm 0.05, D=-0.30 \pm 0.26$$

Questa stima è in accordo con la stima di Jaumé and Sykes.

Per valutare quale delle due relazioni possa essere più adeguata per il territorio italiano abbiamo analizzato la localizzazione di alcune sequenze energetiche note in letteratura come 'Burst' che si sono verificate prima di alcuni forti eventi e che sembrano univocamente appartenere al loro processo di preparazione. La distanza tra tali sequenze e il forte terremoto sembra essere in accordo con la relazione proposta da Bowman.

Si è avviata una stretta collaborazione con la UR 2.4 del progetto al fine di integrare le conoscenze ottenute sul comportamento sismogenetico delle aree analizzate con le informazioni geologico strutturali. Per alcuni eventi per i quali il modello AMR non fornisce risultati soddisfacenti sono stati condotti studi specifici volti ad una rivalutazione della sismicità per comprendere se un'attivazione spesso osservata su faglie limitrofe possa comunque essere riconducibile alla preparazione del forte terremoto e possa quindi contribuire all'analisi. Dall'inversione del campo di stress è stato osservato che l'attivazione sembra a volte interessare faglie che possono essere meccanicamente in relazione tra loro ma che si trovano a distanze superiori rispetto alla stima dell'area interessata dalla preparazione così come ipotizzabile dalle relazioni empiriche utilizzate. Ci si è avvalsi di uno studio sulla sismicità del Gargano (Milano et al., 2005) per comprendere la mancanza di attivazione prima del terremoto del Gargano del 1995. Uno studio su alcune sequenze della Valcomino e di Isernia permette di fornire una interpretazione sismotettonica alla sequenza di Isernia del 2001 che mostra con il metodo AMR una sovrastima della magnitudo. (Milano et al., 2005, 2006). Le osservazioni sul ruolo di alcune sequenze di minore entità che si sono verificate in aree limitrofe a quella interessata dal terremoto del Molise ha motivato uno studio sismotettonico di alcune sequenze dell'appennino centro meridionale i cui risultati sono descritti in un lavoro che è in preparazione. E' in fase di sottomissione un lavoro sull'analisi della sismicità del terremoto di Faenza del 2000 e di Monghidoro del 2003. L'analisi di dettaglio della sismicità della sequenza di Faenza e di Monghidoro ottenuta mediante l'analisi integrata dei dati della Rete Sismica Nazionale e delle reti temporanee interpretata congiuntamente con i dati messi a disposizione dalla UR 2.4 ha permesso di chiarire che i due fenomeni sismici, pur essendo localizzati ad una distanza epicentrale di circa 40 km sembrano non essere in relazione meccanica o cinematica tra di loro. In tal caso il *fit* non soddisfacente del modello AMR può essere dovuto alla impossibilità di prendere in esame per i due eventi aree molto piccole tali da escludere la mutua interferenza tra i due processi sismogenetici.

Per la validazione statistica del metodo, è stata verificata la stabilità dei risultati ottenuti applicando l'AMR ai diversi cataloghi sismici. Un problema critico è la stima della qualità, completezza e omogeneità dei dati che sono utilizzati. L'analisi è stata condotta sul catalogo sismico compilato dall'Istituto Nazionale di Geofisica e Vulcanologia (INGV) per il periodo compreso tra il 1975 e il 1988, aggiornato con i dati del bollettino sismico per il restante periodo. La completezza e omogeneità di questo catalogo è stata stimata con il codice ZMAP ed è $Mc=3.5$ per il periodo 1975-1985 e $Mc=2.3$ per il 1986-1998. Per gli eventi verificatisi dal 1986 al 2002 l'analisi è stata ripetuta utilizzando la versione del catalogo modificata dalla UR 4.7. I risultati mostrano che i due cataloghi utilizzati producono la stessa stima dei parametri del modello AMR. Nel modello AMR una regione che mostra un'accelerazione della sismicità ha un aumento della probabilità di subire un forte terremoto. Non tutte le accelerazioni di rilascio sismico sono però seguite da forti terremoti, come nel caso delle sequenze o sciami precedentemente descritti. Anche nel caso di applicazioni sistematiche dell'AMR ad altre aree sismogenetiche è stata documentata la possibilità dell'esistenza di accelerazioni del rilascio dell'energia che non sono seguite da forti terremoti. Nel caso di 6 forti eventi degli Stati Uniti (San Fernando, Coalinga, Superstition Hills, Loma Prieta, Landers, and Northridge) la probabilità di ottenere tali accelerazioni con cataloghi sismici simulati è inferiore al 25% (Mignam et al.,

2006).

Parametri del modello

Il modello AMR descritto nell'equazione (1)

$$Q(t) = Q(t_1) + A_1 - A_2(t_f - t)^m [1 + c * \cos(2\pi \frac{\log(t_f - t)}{p} - \phi)] \quad (1)$$

prevede l'utilizzo di alcuni parametri che sono peculiari delle singole aree sismogenetiche. I seguenti parametri sono invece utilizzati per selezionare gli eventi che contribuiscono al processo di preparazione dei forti terremoti. Altri parametri in seguito descritti sono stati stimati dall'applicazione del modello stesso.

Parametro Lc

Il parametro Lc rappresenta la dimensione lineare della regione analizzata. Abbiamo scelto Lc=1.5 Reff, con Reff la dimensione lineare della sorgente dell'evento esaminato, determinata mediante relazioni empiriche dall' energia. Per il territorio italiano, in assenza di studi specifici è stata applicata una relazione calcolata per i terremoti della Grecia che lega Reff alla magnitudo dell'evento Log(Reff)=0.44M-1.289

E' stata condotta un'analisi per stimare tale parametro per il territorio italiano (Tyupkin e Di Giovambattista, 2005) ed è in sottomissione un lavoro che descrive un nuovo approccio.

Parametro profondità

L'intervallo di profondità (Zmin, Zmax) degli eventi è scelto in funzione della conoscenza dello spessore sismogenetico per le diverse aree. Dall'analisi dei cataloghi è emerso che la maggior parte della sismicità è concentrata entro i primi 20 km. L'analisi è stata quindi condotta assumendo Zmin=0 km e Zmax=20 km.

Parametro magnitudo

Il livello di completezza del catalogo determina il valore minimo della magnitudo degli eventi che precedono il main-shock e che contribuiscono all'analisi.

Intervallo temporale

L'intervallo di tempo durante il quale avviene il processo di preparazione del forte terremoto dipende dalla magnitudo dell'evento stesso. Per il territorio italiano è stato assunto un intervallo di 2~3 anni.

Parametri stimati dal modello

Parametro m: il grado m dell'esponente nella equazione (1) è il parametro che caratterizza la fratturazione del mezzo nell'area del terremoto in preparazione

Parametri che determinano il trend del modello

Il Parametro A₁ determina la magnitudo predetta del main shock (M_{mod})

Parametri del modello log-periodic

Il modello contiene un termine *log-periodic* per una migliore stima dell'andamento a gradino della cumulata dello stess di Benioff. I parametri del termine *log- periodic* sono: ampiezza c, fase Φ e periodo p.

Procedura per la stima dei parametri

Per stimare i coefficienti del modello abbiamo applicato il metodo dei minimi quadrati minimizzando per tutti e 7 i parametri.

Come introdotto il coefficiente m caratterizza il grado di fratturazione del mezzo nell'area epicentrale del futuro terremoto. Assumendo che le proprietà di fratturazione del mezzo non possano subire forti variazioni nel corso di alcune decadi, il parametro m puo' essere determinato usando degli "eventi di calibrazione", ossia degli eventi per i quali il processo di accelerazione si è manifestato molto chiaramente. Per l'Italia l'evento di

calibrazione scelto è il terremoto dell’Umbria del 1997 per il quale si è ottenuto un valore di $m=0.12$ in accordo a quanto ottenuto in altre aree sismogenetiche. Per i rimanenti terremoti sono stati determinati i 7 parametri del modello assumendo $m=0.12$. I risultati ottenuti sono riportati nella tabella 1. La figura 1 mostra le localizzazioni dei terremoti analizzati e i rispettivi valori di magnitudo predetti.

Bibliografia

Bowman D.D., G.Ouillon, C.G.Sammis, A.Sornette, and D.Sornettee, An observation test of the critical earthquake concept. JGR, N B10, P. 24,359-24,372, 1998.

Bowman DD, GCP King, Accelerating seismicity and stress accumulation before large earthquakes - Geophys. Res. Lett, 28, 1, 4039-4042, 2001

Brehm D.J. and I.W.Braile Intermediate-term earthquake prediction using precursory events in the New Madrid Seismic Zone. Bull. Seismo.; Soc. Am. 88, 564-580, 1998

Knopoff, L., T. Levshina, V. Keilis-Borok, and C. Mattoni (1996), Increased long-range intermediate-magnitude earthquake activity prior to strong earthquakes in California, J. Geophys. Res., 101, 5779– 5796.

Mignan A., D. D. Bowman and G. C. P. King, An observational test of the origin of accelerating moment release before large earthquakes Journal of Geophysical Research, Vol. 111, B11304, doi:10.1029/2006JB004374, 2006

Mignan, A., G. C. P. King, D. D. Bowman, R. Lacassin, and R. Dmowska (2006), Seismic activity in the Sumatra-Java region prior to the December 26, 2004 ($M_w = 9.0\text{--}9.3$) and March 28, 2005 ($M_w = 8.7$) earthquakes, Earth Planet. Sci. Lett., 244, 639– 654, doi:10.1016/j.epsl.2006.01.058.

Milano G., Di Giovambattista R., Ventura G., 2005.Seismic constraints on the present-day kinematics of the Gargano foreland, Italy, at the transition zone between the southern and northern Apennine belts

Geophysical Research Letters, 32, L24308, doi:10.1029/2005GL024604, 2005

Milano G., Di Giovambattista R., Ventura G., 2005, The 2001 seismic activity near Isernia (Italy): Implications for the seismotectonics of the Central-Southern Apennines, Tectonophysics 401 (2005) 167– 178

Milano G., Di Giovambattista R., Ventura G., 2006 Seismicity and stress field in the Sannio-Matese area , Annals of Geophysics, vol48, 881-890

Papazachos, C. B., G. F. Karakaisis, A. S. Savvaidis, and B. C. Papazachos (2002c), Accelerating seismic crustal deformation in the southern Aegean area, Bull. Seismol. Soc. Am., 92, 570– 580, doi:10.1785/0120000223.

Jaumé, S.C. and L.R.Sykes, Evolving towards a critical point: a review of accelerating seismic moment energy release prior to large and great earthquake. Pure and Appl. Geophys., 155, 279-306,1999

Robinson, R., S. Zhou, S. Johnston, and D. Vere-Jones (2005), Precursory accelerating seismic moment release (AMR) in a synthetic seismicity catalog: A preliminary study, Geophys. Res. Lett., 32, L07309, doi:10.1029/2005GL022576.

Sammis, C. G., D. D. Bowman, and G. C. P. King (2004), Anomalous seismicity and accelerating moment release preceding the 2001 and

2002 earthquakes in northern Baja California, Mexico, Pure Appl. Geophys.,
161, 2369–2378.

Tabella 1. Risultati dell'applicazione del modello AMR. $M_{catalog}$ è la magnitudo riportata per l'evento nei cataloghi sismici mentre M_{mod} è la magnitudo stimata dal modello. Gli altri parametri sono descritti nel testo.

Data		$M_{catalog}$	t_f	M_{mod}	A_2	m	c	p	ϕ	Δ
1979.720	Norcia	5.5	1979.75	6.3	104.23	0.12	0.06	0.567	0.906	6.303
1980.898	Irpinia	6.5	-	-	-	0.12	-	-	-	-
1984.352	Val Comino	5.4	1984.42	5.57	36.49	0.12	0.03	1.647	1.271	0.350
1990.951	Sicilia Or.	5.2	1990.95	5.13	17.7	0.12	0.02	2.255	3.307	0.055
1997.737	Umbria	5.6								
1997.738		5.8	1997.80	6.00	86.27	0.12	0.01	1.957	3.245	0.386
1998.692	Lucania	5.5	1998.70	5.33	32.964	0.12	0.17	0.250	2.875	0.056
2002.73	Palermo	5.8	2002.34	6.2	45	0.12	0.02	1.7	3.122	0.312
2003.70	Monghidoro	5.3	2003.35	6.2	60	0.12	0.03	1.6	2.997	0.374

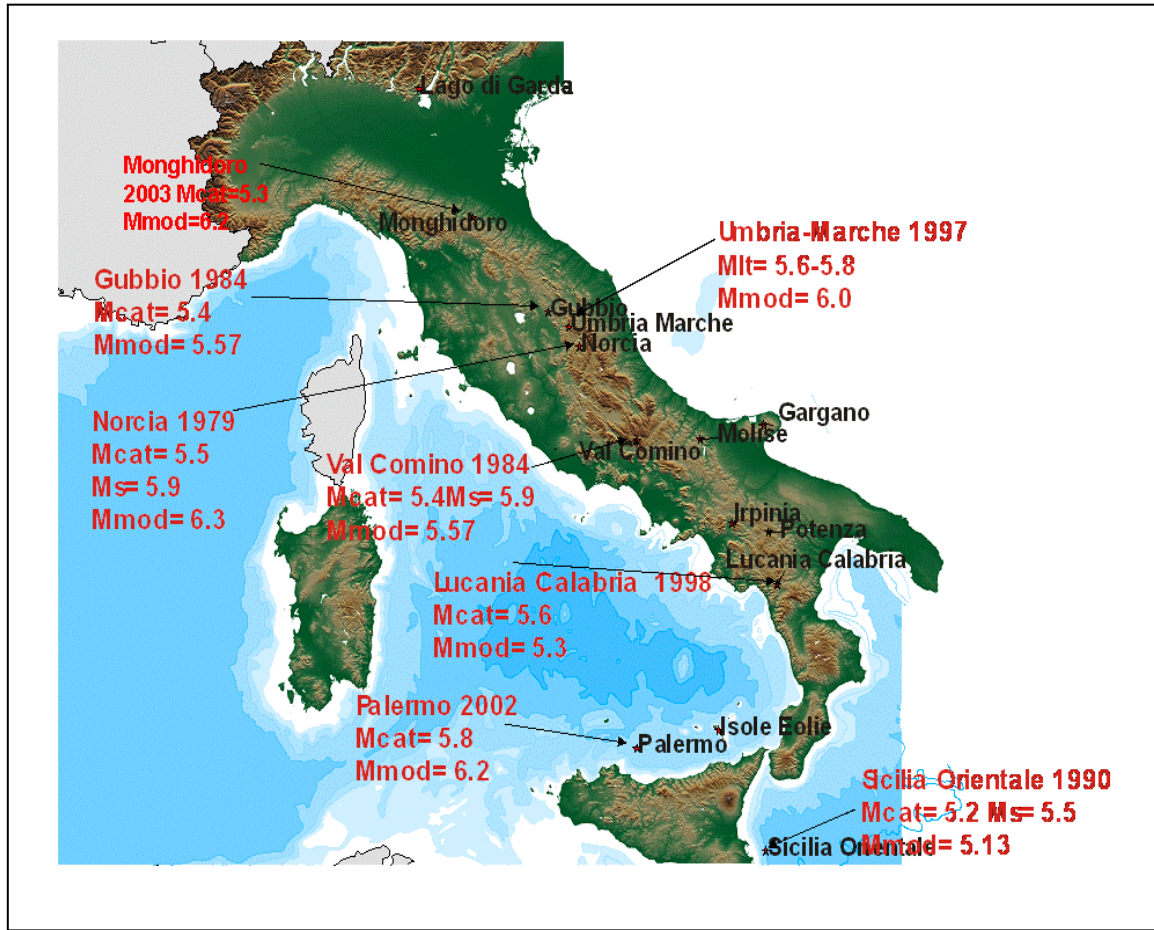


Figura 1 –Localizzazione degli eventi analizzati. Il terremoto del Lago di Garda e i due terremoti siciliani, pur non appartenendo alle aree selezionate per il test sono stati comunque analizzati. Per il terremoto dell’Irpinia del 1980 non si hanno dati sufficienti per l’analisi. I terremoti del Gargano, Potenza e Molise non sono stati preceduti da attivazioni significative.



UR 4.3 - Coordinatore: Francesca Romana Cinti (INGV-Roma)

I principali obiettivi della ricerca svolta dalla UR sono:

- 1) Verificare gli effetti dell'interazione tra faglie sulla distribuzione spazio-temporale dei terremoti medio-forti confrontando le caratteristiche statistiche di cataloghi sintetici con quelle del catalogo reale;
- 2) Studiare l'effetto della "non completa" conoscenza delle strutture sismogenetiche e delle incertezze epistemiche sul sistema di faglie e sulle singole strutture sismogenetiche.

Metodo:

Abbiamo analizzato il comportamento di una popolazione di strutture sismogenetiche realistica integrando informazioni geologiche/strutturali con una modellistica fisica e statistica. Il procedimento consiste nel i) definire il sistema di faglie, individuando gli eventuali limiti che lo caratterizzano; ii) definire il comportamento sismogenetico delle singole strutture e un modello di interazione co- e post-sismica tra le strutture sismogenetiche; iii) creare i cataloghi sintetici utilizzando i punti precedenti; iv) studiare l'effetto delle interazioni tra strutture e delle incertezze epistemiche (relative al sistema di faglie ed al modello) sulla distribuzione spazio-temporale dei terremoti.

Attività e Risultati:

La ricerca si articola in tre attività principali:

- 1) Scelta e definizione della popolazione di strutture sismogenetiche (scala regionale)
- 2) Messa a punto del modello di ricorrenza delle strutture e di interazione tra faglie e creazione di cataloghi sintetici
- 3) Analisi dei risultati

Attività 1):

Analizzando il quadro delle conoscenze geologiche e sismotettoniche dell'Italia è apparso chiaro che il settore centrale della Penisola è quello in cui le informazioni di tettonica attiva sono maggiori, abbiamo pertanto applicato la nostra ricerca in tale settore. Abbiamo definito un primo sistema di faglie responsabili o capaci di produrre eventi sismici di $M \geq 5.5$. Tale assetto di base include tutte le strutture, n. 38 faglie, presenti nel DISS *Working Group, versione 3.0.1* (dicembre 2005 - www.ingv.it/banchedati/banche.html). Ad incremento del DISS, abbiamo aggiunto strutture definite in ex progetti GNDT e in elaborazioni successive quali *Barchi et al. (2002)*, *Galadini et al. (2000)* e (2001), ma non presenti nel DISS. Da questa combinazione, da noi denominata DISSPLUS, si raggiunge un numero totale di n. 46 faglie sismogenetiche nell'area selezionata.

Il quadro della popolazione di faglie così ottenuto è certamente più completo, sebbene la qualità dei parametri di faglia ha ancora una grande variabilità ed inoltre il numero delle faglie è ragionevolmente ancora sottostimato. Considerando infatti una ricorrenza di eventi medio-forti su una singola faglia dell'ordine di alcune migliaia di anni, relativamente alla lunghezza del catalogo sismico a disposizione (*Gruppo di lavoro CPTI, 2004*; *Castello et al., 2005*), è ragionevole assumere che non più di un singolo evento su una specifica faglia può essere registrato nella memoria storica. In altre parole, il numero degli eventi approssimerebbe il numero delle faglie. All'interno dell'area studiata, la maggior parte delle faglie hanno assegnato un evento più recente che appare nel catalogo storico, come da testimonianza diretta o da studi paleosismologici (poche strutture) o come da dati macrosismici e localizzazioni epicentrali (la maggior parte delle strutture). Oltre a

questi eventi per i quali la faglia attivata è riconosciuta, si contano 23 eventi che hanno colpito l'area dal 1100 A.D. ad oggi per i quali non è riconosciuta la relativa struttura. Al fine di colmare questa "mancanza" ed utilizzare nella nostra analisi una popolazione di strutture sismogenetiche più realistica possibile, abbiamo riprodotto un terzo set di strutture denominato Large Structures Dataset - LSD. Questo include nuove strutture ipotizzate specificatamente per questo studio. Ad ogni evento "orfano" abbiamo associato una faglia ex-novo e definito i parametri di faglia utilizzando le informazioni storiche sull'evento, quali localizzazione epicentrale ed intensità, caratteristiche di sismicità e tettonica regionale e locale e formule empiriche, inoltre si è proceduto per analogia con faglie adiacenti. Abbiamo così raggiunto un totale di n. 69 faglie presenti in questo settore di Italia centrale (*Figura 1*), ossia 23 strutture sismogenetiche in più (circa il 60%) rispetto al set delineato usando come base il DISS 3.0.1.

Si ribadisce che analizziamo il comportamento dei tre dataset di faglie allo scopo di verificare gli effetti dei diversi gradi di completezza sulla distribuzione statistica spazio-temporale degli eventi.

Ad ogni faglia abbiamo assegnato i parametri geometrici e cinematici che vengono considerati nel modello di interazione: localizzazione, dimensione, profondità, direzione, immersione, rake, slip (dalla magnitudo), tempo di ricorrenza. Alcuni di questi parametri erano sconosciuti per le strutture integrate da ex-progetti GNDT, così come tutti i valori delle faglie appartenenti al dataset finale (LSD) che sono stati quindi definiti ex-novo dai componenti della UR specificatamente per questo lavoro. Riguardo i tempi di ricorrenza assegnati alle faglie, abbiamo riscontrato un'elevata variabilità, e sulla base degli intervalli e delle medie derivate abbiamo così definito ed assegnato delle classi di valori (1200-2000-3500).

Attività 2):

E' stato realizzato e verificato il codice per modellare il comportamento delle singole strutture e l'interazione tra di esse. Il modello assume per le strutture sismogenetiche un comportamento di tipo "terremoto caratteristico" (comportamento periodico e magnitudo ripetuta) con un carico tettonico costante e aggiunge il contributo delle perturbazioni co-sismiche (modello di Okada) e post-sismiche dovute agli eventi avvenuti sulle strutture. L'interazione tra le faglie viene stimata tramite Coulomb Failure Function. L'effetto post-sismico viene calcolato attraverso una relazione empirica con il co-sismico calcolato, ed evolve nel tempo con tempi di rilassamento caratteristici che dipendono dalla viscosità astenosferica (*Marzocchi et al., 2003; Schiavardi, 2003*).

$$\begin{aligned} &\text{Co-seismic part} \quad \text{Post-seismic part} \\ &\sigma(t) = Mo_i(\Delta_{CO}(x_i)H(t-t_i) + \Delta_{POST}(x_i)\Omega(t-t_i)) \\ &\Delta_{POST}(x) = \Delta_{CO}(x)(0.012\delta + 1) \\ &\Omega(t^*) = 1 - \exp(-t^*/\tau) \end{aligned}$$

σ : Stress perturbation on a fault

$\Delta_{CO}(x)$: Co-seismic Coulomb Failure Function (CFF) through Okada's model

Mo_i : Seismic moment of the i-th earthquake

$H(y)$: Heaviside function

τ : "Relaxation" time of the viscous layers (30 years in this application)

δ : Dimensionless value, corresponding numerically to the distance in km

t_i : Time of occurrence of the i-th earthquake

Alcuni dei parametri del modello sono soggetti a forti fluttuazioni legate alla scarsa conoscenza dei parametri reali, come per esempio i tempi di ricorrenza (tutti uguali oppure diversi da struttura a struttura) e la statistica degli intereventi (terremoto caratteristico o Poisson) delle singole strutture, ed il tempo caratteristico per il post-sismico (30 e 300 anni). Per questo motivo abbiamo proceduto con una serie di simulazioni, con relativa produzione di cataloghi sintetici, realizzate con le diverse scelte, e proceduto all'analisi della stabilità dei risultati. Inoltre si sono prodotti diversi cataloghi sintetici anche assumendo i tre assetti di strutture (diverso numero di faglie) al fine di verificare l'effetto di dataset con diverse completezze.

Per quanto riguarda l'aspetto temporale delle simulazioni, il sistema faglie ed interazioni è stato fatto evolvere per un tempo molto lungo (3 milioni di anni). E' stata poi analizzata l'ultima parte del catalogo sintetico (1 milione di anni) al fine di studiare il comportamento asintotico ed indipendente dalle condizioni iniziali imposte.

Attività 3):

L'analisi e' stata fatta su due piani distinti. Da un lato si è confrontato il catalogo reale con quelli sintetici sul piano regionale (catalogo completo); dall'altro, si sono analizzati i comportamenti delle singole strutture.

In Figura 2 sono riportate le cumulative dei tempi di intervento osservati nel catalogo reale e nel catalogo sintetico (in rosso), confrontandole con un modello poissoniano (in blu). I cataloghi sintetici riproducono l'effetto di cluster su pochi anni, osservato anche nel catalogo sismico reale degli ultimi secoli.

In *Figura 3* abbiamo riportato un confronto tra il rateo osservato e quello modellato (in una finestra casuale di 1000 anni). Entrambi i ratei sono caratterizzati da significative non stazionarietà con tempi caratteristici di secoli, minori delle ricorrenze sulle singole strutture (dell'ordine di 2000 anni) e maggiori del tempo di interazione (30 anni). Questi risultati sono stabili rispetto alle variazioni del catalogo delle strutture e del modello fisico.

Dallo studio delle singole strutture, si evidenzia che le interazioni influenzano il comportamento delle faglie nel tempo, ovvero cambiano i tempi di ricorrenza sulle singole strutture in maniera significativa (*Figura 4*). Infatti introducono comportamenti multi-modali, così come significative accelerazioni o decelerazioni dei cicli sismici. Un aspetto importante è che non si osservano gruppi di faglie con una interazione privilegiata (effetto di sincronizzazione). Questo significa che non si osserva una relazione immediata tra poche strutture ben specificate, ma piuttosto il comportamento di ogni struttura è legato all'effetto cumulato di tutte le altre strutture (sia grandi e lontane, sia piccole ma vicine; esemplificativo di questo sia il mancato accoppiamento delle faglie Ovindoli Pezza e Fucino dovuto al sistema locale di strutture "minori"). Questo comportamento è strettamente connesso al fatto che l'accoppiamento geometrico agisce in maniera fortemente assimmetrica. L'aggiunta o la rimozione di una faglia dal sistema non induce cambiamenti a livello regionale ma modifica il comportamento nel tempo delle strutture vicine. Le non stazionarietà osservate a livello regionale sono quindi legate ad effetti nel tempo tipo "battimenti" piuttosto che a un comportamento a gruppi. Quanto detto mostra che la statistica temporale delle singole strutture è estremamente sensibile all'eventuale incompletezza del catalogo delle strutture.

In *Figura 4* si riportano alcuni esempi su come l'interazione tra le strutture induce perturbazioni significative dello stress sulla singola faglia e conseguentemente sulla ricorrenza degli eventi generati nel tempo su di esse.

Conclusioni

Il modello è in grado di riprodurre le caratteristiche del catalogo regionale quali clusterizzazione e non-stazionarietà. A livello delle singole strutture, il modello evidenzia che la completezza del catalogo delle strutture può avere un effetto dominante sul comportamento delle singole strutture, e quindi sulla capacità previsionale del loro comportamento temporale. In particolare:

- ✓ *L'interazione tra le faglie* induce cambiamenti significativi sui tempi di ricorrenza delle singole strutture sismogenetiche
- ✓ Alcune faglie mostrano tempi di ricorrenza *multimodali*
- ✓ Alcune faglie subiscono sensibili “*accelerazioni*” e/o “*decelerazioni*”; i cambiamenti dei tempi di interevento sono fortemente dipendenti dall’effetto cumulato delle faglie nelle vicinanze (forti effetti di faglie “minori”)
- ✓ Non troviamo *sincronizzazioni* di faglie statisticamente significative (accoppiamento di singole faglie)

Presentazioni a convegni inerenti la ricerca svolta

Selva J., F.R. Cinti, W. Marzocchi, P. Montone, S. Pierdominici and R. Schivardi (2005). Temporal evolution of a realistic faults system: some insights from a seismic area in central Italy, Eos Trans. AGU, 86(52), Fall Meet. Suppl., Abstract S53A-1083.

Selva, J., F.R. Cinti, W. Marzocchi, P. Montone, S. Pierdominici and R. Schivardi (2006). Seismic Stress Interaction among active Faults in Central Italy: implications on the spatio-temporal earthquake distribution, EGU Gen. Assembly 2006, Vienna April 2006.

Marzocchi, W., J. Selva, F.R. Cinti, P. Montone, S. Pierdominici, R. Schivardi and E. Boschi (2006). On the Recurrence of Large Earthquakes: Some Insights From a Model Based on a Realistic Interacting Fault System, Eos Trans. AGU, 87(52), Fall Meet. Suppl., S12A-05

Selva, J., W. Marzocchi, F.R. Cinti, P. Montone, S. Pierdominici and R. Schivardi (2007). On the recurrence of large earthquakes: some insights from a model based on a realistic interacting fault system, IUGG Perugia -Italy 2-13 Luglio 2007.

Bibliografia

- Barchi, M., F. Galadini, G. Lavecchia, P. Messina, A.M. Michetti, L. Peruzza, A. Pizzi, E. Tondi and E. Vittori (2000). Sintesi delle conoscenze sulle faglie attive in Italia Centrale: parametrizzazione ai fini della caratterizzazione della pericolosità sismica. CNR - Gruppo Nazionale per la Difesa dai Terremoti - Roma, 2000, 62 pp.
- Castello, B., G. Selvaggi, C. Chiarabba and A. Amato (2005). CSI Catalogo della sismicità italiana 1981-2002, versione 1.0. INGV-CNT, Roma, <http://www.ingv.it/CSI/>
- Cinti, F.R., L. Faenza, W. Marzocchi, and P. Montone (2004). Probability map of the next ≥ 5.5 earthquakes in Italy, *Geochem. Geophys. Geosy.*, 5, N. 11, 2 November 2004, Q11003, doi:10.1029/2004GC000724.
- DISS Working Group (2005). Database of Individual Seismogenic Sources (DISS), Version 3.0.1: A compilation of potential sources for earthquakes larger than M 5.5 in Italy and surrounding areas. <http://www.ingv.it/banchedati/banche.html>
- Faenza, L., W. Marzocchi and E. Boschi (2003). A nonparametric hazard model to characterize the spatio-temporal occurrence of large earthquakes: An application to the Italian catalogue, *Geophys. J. Int.*, 155(2), 521–531.
- Galadini, F., C. Meletti and A. Rebez (2000). Le ricerche del GNDT nel campo della pericolosità sismica (1996-1999). CNR - Gruppo Nazionale per la Difesa dai Terremoti - Roma, 2000, 397 pp.
- Galadini, F., C. Meletti and E. Vittori (2001). Major active faults in Italy: Available superficial data, *Neth. J. Geosci. Geol. Mijnb.*, 80(3-4), 273–296.
- Gruppo di lavoro CPTI (2004). Catalogo Parametrico dei Terremoti Italiani, versione 2004 (CPTI04). INGV, Bologna. <http://emidius.mi.ingv.it/CPTI/>
- Marzocchi, W., J. Selva, A. Piersanti and E. Boschi (2003). On the long-Term interaction among earthquakes: Some insights from a model simulation. *J. Geophys. Res.*, 108 (B11), 2538, doi:10.1029/2003JB002390.
- Schivardi R. (2003) – Modello di interazione co- e post-sismica tra faglie: implicazioni sulla distribuzione spazio-temporale dei terremoti. Univ. di Bologna, Anno Acc. 2002/2003. Tesi di Laurea (inedita).
- Selva, J., W. Marzocchi, F. Zencher, E. Casarotti, A. Piersanti and E. Boschi (2004). A forward test for the interaction between remote earthquakes and volcanic eruptions: the case of Sumatra (Jun. 2000), and Denali (Nov. 2002) earthquakes. *Earth Planet. Sci. Lett.*, 226, 383-395.

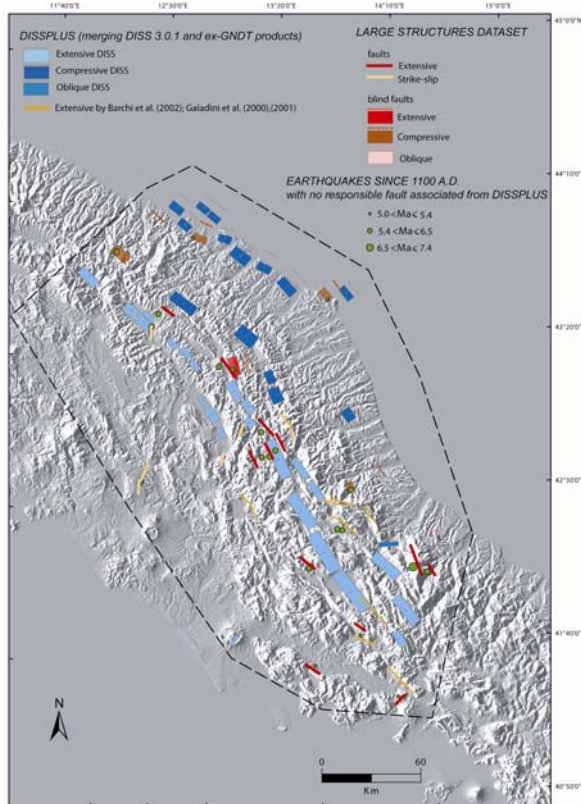
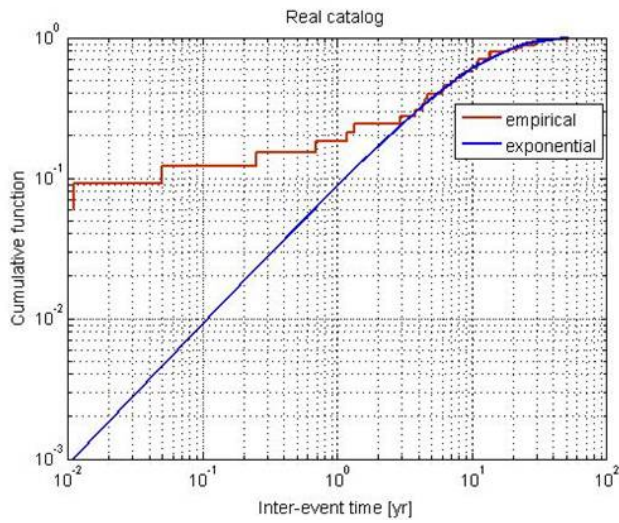
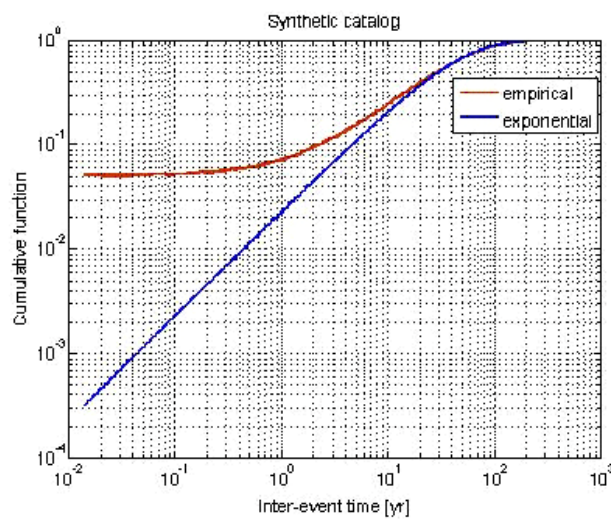


Figura 1 - Sistema di faglie responsabili dei terremoti medio-forti nell'area in esame. Sono riportati i tre dataset Diss-Dissplus e LSD. Sono plottati gli epicentri degli eventi non associati alle faglie disponibili in letteratura, ad ognuno dei quali abbiamo assegnato una struttura ex-novo.



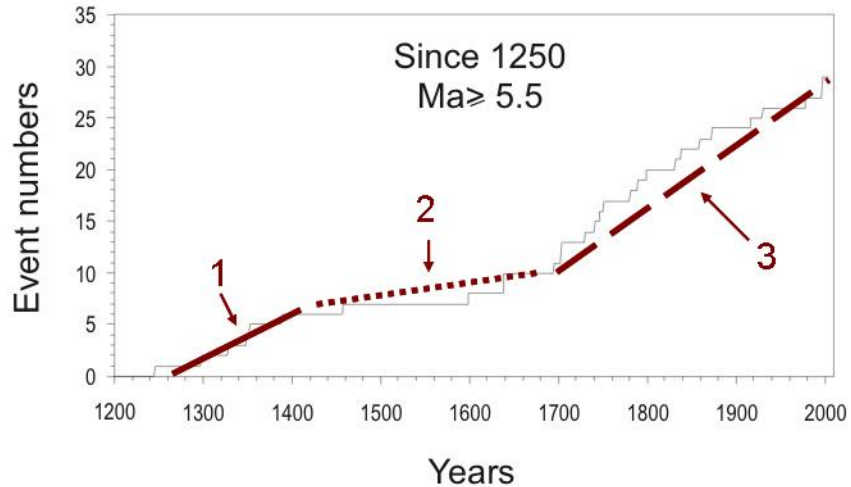
(a)



(b)

Figura 2 - Distribuzione cumulativa dei tempi di interevento osservati nel catalogo reale (a) e catalogo sintetico (b). Gli eventi appaiono clusterizzati rispetto all'andamento poissoniano (linea blu); il cluster ha tempi caratteristici di alcuni anni, quindi tempi confrontabili con quelli osservati nel catalogo reale (Faenza et al., 2003; Cinti et al., 2004).

(a) *Real catalog*



(b) *Synthetic catalog*

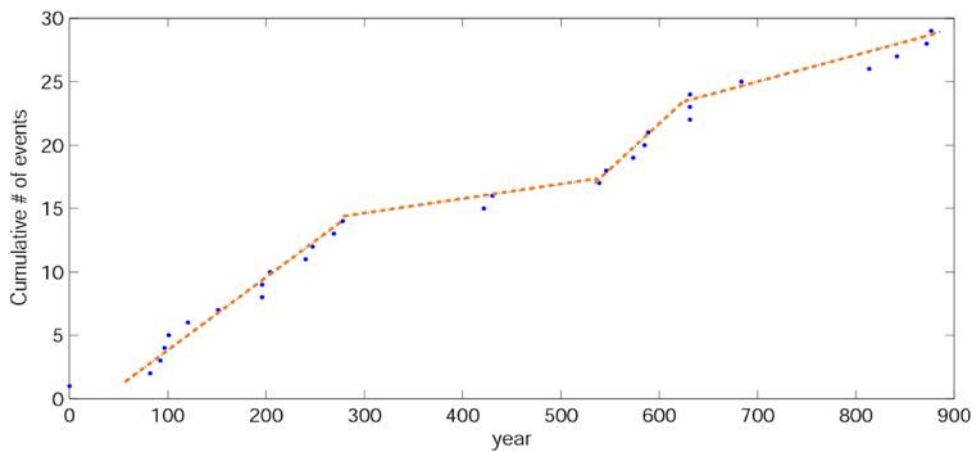


Figura 3 - Rateo sismico cumulativo osservato nel catalogo reale (a) e rateo cumulativo in una finestra temporale di 1000 anni selezionata a caso all'interno del catalogo sintetico (b). Il rateo sismico non appare essere costante, ma è significativamente non stazionario. Si osservano periodi (lunghi secoli) dove avvengono molti eventi rispetto ad altri periodi con molto meno eventi.

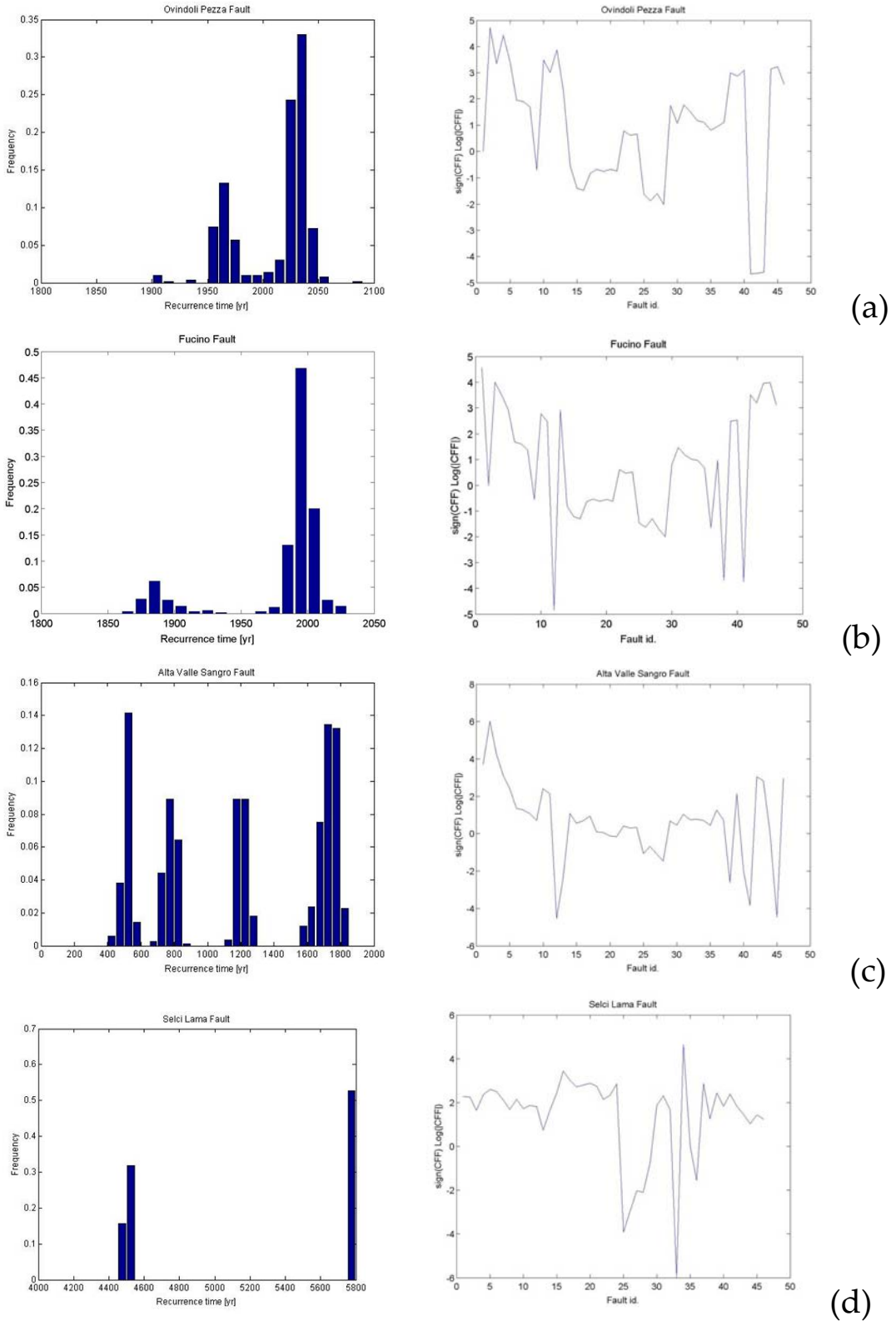


Figura 4 - Frequenze dei tempi di ricorrenza osservati (sinistra) e valore dell'interazione co-sismica (destra) su diverse strutture: (a) Ovindoli Pezza, (b) Fucino, (c) Alta Valle Sangro e (d) Selci Lama.



UR 4.4 - Coordinatore: Elsa Garavaglia (Politecnico di Milano, DIS)

In the time period during which the Project S2 has been developed, the UR_PoliMi, Task4_4, involved into the research field dealing the prediction of the next events during the interval 2005 – 2035, has focused its work at providing a predictable earthquake model, able to interpret a characteristic earthquake (CE) even if clusters or other kind of frequent and irregular earthquakes are present. In other words the model would be reliable even if the presence of a CE is debatable: the spread interoccurrence times (IT) with coefficient of variation (COV) near to the unity could make *not rejectable* also the poissonian hypothesis.

1- Problem position

The proposed model is a renewal process (RP). Only strong earthquakes are modelled, with magnitude M>5.3. The procedure is purely probabilistic, but at least two physical hypotheses are included:

- 1) a weak dependence on the past history, expressed with the use of a RP;
- 2) a stationary asymptotic behaviour of the hazard: a very long seismic silence in a zone could be reasonably interpreted like an energy release occurred somewhere, rather than a continuous enormous accumulation of energy in progress in the zone.

Precisely the property 1) means that the probability of an earthquake depends on the elapsed time t_0 from the last event. The property 2) means that the hazard increases with t_0 but, after a peak value, if the earthquake did not occur, it decreases and reaches a stable value, describing for every next instant (always if the seismic silence is going on) a constant probability of occurrence.

In order to satisfy the property 2), an exponential-Weibull (ex-w) mixture is adopted, with the Weibull's form parameter $\alpha > 1$.

$$1 - F_\tau(t_0) = (1-p)\exp[-bt_0] + p \exp[-(\rho t_0)^\alpha] \quad (1)$$

The exponential distribution mainly interprets the short IT, while the Weibull distribution mainly interprets the regular IT related to CE. Nevertheless both distributions are defined in $[0, \infty)$ without a threshold of separation between the two families of events. Indeed, a threshold could be hardly defined. The more the tails overlap, the less the CE is evident. In any case the mixture distribution overcomes the drawback of a single distribution that in general is not able to fit the entire class of IT. The mixtures (1) model a wide class of earthquake IT whose hazard rate (HR) is given by:

$$\lambda(t_0) = \frac{f_\tau(t_0)}{1 - F_\tau(t_0)} \quad (2)$$

It is shaped as required from property 2). Because of the variability of the parameter p , the distributions (1) can explore all degree of CE evidence: increasing values of p mean larger and larger evidence of CE; $p=1$ means lack of the irregular short IT. In the two extreme cases $p=0$ and $p=1$ the mixture distribution (1) becomes, respectively, exponential and Weibull and the property 2) fails: when $p=0$ the HR is constant in time and the predictability is missing; when $p=1$ the HR is continuously increasing until the asymptotic

certainty of an occurring earthquake.

The Eq. (2) furnishes the prediction in a very short (infinitesimal) next time interval dt :

$$\lambda(t_0) = \lim_{\Delta t_0 \rightarrow 0^+} \frac{\Pr\{t_0 < \tau \leq t_0 + \Delta t_0 | \tau > t_0\}}{\Delta t_0} = \frac{f_\tau(t_0)}{1 - F_\tau(t_0)} \quad (3)$$

while the medium term Δt prediction is:

$$P_{\Delta t_0 | t_0} = \frac{F_\tau(t_0 + \Delta t_0) - F_\tau(t_0)}{1 - F_\tau(t_0)}. \quad (4)$$

Note explicitly that, in this contest, prediction means, at each instant, conditional probability of an earthquake ($M > 5.3$) in the next time interval (dt or Δt), given the length of the preceding seismic gap.

The presence of four parameters is the main drawback of Eq. (1) in estimation procedure. To avoid this shortcoming, we propose the following time scale transform:

$$h = \frac{t_0}{\mu} \quad (5)$$

where $\mu = (1-p)\mu_1 + p\mu_2$ is the global return period of the earthquake process weighted sum of the two component periods μ_1 and μ_2 . Eq. (5) transforms Eq. (1) in adimensional terms as follows:

$$1 - F(h) = (1-p) \exp\left[-\frac{h}{k_1}\right] + p \exp\left\{-\left[\Gamma\left(1 + \frac{1}{\alpha}\right) \frac{h}{k_2}\right]^\alpha\right\} \quad (6)$$

where $k_1 = \mu_1/\mu$, $k_2 = \mu_2/\mu$ are the two return period components expressed in adimensional terms; under this assumption the values assumed by k_1 and k_2 are respectively: $k_1 < 1$ and $k_2 > 1$. Eq. (6) offers the advantage of presenting the possible earthquakes panorama independently of their return periods. In adimensional form becomes $1 = (1-p)k_1 + pk_2$ and p now can be estimated as:

$$p = \frac{1-k_1}{k_2 - k_1}.$$

Three parameters remain to be estimated in Eq. (6). In order to make the estimate procedure easier and more stable, we proceed assuming $\alpha = constant$ with different trial values; then we choose the best one in respect to likelihood function. In this way only k_1 and k_2 have to be estimated: they can be directly read in the sample, at least if the ratio $r = k_2/k_1$ is large enough to ensure weak overlap of the two component densities. In this case the mean values of $IT < 1$ and $IT > 1$ give empirical estimates of k_1 and k_2 , respectively.

Varying k_2 and k_1 we obtain different families of earthquake processes, representing conjectural "truths". An example is reported in figure 1 in a compact form through the adimensional HR $\tilde{\lambda}$.

2 - Comparison between estimated procedures

Different estimate procedures are taken into consideration.

The first one assumes the mathematical model (6) and uses the classical method of maximum likelihood (ML) for the estimation of the parameters k_1 and k_2 .

The second one, that we call threshold method (TR), also assumes the mathematical model (6) and accepts as estimation of k_1 and k_2 the mean of the IT, respectively $\langle 1 \rangle$ and $\langle 2 \rangle$, as explained above.

As we will see in the following, if r assumes values around 4 or more, the TR method is also better than ML method: indeed it is able to catch the contribution of the few IT in the tail better than the ML that is sensitive to the total contribution of the IT. On the contrary the TR fails for low values of r , i.e. if the tails of the two components of the mixture overlap.

A third method (ME) is based on the maximum entropy principle that implies the use of a generalized exponential distribution. This is, indeed, the distribution that incorporates only the information inherent in dataset (so maximizing the entropy). This method does not agree with our choice of limited λ_∞ , but it is useful in a qualitative sense because it is very sensitive to the dataset and is free from the CE hypothesis.

Finally an empirical method (EMP) consists in reading directly on the cumulative frequency polygon F^* the values of λ^* and $P_{\Delta h|h}$. Precisely the empirical value λ^* is:

$$\lambda^*(h) = \frac{(tg\theta)_h}{1 - F^*(h)}$$

being $(tg\theta)_h$ the angular coefficient of that polygon F^* side which h belongs to. The Eq. λ^* becomes meaningless at the end of the polygon, but, before the end, it offers an empirical rough prediction directly coming from dataset and without any subjective assumption (but the piecewise linearity of the polygon). Moreover the dataset can suggest possible variability on the hazard that the structure of the chosen mathematical model cannot incorporate; typically a possible multimodality of the hazard will be suggested from the empirical method. Obviously, this rough empirical method EMP can not be considered a reliable non parametric procedure, but it would only furnish complementary qualitative considerations.

3 - Credibility Procedure

Following a procedure developed during the previous project (Progetto Quadro CNR-GNDT 2000-2002 (Coor. da A. Amato)) the credibility of a procedure has been defined aimed at measuring the error, respect to a conjectural truth F° , when a quantity A is estimated with that procedure. Let be A° the true value of A (in the conjectural truth) and \hat{A}_r its estimator with the procedure r . The credibility Δ_r° of the procedure r relative to the truth F° (that here is simply a given distribution) is defined as follows:

$$\Delta_r^\circ = \Pr\{A^\circ - kA^\circ \leq \hat{A}_r \leq A^\circ + kA^\circ\}. \quad (7)$$

In other words, Δ_r^o is the probability of an error (in absolute value) not larger than a given value k in the estimate of the quantity A .

Thanks to this introduced credibility, competing models can be compared in the frame of the conjectural chosen truths. The values of Δ are obtained with Monte Carlo simulation.

In Table 1 the values Δ are shown, relative to some conjectural F^o identified through their single parameter k_2^o , being the comparison done with the same values of p and α : $p=0.5$ and $\alpha=4$ are the assumed values that are frequently observed in the studied zones; the parameter k_1^o is evaluated through $1=(1-p)k_1+p k_2$. In Table 1 the sample size is $v=20$ that represent a more realistic value compared with a real database of seismic events. The results obtained confirm a suitable reliability of the TR method when the ratio $r=k_2/k_1$ is large ($r > 4$).

4 - Robustness

The ex-w mixture model has the advantage of robustness, at least in respect to the poissonian hypothesis. In other words the mixture model gives a reliable prediction even if the true distribution is exponential. In fact the flexibility of the mixture distribution gives HR estimate with very moderate variability, for samples drawn from an exponential. This, in terms of credibility, is shown in Table 2 where Δ_{ex-w}^{exp} is the credibility of the mixture procedure when the truth is exponential. Its values are rather high, even if a realistic small size of the samples ($v=20$) has been chosen.

5 - Applications

The aim of the Project S2 is to assign to each Italian seismogenetic area an occurrence probability of event into the interval 2005-20035. The catalogues taken into consideration for the application of the procedures proposed are obtained by the associations of the events of the Italian historic catalogue CPTI04 (CPTI Working Group, 2004. Catalogo Parametrico dei Terremoti Italiani-Versione 2004 (CPTI04) INGV, Bologna) with the seismogenetic source areas (SA Sources-DISS03, INGV). These new catalogues are put at disposal by the members of Project S2-Task 1, so like the association of SA Sources to eight Macro Regions (MR) that are permitted to bypass the problem of few data in some areas (Fig. 2a,b). The prevision deals with events from 1600 to 2002 with magnitude $Maw>5.3$.

The application of the three proposed methods (ML, TR and ME) has required the building of interoccurrence times data sets. Starting form the historic catalogue CPTI04, the interoccurrence times have been evaluated for each SA involved into a given MR, the interoccurrence times so evaluated for all the SA inside the MR analysed represent the MR interoccurrence times data set.

The application has been made on the 8 Italian MR. For each MR the data have been organized as shown in Fig. 3: Table with MR catalogue in dimensional and adimentional forms, return period μ of the MR, parameter p representative of the evidence of CE and the asymptotic hazard rate value λ_∞ of the MR investigated. The figures shown the $\hat{F}(h)$ and $\hat{\lambda}(h)$ estimations with the three methods in adimentional form. In figures also the experimental hazard rate λ^* is presented. Its behaviour is useful to investigate anomalies in the data sets not captured by ML, TR and ME. All the data produced are present in [3]:

www.mate.polimi.it/biblioteca/qddview.php?id=1329&L=i

By the implemented elaborations, it is clear that an exponential distribution seems inadequate to model the investigated process; the mixture ex-w, supported by the proposed credibility analysis, seems more adequate.

For each SA we have evaluated the probability of occurrence $\hat{P}_{\Delta t|t_0}$ for different Δt (5, 10, 20, 30 50 and 100 years) starting from last event in each SA and assuming last year reported in CPTI04 (2002) like date of reference. The probability is reported both in tables (an example is reported in Fig. 3) and in maps (an example is reported in Fig. 4, 5, 6). The results put in evidence that the Central Northern Apennines and Calabrian Arc seismogenetic areas present the biggest risk of occurrence of earthquake with magnitude greater than 5.3.

Bibliografia essenziale

E. Guagenti Grandori, L. Petrini, E. Garavaglia, "Ipotesi e modello di terremoto caratteristico perturbato", *Atti di ANIDIS07, XII Conv. Naz. "L'Ingegneria sismica in Italia"*, Pisa, 10 – 14 Giugno 2007, Editors F. Braga e W. Salvatore, Edizioni PLUS, Pisa, CD-ROM, paper n. 5, ISBN 978-88-8492-458-2.

E. Garavaglia, E. Guagenti, L. Petrini "The earthquake predictability in mixture renewal models" *Proc. of Società Italiana di Statistica, SIS Intermediate Conference 2007 Risk and Prediction*, Venezia, June 6 – 8 2007, Invited Section, Editor Società Italiana di Statistica, Ed. CLEUP, Venezia, Vol. I, pp 361-372, ISBN 978-88-6129-093-8.

E. Garavaglia, E. Guagenti, R. Pavani, L. Petrini "La predicitività di un terremoto caratteristico nell'ipotesi dei processi di rinnovo del tipo mistura", *Quaderni del Dipartimento di Matematica*, QDD 20, Politecnico di Milano, versione elettronica in:

<http://www.mate.polimi.it/biblioteca/qddview.php?id=1329&L=i>

E. Garavaglia, R. Pavani "About earthquake forecasting by Semi - Markov renewal processes", *Jour. Methodology and Computing in Applied Probability*, Spring Ed., US, (Submitted).

Table 1 Values of $\Delta = \Pr\left\{\left|\frac{\hat{\lambda}(h) - \lambda^\circ(h)}{\lambda^\circ(h)}\right| < 0.3\right\}$ with samples size: $n=20$

h k_2^0	methods	0.5	1	1.5	2	2.5	h_{max}
1.2	ML	0.71	0.57	0.57	0.19	0.50	0.49
	TR	0.91	0.21	0.37	~0.0	~0.0	~0.0
1.4	ML	0.67	0.61	0.46	0.38	0.25	0.36
	TR	0.91	0.65	0.54	0.68	0.14	0.70
1.6	ML	0.58	0.59	0.41	0.39	0.34	0.69
	TR	0.87	0.70	0.54	0.54	0.58	0.69
1.8	ML	0.33	0.41	0.36	0.34	0.34	0.43
	TR	0.38	0.49	0.38	0.38	0.40	0.57

Table 2 Values of Δ_{ex-w}^{exp} for estimate with ML of λ and $P_{0.1|h}$; $n=20$

h	0.5	1	1.5	2	2.5	h_{max}
λ	0.92	0.95	0.70	0.57	0.48	0.42
$P_{0.1 h}$	0.94	0.95	0.71	0.59	0.50	0.44

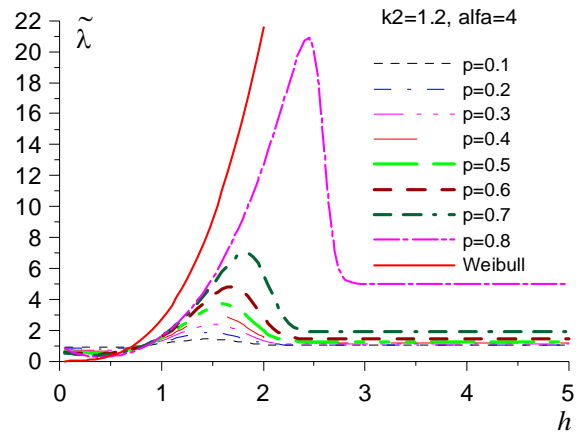


Figura 1

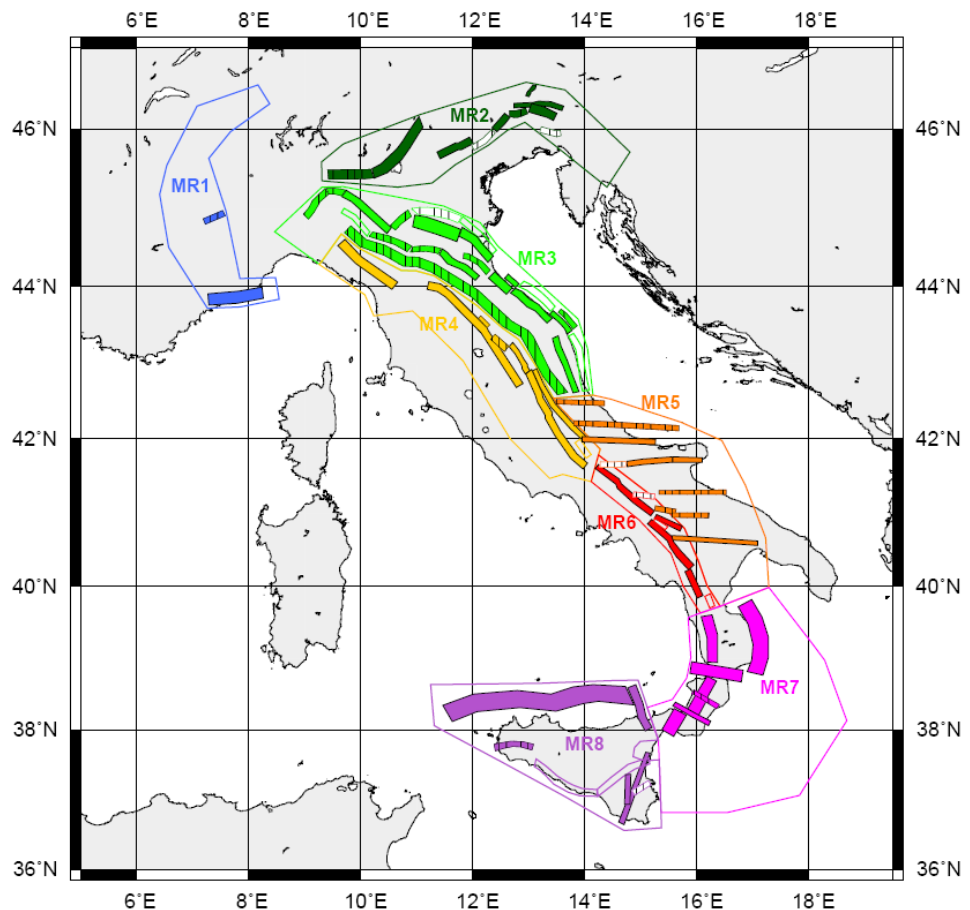


Figura 2a

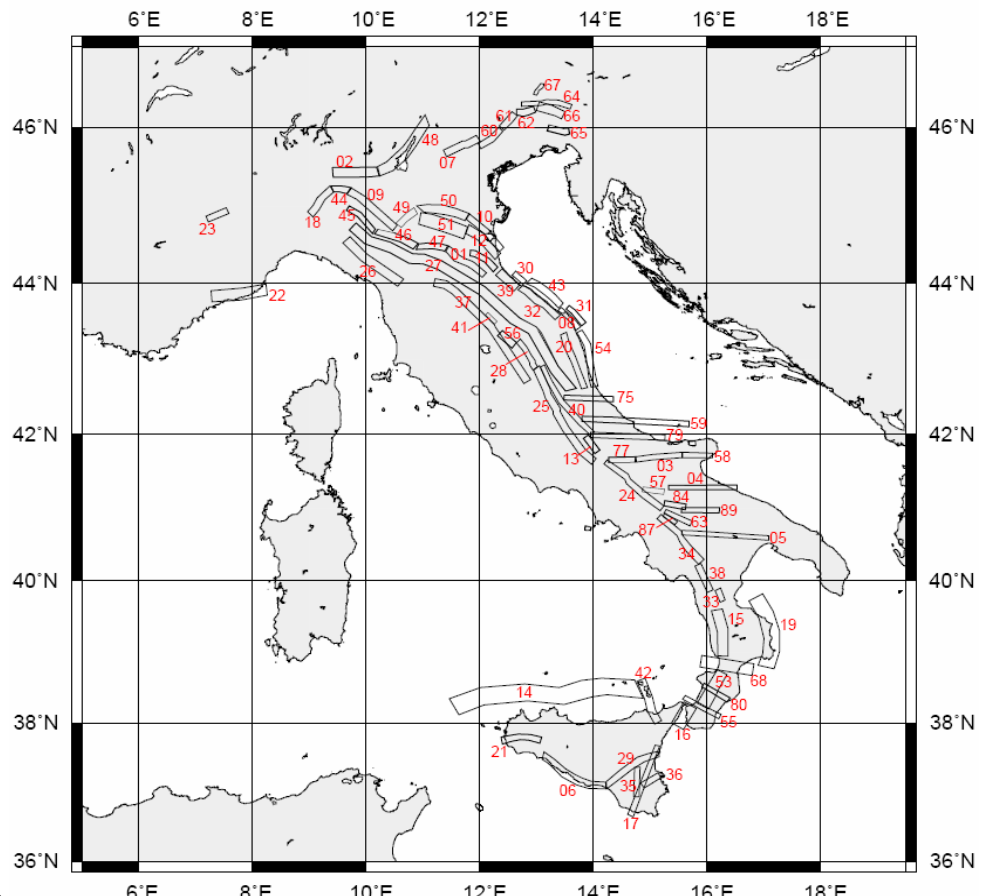


Figura 2b

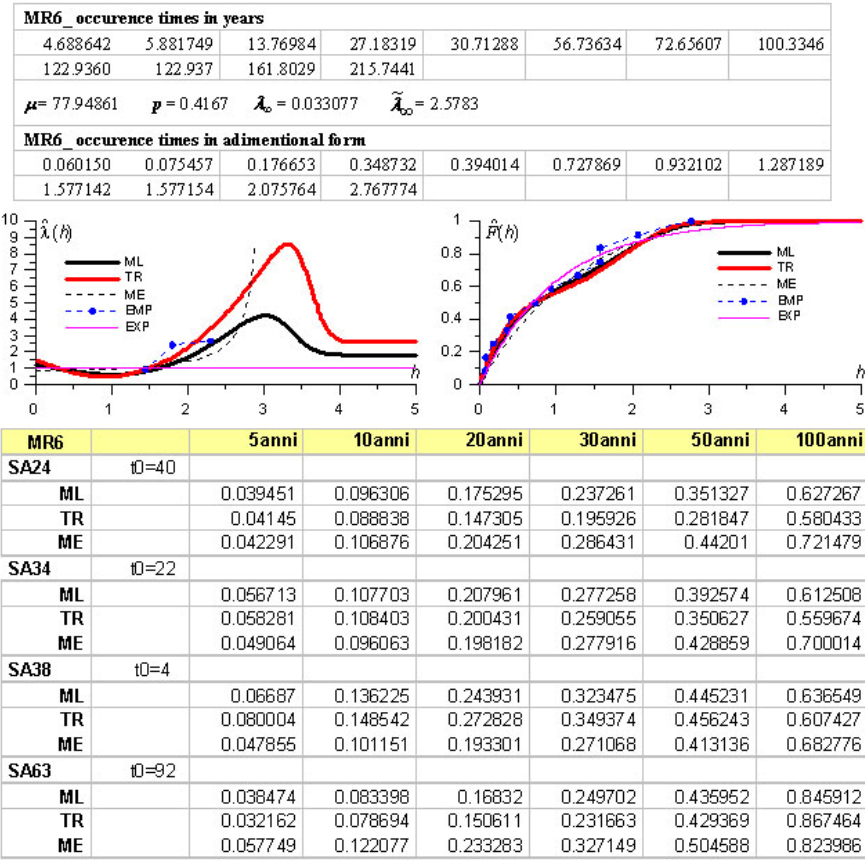


Figura 3 -

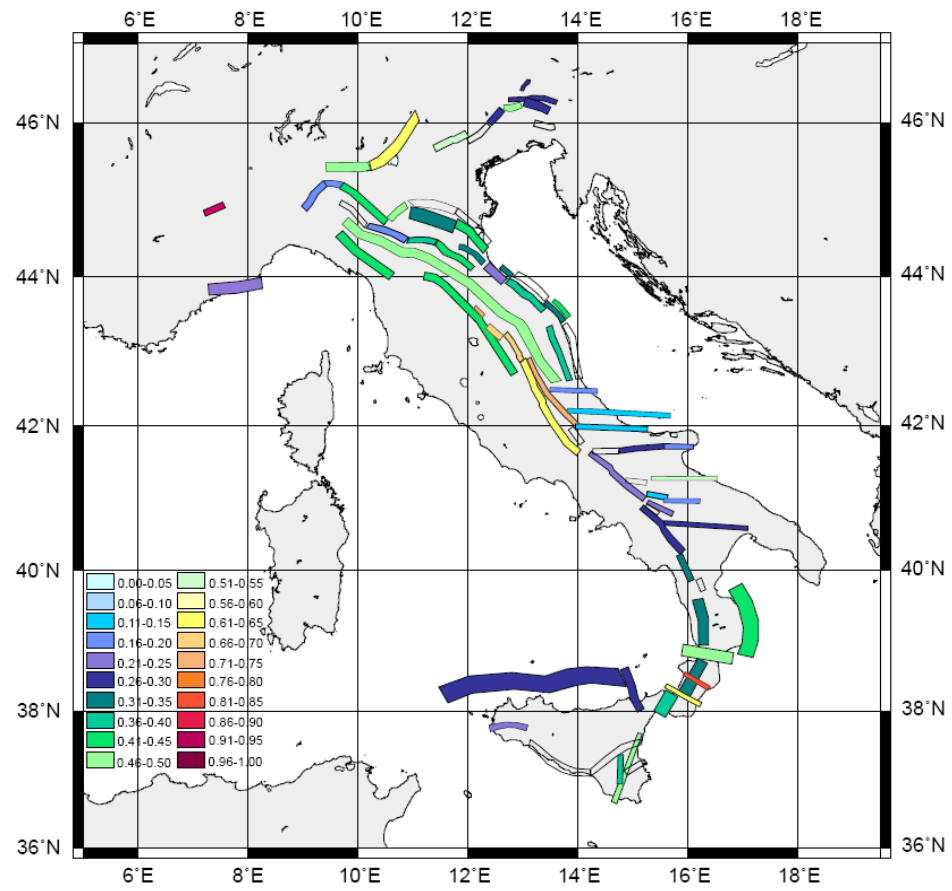


Figura 4 - $\Delta t=30$ anni, ML Method

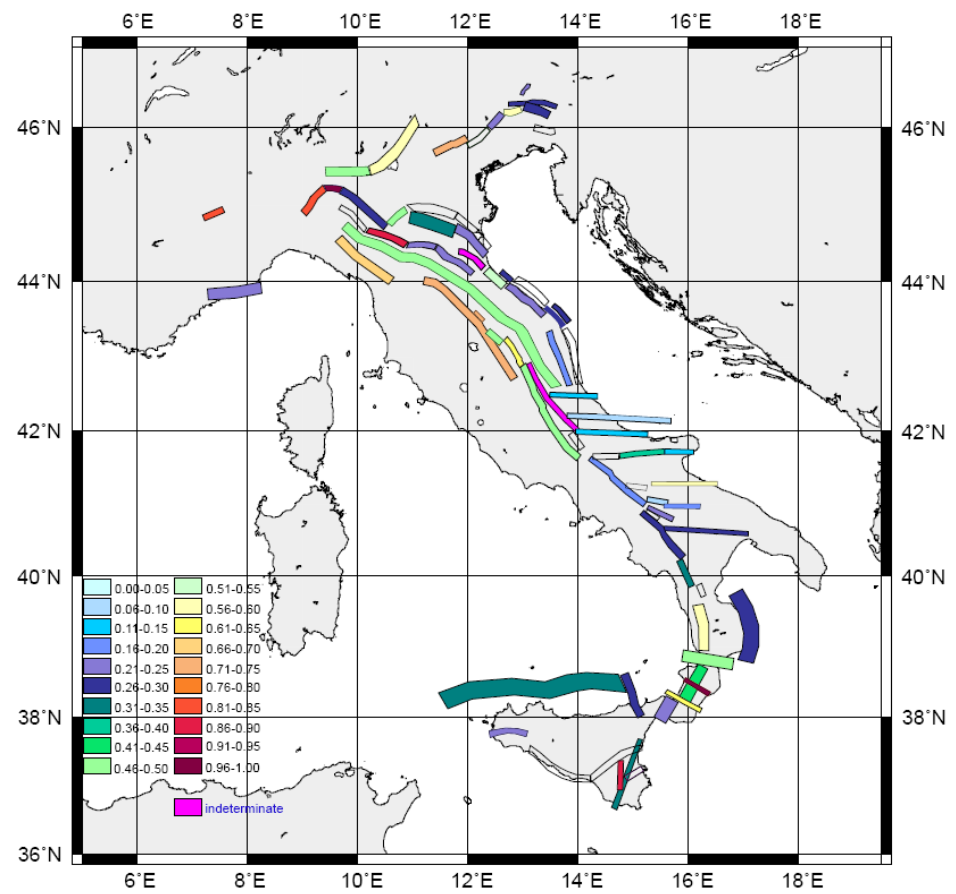


Figura 5 - $\Delta t=30$ anni, TR Method

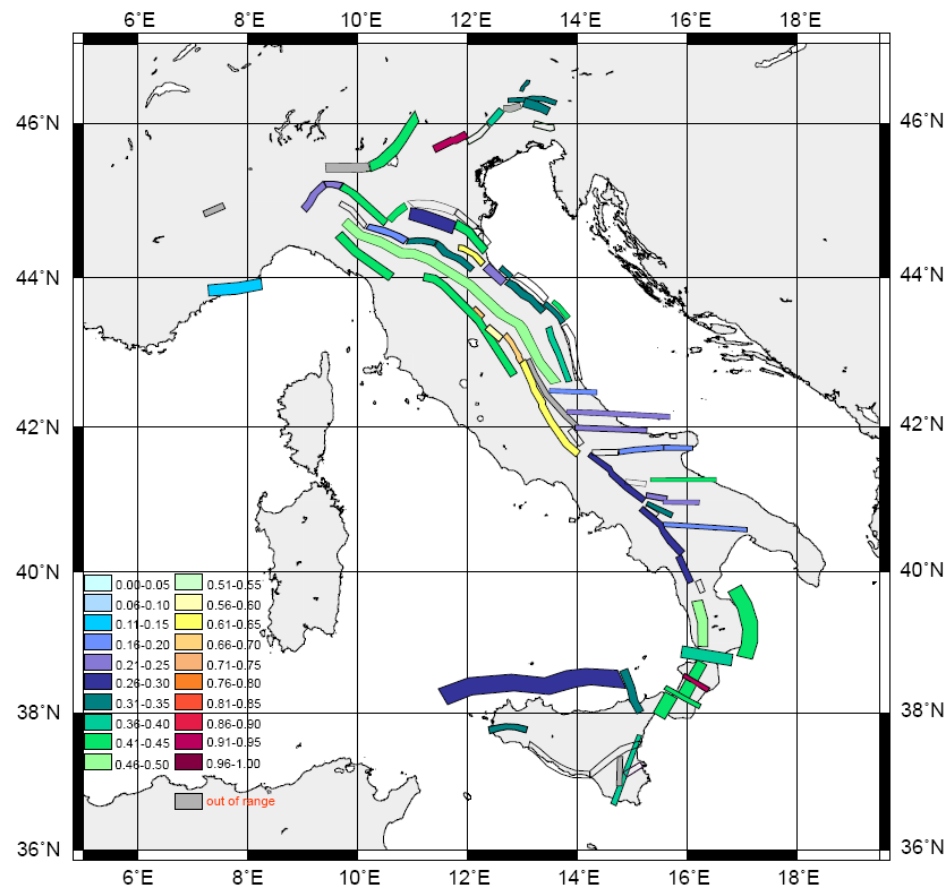


Figura 6 - $\Delta t=30$ anni, ME Method



UR 4.5 - Responsabile Cataldo Godano (Department of Environmental Sciences and CNISM, Second University of Naples, 81100 Caserta)

1 - Abstract, objectives of the project

The main aim of this project was the developing of a new stochastic model of earthquake occurrence which should improve the traditional ETAS one [1] taking into account of magnitude, space a time correlations between successive earthquakes. On the base of this model the occurrence probability of the next earthquake of magnitude m in the next 30 years can be evaluated for Italian region. As result we are able to produce the probability maps of these events.

2 - Scientific background

Since the Omori observation [2], temporal clustering is considered a general and distinct feature of seismic occurrence. Clustering in space has also been well established [3] and, together with the Omori law and the GutenbergRichter law [4], is the main ingredient of probabilistic tools for timedependent seismic hazard evaluation [5]. The distribution $D(\Delta t)$ of the intertime Δt elapsed between two successive events is a suitable quantity to characterize the temporal organization of seismicity. Analogously, the distribution $D(\Delta r)$ of the distance Δr between subsequent epicenters provides useful insights in the spatial organization. Both distributions have been the subject of much interest in the last years [6, 7, 8, 9, 10, 11, 12, 13, 14, 15]. In particular, they exhibit universal behavior essentially independent of the space region and the magnitude range considered [8, 11, 12, 13]. Furthermore, the question of the existence of correlations between magnitudes of subsequent earthquakes has been also recently addressed [14, 15]. Corral [14] has shown that the Southern California Catalog exhibits possible magnitude correlations that are small but different from zero. However, restricting his investigation to earthquakes with Δt greater than 30 minutes, he observes that correlations reduce and become smaller than statistical uncertainty. Magnitude correlations have been, therefore, interpreted as a spurious effect due to short term aftershock incompleteness (STA) [16]. According to this hypothesis, aftershocks, in particular small events, occurring closely after large shocks are not reported in the experimental catalog. This interpretation agrees with the standard approach that assumes independence of earthquake magnitudes: an earthquake "does not know how large it will become". This has strong implications on the still open question of earthquake predictability. On the other hand, a recent analysis of the Southern California Catalog [15] has shown the existence of nonzero magnitude correlations, not to be attributed to STA. These are observed by means of an averaging procedure that reduces statistical fluctuations.

3 - Results of UR 4.5

A dynamical scaling hypothesis relating magnitude to time differences has been proposed to explain the observed magnitude correlations. A better description of real seismicity can be obtained if correlations between time, space and magnitude are properly taken into account. As in dynamical critical phenomena where energy and time fix a characteristic length scale, similar ideas can be used to introduce magnitude correlations within standard trigger models for seismicity. In trigger models [17], the probability to have the next earthquake in

the time window $[t; t + \delta t]$, with epicenter in the region $[\vec{r}; \vec{r} + \delta \vec{r}]$ and magnitude in

the range $[m; m + \delta m]$ is given by the superposition

$$P(t; \vec{r}; m) = \sum_j P(t - t_j, |\vec{r} - \vec{r}_j|, m, m_j) \quad (1)$$

where $P(t - t_j, |\vec{r} - \vec{r}_j|, m, m_j)$ is the probability conditioned to the occurrence of an earthquake of magnitude m_j , at time $t_j < t$, in the position \vec{r}_j . In the widely accepted ETAS model [1] $t - t_j, |\vec{r} - \vec{r}_j|, m$ and m_j are all independent quantities and empirical laws are used to characterize their distributions. Hence, by construction, the ETAS model does not take into account magnitude correlations and their dependence on time and space. In order to reproduce the experimental findings, we introduce $\tau_{ij} = k_t 10^{b(m_i - m_j)}$ and $r_{ij}^z = k_r |\vec{r}_i - \vec{r}_j|^z$ which fix two characteristic time scales $\Delta t_{ij} = t_i - t_j$ leading to the scaling behaviour with

$$P(\Delta t_{ij}, |\vec{r}_i - \vec{r}_j|, m_i, m_j) = \Delta t_{ij}^{2/z} H\left(\frac{\tau_{ij}}{\Delta t_{ij}}, \frac{r_{ij}}{\Delta t_{ij}^{1/z}}\right) \quad (2)$$

The exponent $2/z$ is determined by imposing the condition

$$\int d\vec{r}_i P(\Delta t_{ij}, |\vec{r}_i - \vec{r}_j|, m_i, m_j) = H_1\left(\frac{\tau_{ij}}{\Delta t_{ij}}\right) \quad (3)$$

where the function $H_1(x)$ must satisfy the normalization condition

$$\int dx H_1(x) = 1 \quad (4)$$

In order to simplify the numerical procedure, we consider a special case of Eq.(2)

$$H\left(\frac{\tau_{ij}}{\Delta t_{ij}}, \frac{r_{ij}}{\Delta t_{ij}^{1/z}}\right) = H_1\left(\frac{\tau_{ij}}{\Delta t_{ij}}\right) H_2\left(\frac{r_{ij}}{\Delta t_{ij}^{1/z}}\right) \quad (5)$$

4 - Description of the deliverables: Evaluation of the probability maps

In the numerical code we used for H_1 and H_2

$$H_1(x) = \frac{1}{e^x - 1 + \gamma_1} \quad (6)$$

and

$$H_2(x) = \frac{1}{x^\mu + \gamma_2} \quad (7)$$

For the evaluation procedure, we divided the Italian region in 40x40 cells and calculate, in each cell and for each time interval, the occurrence probability of an earthquake for a magnitude m_i based on all the earthquakes recorded in the Italian catalog (CSI) from January 1981 to December 2002 using as a completeness threshold of magnitude 2.5. Then the probability has been integrated over a period of 30 years after the occurrence of the last event in the catalogue. The results are reported in figure 1 and 2 for a magnitude 3 and 4. The probability values are showed in a log scale in order to don't saturate the color scale rapidly. Probability maps for higher values of the magnitude are not reported because for $m > 4$ the occurrence probability is very close to zero due to the absence of earthquakes with magnitudes greater than 5.8 in the used catalogue. This implies that for these seismic events the dominating term in the occurrence probability is Poissonian. As a consequence we should evaluate this parameter as a function of space. This requires the evaluation of a likelihood function which shall be matter of our future work.

References

- Y. Ogata, *J. Amer. Stat. Assoc.* 83, 9, (1988).
- F. Omori, *J. Coll. Sci. Imp. Univ. Tokyo* 7, 111, (1894).
- Y.Y. Kagan, L. Knopoff, *Geophys. J. Roy. Astron. Soc.* 62, 303 (1980).
- B. Gutenberg, C.F. Richter, *Bull. Seism. Soc. Am.* 34, 185, (1944).
- M.C. Gerstenberger, S. Wiemer, L.M. Jones, P.A. Reasenberg, *Nature* 435, 328, (2005).
- P. Bak, K. Christensen, L. Danon, T. Scanlon, *Phys. Rev. Lett.* 88, 178501, (2002).
- M.S. Mega et al., *Phys. Rev. Lett.* 90, 188501 (2003).
- A. Corral, *Phys. Rev. Lett.* 92, 108501 (2004).
- V. N. Livina, S. Havlin, A. Bunde *Phys. Rev. Lett.* 95, 208501 (2005).
- E. Lippiello, C. Godano, L. de Arcangelis, *Europhys. Lett.* 72, 678 (2005).
- A. Saichev, D. Sornette, *Phys. Rev. Lett.* 97, 078501 (2006).
- J. Davidsen, M. Paczuski, *Phys. Rev. Lett.* 94, 048501 (2005).
- A. Corral, *Phys. Rev. Lett.* 97, 178501 (2006).
- A. Corral, *Phys. Rev. Lett.* 95, 028501 (2005).
- E. Lippiello, C. Godano, L. de Arcangelis, *Phys. Rev. Lett.* 97, 178501 (2007).
- Y.Y. Kagan, *Bull. Seism. Soc. Amer.*, 94(4), 1207 (2004).
- J. F. D. VereJones, *J. Roy. Statist. Soc.*, B32, 1, (1970).



U.R. 4.6 - Coordinator: Enzo Mantovani (Dip. Scienze della Terra Univ. di Siena)
Research team: Albarello Dario, Babbucci Daniele, Mini Silvia and Viti Marcello

Final report

Basic concepts of the adopted approach.

To achieve the main objective of this project, one must take into account a basic feature of seismic history recognized in several seismic zones of Italy, that is the clearly discontinuous time pattern of seismicity, characterized by short periods of intense activity and long periods of quiescence or minor activity. This implies that seismic hazard in such zones is higher than average for short time intervals and lower than average for most of the time. This discontinuous pattern may result from the fact that the probability of major earthquakes in such zones is strongly influenced by the occurrence of particular seismotectonic conditions in the surrounding regions, whose occurrence determines the temporary increase of seismic hazard.

The results of previous studies about this problem (e.g., Anderson, 1975; Rydelek and Sacks, 1990, 2003; Mantovani and Albarello, 1997; Pollitz et alii, 1998; Mantovani et al., 2001; Viti et al., 2003) suggest that such conditions are generally represented by the occurrence of major decoupling earthquakes in key tectonic belts, whose activation induces acceleration of deformation in the connected seismic zones. The fact that the effects of such acceleration occur with a time delay of months to several years from the triggering earthquake is due to the relatively slow migration of the post-seismic strain perturbation, which is controlled by the structural/rheological properties of the crust-upper mantle system in the region involved.

The results obtained in this research suggest that the approach described above may provide an efficient tool for estimating the time pattern of seismic hazard in some zones of the Apennines belt.

Main results obtained

The main information acquired during this Project can be synthesized as follows:

- 1)** Definition of the ongoing tectonic processes in the Central Mediterranean region, Italy in particular, responsible for seismic activity.
- 2)** Recognition of the tectonic mechanisms that are supposed to underlie the seismic interrelations observed in the study area.
- 3)** Information on the effects of post-seismic relaxation processes in the study area and comparison of such effects with the main features of the observed seismic interrelations.
- 4)** Definition of the possible outcomes of the results obtained for Civil Defense in Italy.

Description of the results

1) Definition of the ongoing tectonic processes in the Central Mediterranean region

Starting from the results obtained in previous investigations (Mantovani, 2005; Mantovani et al., 2006 and cited references), new important insights have been gained into the present tectonic setting of the Apennines belt and the related geodynamic context, fully described by Viti et al. (2006).

To achieve such result, it has been first necessary reconstructing the Neogene evolutionary history and geodynamic context of the entire Mediterranean region. This reconstruction has been achieved by the definition of the constraints implied by geological, geophysical and volcanological evidence in the study area and then by a systematic search of the geodynamic model and evolutionary history which can plausibly

and coherently explain the above constraints. This investigation must be continuously updated as new and new data are reported in the relevant literature. A detailed description of the arguments and evidence that support the proposed evolutionary reconstruction and geodynamic setting is described in a number of works (e.g., Mantovani, 2005; Mantovani et al., 2006; Viti et al., 2006). In order to provide information on the Mediterranean geodynamics not only limited to the interpretation we propose, a critical analysis of our and the other geodynamic models so far proposed, analysing the consistency of their implications with the observed deformation pattern, has been distributed to all researchers possibly interested in this problem (as background information for the meeting on Mediterranean geodynamics held in Siena in February 2006).

Using the constraints implied by the recent/present deformation (inferred from neotectonic data, seismic surveys and seismological evidence) and considering the need of satisfying the continuity between the present geodynamic setting and the one recognized in the Pliocene-Quaternary evolution, we propose a well defined hypothesis (Fig.1) on the ongoing tectonic setting that can be adopted as responsible for seismic activity (Viti et al., 2006).

The proposed model provides that major deformation in the axial part of the Apennines (where most seismic zones are located) and the associated seismic activity is a consequence of the progressive separation between the external and internal sectors of the belt. This divergence is due to the fact that the external belt is dragged by the Adriatic plate (stressed by the motion of the confining plates), whereas the internal belt is characterized by very low mobility, being now connected with the Tyrrhenian domain (Fig.1).

The implications of the proposed interpretation, in terms of velocity and strain fields have been quantified by numerical modelling, carried out by the finite element analysis of deformation of an elastic thin sheet with kinematic boundary conditions in the plane stress approximation. Details on the methodological approach adopted are given by Mantovani et al. (2001), Viti et al. (2004) and Mantovani et al. (2007). The preferred solution and the boundary conditions adopted are shown in Fig.2. The choice of this solution has been made on the basis of the agreement between the computed and observed strain fields. The last one has been inferred from neotectonic and seismological evidence.

The model described above has then been used to compute the amplitude and strain regime in the Italian seismic zones (DISS) identified in the framework of this project (Fig. 3).

2) Recognition of the tectonic mechanisms underlying the seismic interrelations observed in the study area.

In previous works (Mantovani and Albarello, 1997; Viti et al., 2003, 2004, 2006 and references) we have pointed out possible regularity patterns of seismicity in the Southern and Northern Apennines. The main features of such patterns can be synthesized as follows:

-In the last two centuries major earthquakes in the Southern Apennines have been always preceded by intense seismicity in the zone lying on the eastern side of the Adriatic plate, the Albania-Montenegro zone.

- The most intense historical earthquake (Avezzano, 1915 M=6.9) ever recorded in the central part of the Latium-Abruzzi platform (Central Apennines), has been followed by an exceptional concentration of major shocks (M>5.5) throughout the Northern Apennines.

During the present Project, we have tried to improve our knowledge of the tectonic mechanisms that may be responsible for the observed seismic correlations.

Southern Apennines

This correlation might be connected with the fact that strong earthquakes in the Southern Dinarides favour a decoupling of the Adriatic plate from the Balkan structures, allowing a temporary acceleration of the Adriatic plate (induced by the present boundary conditions in the Central Mediterranean region). In the framework of the kinematic scheme shown in Fig.1, the acceleration the Adriatic favours the separation between the external part of the Apennines belt with respect to the internal one, thus increasing the probability of seismic dislocation at the normal faults recognized in the Southern Apennines active zones (the sector of the belt nearest to the strong Montenegro-Albania decoupling earthquakes). Other information about the tectonic setting and the proposed interpretation are given by Mantovani et al. (1997) and Mantovani and Albarello (1997).

Northern Apennines

The dependence of Northern Apennines seismicity from strong shocks in the Central Apennines might be connected with the fact that major seismic events in the second zone favours the decoupling between the eastern part of the Latium-Abruzzi platform (ELA) from the western part. The consequent temporary acceleration of the eastern ELA, that is triggered by such decoupling events, increases stresses and strains in the Northern Apennines, with the mechanism schematically shown in Fig.4.

The evidence and arguments (even quantitative) that support the above mechanism are given by Viti et al. (2004). The proposed tectonic interpretation might explain why in the period 1915-1920, just following the strong 1915 Avezzano event, most of the Northern Apennines seismic zones have been activated by intense shocks ($M>5.5$), as shown in Fig.5.

Important evidence in support to the proposed interpretation are provided by the results of seismic surveys (CROP Project, Finetti et al., 2005) in the Northern Apennines (Fig.6). In particular, the cross section reported in this figure helps to delineate the main features of the crustal wedge that is undergoing lateral extrusion in response to the driving mechanism implied by the proposed model (Figs.1 and 4). This wedge is confined to the shallow part of the crust lying above the thick layer of Triassic evaporites where the main decoupling normal faults are rooted and strong earthquake nucleates. The figure also evidences the lateral shift of old thrust faults (by younger normal faults), which allows estimating the average migration rate (few mm/y) of the extruding wedge since the Pliocene (Cenni et al., submitted).

3) Information on the effects of post-seismic relaxation processes in the central Mediterranean region and comparison of such effects with the main features of the observed seismic correlations

Southern Apennines

The results of numerical simulation of postseismic relaxation, carried out with an elasto-viscous thin sheet model (Viti et al., 2003), indicate that in the Southern Apennines the time pattern of the strain rate induced by Dinaric strong earthquakes is characterized by a peak of amplitude that occurs at 1-2 years after the triggering shock (modelled with the parameters of the 1979 Montenegro earthquake). This result provides significant support to the proposed interpretation since it may explain why major earthquakes in the

southern Apennines have fairly regularly occurred with a time delay of 1-3 years from the ones in the Albania-Montenegro zone. Other experiments, carried out during this project have allowed to gain insights into the dependence of post-seismic relaxation on the features of the seismic source in the Dinaric zones, the rheological properties of the Adriatic structure and the lateral heterogeneity of the crust-mantle system in the Adriatic-Apennines region. In particular, these experiments indicate that the presence of a lithospheric root under the Apennines (possible remnant of the old subduction process under that zone) may produce a slower propagation of seismic relaxation effects induced by Dinaric events.

Northern Apennines

The main results of numerical experiments (Fig.7) show that in the Northern Apennines the time pattern of the strain rate induced by strong earthquakes in the Central Apennines is characterized by a peak of amplitude that occurs with delays of 1 to 5 years (depending on the position of seismic zones along the Northern Apennine arc, from the Tiber Valley to the Garfagnana troughs) from the triggering event (modelled with the parameters of the 1915 Avezzano earthquake).

General remarks

Numerical modelling has allowed estimating the main features of the velocity field expected in the Southern and Northern Apennines as an effect of post-seismic relaxation. The velocity values indicated by such investigation, which can reach up to several tens of mm/y, clearly indicate that the presence of transient effects can be revealed by permanent geodetic monitoring, being such observation characterized by a resolution of the order of few mm/y.

The possibility of recognizing eventual future anomalous values of velocity and strain rate in the zones mentioned above is considerably favoured by the results of geodetic monitoring which have been carried out in those regions during the last years. For instance, the velocity field evaluated in the Northern Apennines in the last 4 years (Fig.8) is characterized by average velocities of few mm/y, which are clearly lower than the ones expected from post-seismic relaxation of strong earthquakes. In the above velocity field it may be interesting to note that velocities in the external part of the belt (2-3 mm/y) are systematically higher than the ones measured in the internal part (almost null). This result, if confirmed by further measurements, could indicate that the long term behaviour that our interpretation (Fig.1) predicts for the Apennines belt also develops in the periods of minor deformation, that is far from major decoupling earthquakes in the Dinaric and Central Apennines zones.

4) Possible outcomes for Civil Defence in Italy

1) The results obtained during this project indicate that for some seismic zones of Italy, in particular the Southern and Northern Apennines, it may be possible recognizing the conditions that precede the periods of increased seismic hazard. This possibility derives from the fact that deformation (and the associated seismic activity) accelerates in the above zones in response to strong decoupling earthquakes in other seismic belts, respectively located in the Southern Dinarides and Central Apennines. The arguments and evidence in support of such interpretation are explained in detail in several works (see the list of references and cited papers).

2) The study of post-seismic relaxation indicates that the most favourable conditions for

the occurrence of induced earthquakes in the Southern and Northern Apennines will occur with delays comprised from some months to some years after the triggering decoupling events. This implies that Civil Protection would have significant times to organize eventual initiatives for mitigating the effects of future strong earthquakes in the above zones.

3) The supposed interconnection between seismic sources is based on a well known physical phenomenon (post-seismic relaxation by stress diffusion in the lithosphere), whose development in the zones considered can be both predicted by numerical modelling (based on realistic earthquake source geometry and structural/rheological parameterization) and even monitored by geodetic measurements or studies of the time pattern of minor seismicity or other geophysical observations.

The eventual prosecution of the research carried out in this project could allow to improve our understanding of the proposed precursory patterns, by a deeper knowledge of the tectonic setting in the Italian region, the tectonic connection between seismic zones and the dependence of post-seismic relaxation on the structural/rheological features of the crust-mantle system in the Adriatic-apennines region. Furthermore, the results of some preliminary investigations encourage to think that the possibility of recognizing the periods of highest seismic hazard could be extended to other Italian zones.

References

- Anderson D.L., 1975. Accelerated plate tectonics. *Science*, 167, 1077-1079.
- Cenni N., Viti M., Baldi P., Mantovani E., Ferrini M., D'Intinoante V., Babbucci D., Albarello D. Short-term (geodetic) and long-term (geological) velocity fields in the Northern Apennines. Submitted to *Bollettino della Società Geologica Italiana*.
- Finetti I.R. (Ed), 2005. Deep Seismic Exploration of the Central Mediterranean and Italy, CROP PROJECT. Elsevier, Amsterdam, 794 pp.
- Finetti I.R., Boccaletti M., Bonini M., Del Ben A., Pipan M, Prizzon A., Sani F., 2005. Lithospheric Tectono-Stratigraphic setting of the Ligurian Sea-Northern Apennines-Adriatic Foreland from integrated CROP seismic data. In: Finetti I.R. (ed) Deep Seismic Exploration of the Central Mediterranean and Italy, CROP PROJECT, Elsevier, 20, 119-158.
- Gruppo di lavoro CPTI, 2004. Catalogo parametrico dei terremoti italiani. Edit. Compositori, Bologna, Italy, pp.92.
- Mantovani E., 2005. Evolutionary reconstruction of the Mediterranean region: extrusion tectonics driven by plate convergence. In: Finetti I.R. (ed) Deep seismic exploration of the Mediterranean region. CROP PROJECT, Elsevier, 32, 705-746.
- Mantovani E., Albarello D., 1997. Medium-term precursors of strong earthquakes in southern Italy. *Phys.Earth Planet.Int.*, 101, 49-60.
- Mantovani E., Albarello D., Tamburelli C., Babbucci D., Viti M., 1997. Plate convergence, crustal delamination, extrusion tectonics and minimization of shortening work as main controlling factors of the recent Mediterranean deformation pattern. *Annals of Geophysics*, 40, 611-643.
- Mantovani E., Cenni N., Albarello D., Viti M., Babbucci D., Tamburelli C., D'Onza F., 2001. Numerical simulation of the observed strain field in the central-eastern Mediterranean region. *J. Geodyn.*, 31, 519-556.
- Mantovani E., Albarello D., Babbucci D., Tamburelli C., Viti M., 2002. Trench-Arc-BackArc systems in the Mediterranean area: examples of extrusion tectonics. *J. Virtual Explorer*, 8, 125-141.
- Mantovani E., Viti M., Babbucci D., Tamburelli C., Albarello D., 2006. Geodynamic correlation between the indentation of Arabia and the Neogene tectonics of the central-eastern Mediterranean region, Post-collisional tectonics and magmatism in the eastern Mediterranean region. In: Dilek Y., Pavlides S. (eds) *Geol. Soc. of Am. Special Paper*, 409, 15-41.
- Mantovani E., Viti M., Babbucci D., Albarello D., Tamburelli C., Mini S., 2007. Meccanismi di generazione di sistemi arco-fossa-retroarco. Caso della regione mediterranea. Dipartimento di Scienze della Terra, Università di Siena, pp.74. Available on request.
- Pollitz F.F., Burgmann R., Romanowicz B., 1998. Viscosity of the oceanic asthenosphere inferred from remote triggering of earthquakes. *Science*, 280, 1245-1249.

Rydelek P.A., Sacks I.S., 1990. Asthenospheric viscosity and stress diffusion: a mechanism to explain correlated earthquakes and surface deformation in NE Japan. *Geophys.J.Int.*, 100, 39-58.

Rydelek P.A., Sacks I.S., 2003. Triggering and inhibition of great Japanese earthquakes: the effect of Nobi 1891 on Tonankai 1944, Nankaido 1946 and Tokai. *Earth Planet.Sc.Lett.*, 206, 289-296.

Serpelloni E., Anzidei M., Baldi P., Casula G., Galvani A., 2005. Crustal velocity and strain rate fields in Italy and surrounding regions: new results from the analysis of permanent and non permanent GPS networks. *Geophys J. Int.*, 161, 861-880.

Viti M., Albarello D., Mantovani E., 2001. Classification of seismic strain estimates in the Mediterranean region from a 'bootstrap' approach. *Geophys. J. Int.*, 146, 399-415.

Viti M., D'Onza F., Mantovani E., Albarello D., Cenni N., 2003. Post-seismic relaxation and earthquake triggering in the southern Adriatic region. *Gephys.J.Int.*, 153, 645-657.

Viti M., De Luca J., Babbucci D., Mantovani E., Albarello D., D'Onza F., 2004. Driving mechanism of tectonic activity in the northern Apennines: quantitative insights from numerical modelling. *Tectonics*, 23, TC4003, doi:10.1029/2004TC 001623.

Viti M., Mantovani E., Babbucci D., Tamburelli C., 2006. Quaternary geodynamics and deformation pattern in the Southern Apennines: implications for seismic activity. *Boll. Soc. Geol. It.*, 125, 273-291.

Wang K., 1995. Coupling of tectonic loading and earthquake fault slips at subduction zones. *Pure Appl.Geophys.*, 145, 537-559.

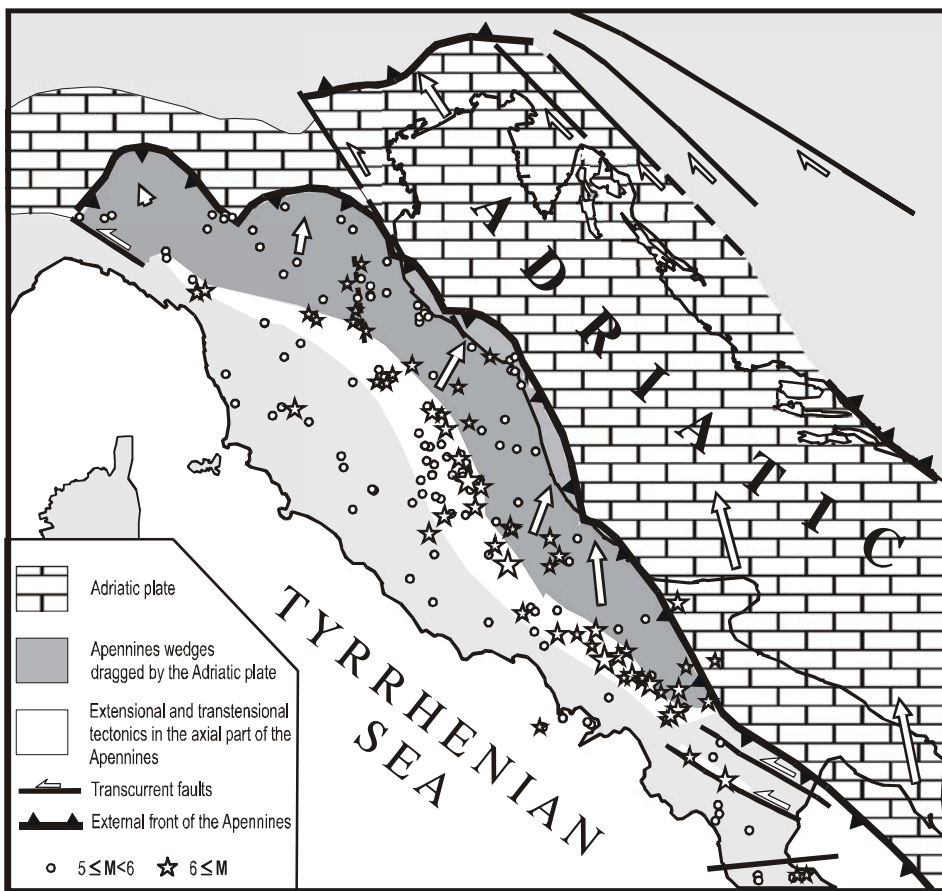


Figure 1 - Tentative reconstruction of the post-middle Pleistocene kinematic pattern (large arrows) in the central Mediterranean region, slightly modified after Viti et al (2006). The external sector of the Apennines belt (dark grey), being dragged by the Adriatic plate, moves faster than the internal Tyrrhenian side of the belt (light grey). The divergence of these two Apennines sectors is accommodated by tensional to transtensional deformation in the axial zone of the belt, associated with most strong earthquakes (stars) and neotectonic activity. Seismicity information is taken from Gruppo di lavoro CPTI (2004), available at <http://emidius.mi.ingv.it/CPTI>.

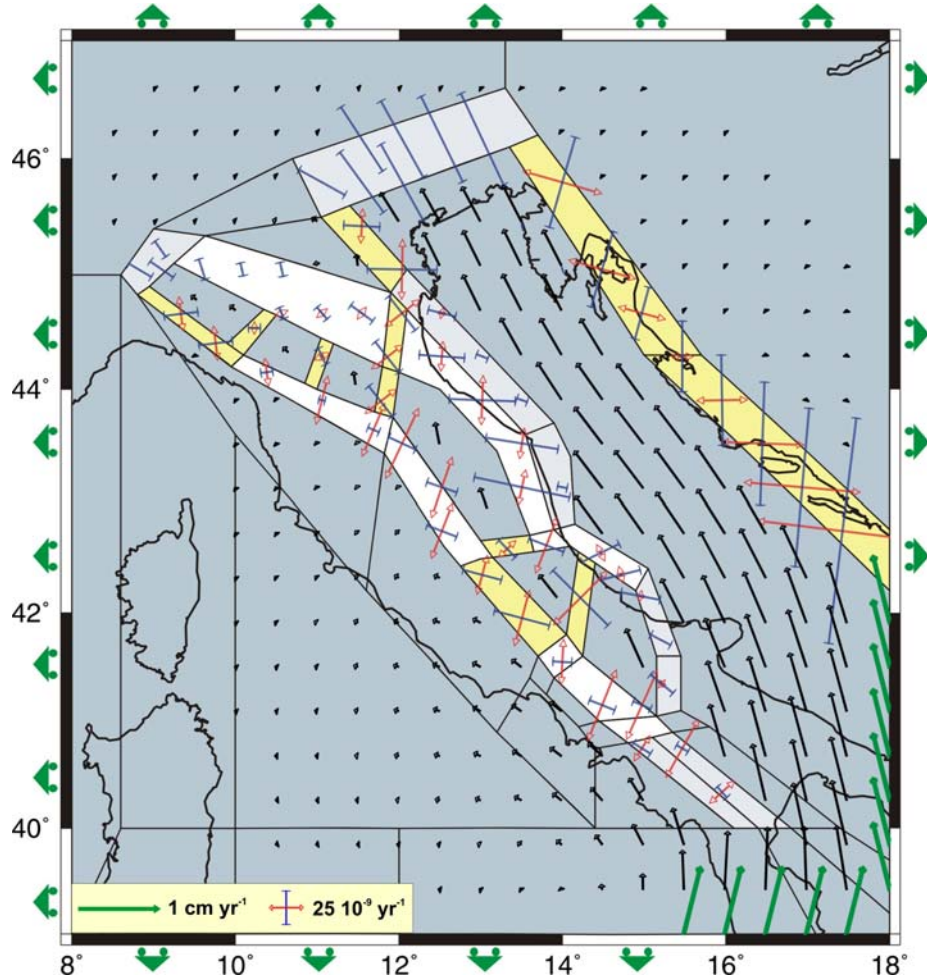


Figure 2 - Finite element modelling of the proposed tectonic interpretation (Fig.1). The mechanical properties of the study area are tentatively reproduced by a mosaic of stiff (blue) and soft (white/light blue and yellow) elastic zones. Soft zones correspond to main tectonically active belts, recognized by neotectonic and seismic evidence. Thrust or extensional belts are white or light blue. Strike-slip fault zones, locally transpressional or transtensional, are yellow. The elastic model is stressed by kinematic boundary conditions (green arrows along the external border), compatible with the convergence of the confining plates (Viti et al., 2006). To avoid clutter in the figure, strain regimes are only reported in the soft zones, and the velocity field only in the stiff domains. The adopted methodology and model parameterization are described by Mantovani et al. (2001) and Viti et al. (2004).

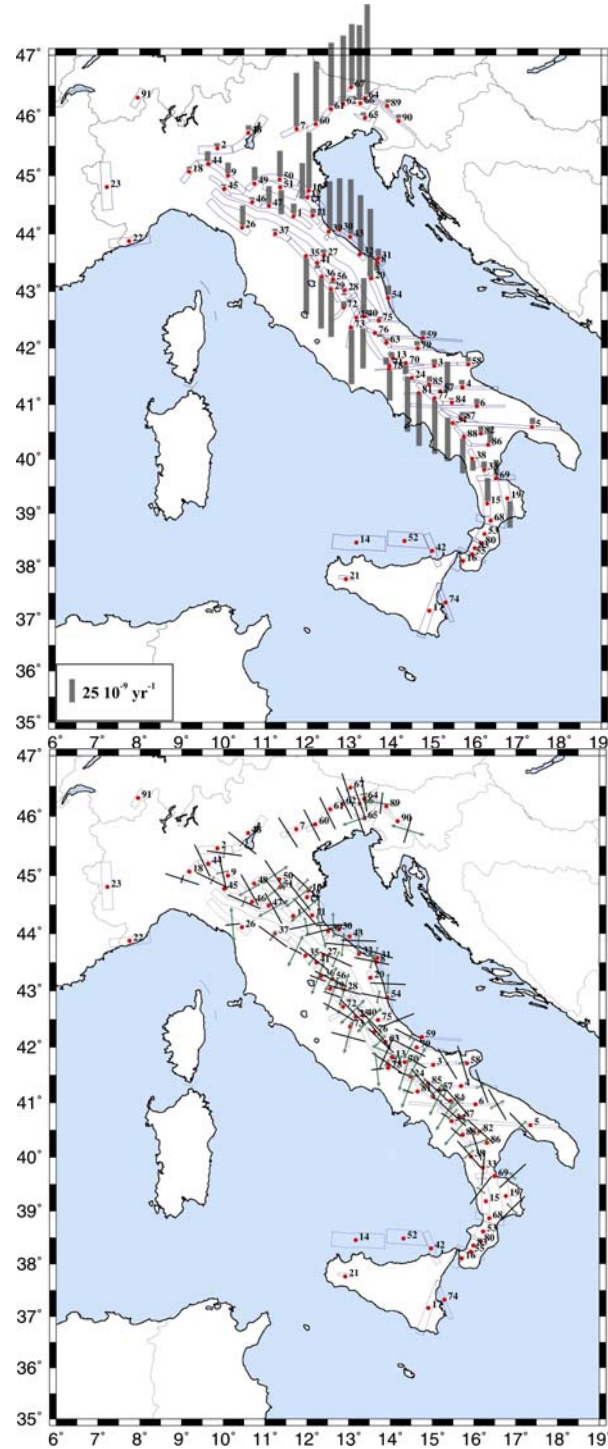


Figure 3 - Amplitude and principal axes of the horizontal strain rate field computed in DISS zones by the finite element model shown in Fig.1. **Left panel:** amplitude of the scalar strain rate (in strain yr^{-1}), as defined by Viti et al. (2001). **Right panel:** Principal strain axes. Shortening and lengthening are indicated by black bars and green diverging arrows, respectively. For each DISS zone, the length of the axes reproduces the ratio of absolute values of the two principal strain rates. Both magnitude and strain regime are computed in the centroid of the zone, identified by the red point with number (DISS catalogue available at <http://www.ingv.it/DISS>).

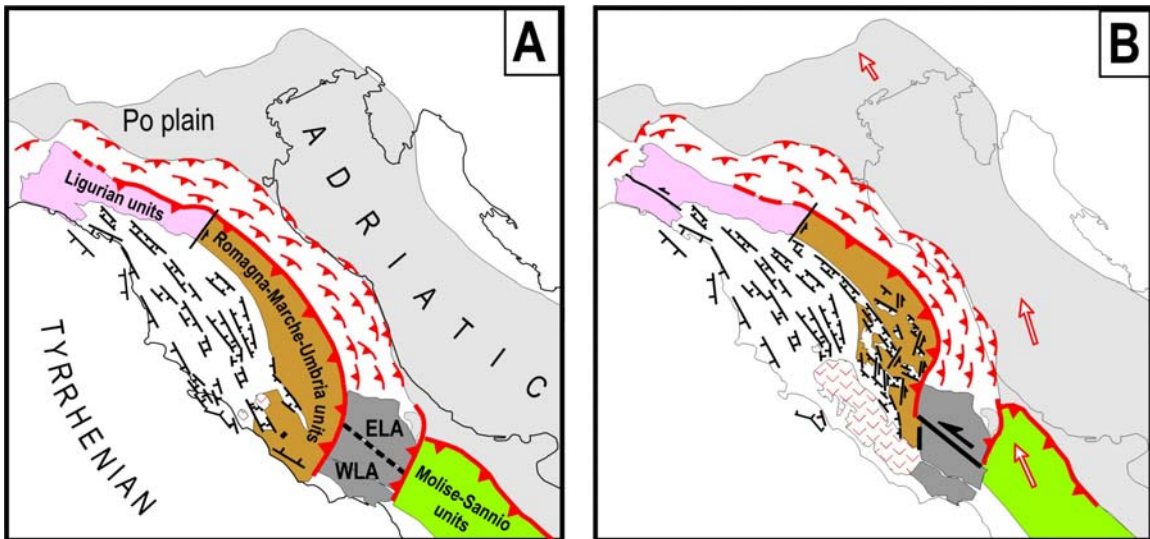


Figure 4 - Tentative reconstruction of the post-middle Pleistocene deformation pattern of the external sector of the Northern Apennines in response to the indentation of the eastern LA platform: A) Lower Pleistocene configuration B) Present tectonic setting. Arrows in the Adriatic plate and the Molise-Sannio units indicate the kinematic boundary conditions which drives the deformation of the Central-Northern Apennines. ELA, WLA = Eastern and Western parts of Latium-Abruzzi platform respectively.

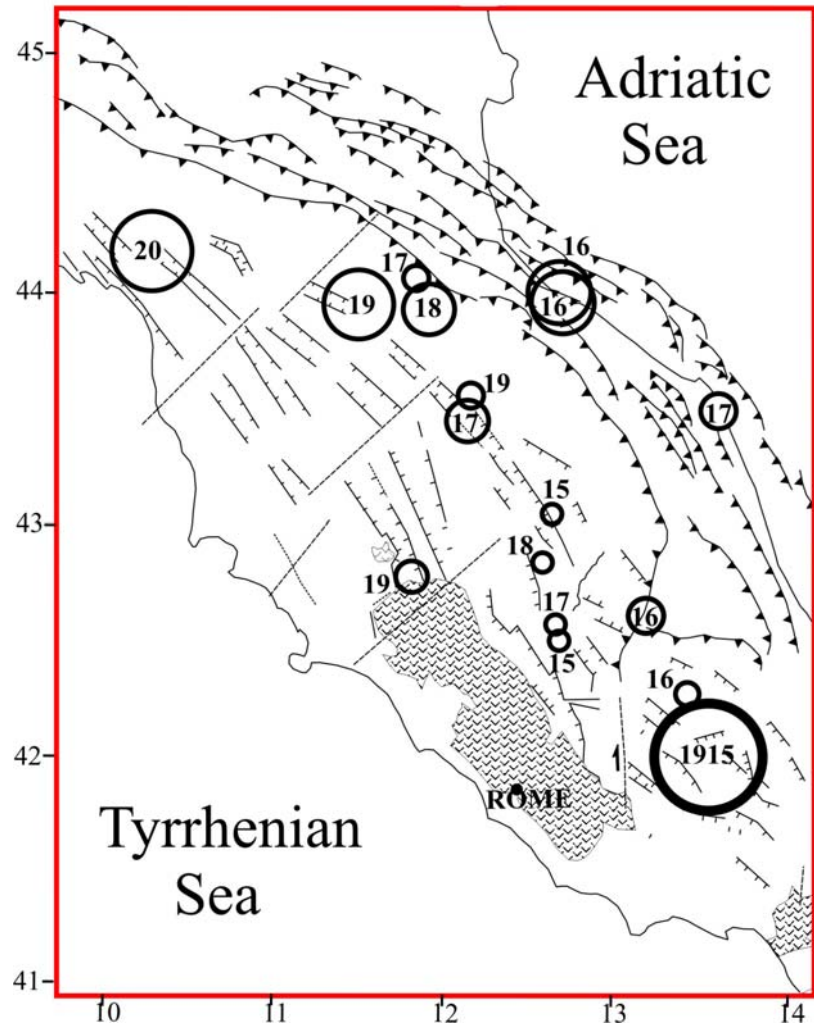


Figure 5 - Distribution of major earthquakes ($M > 4.5$) occurred in the Northern Apennines in the period 1915-1920, following the strong 1915 Avezzano earthquake ($M=6.9$). Data from Gruppo di lavoro CPTI (2004). Numbers inside or close to circles indicate the year of earthquake occurrence (after Viti et al., 2004).

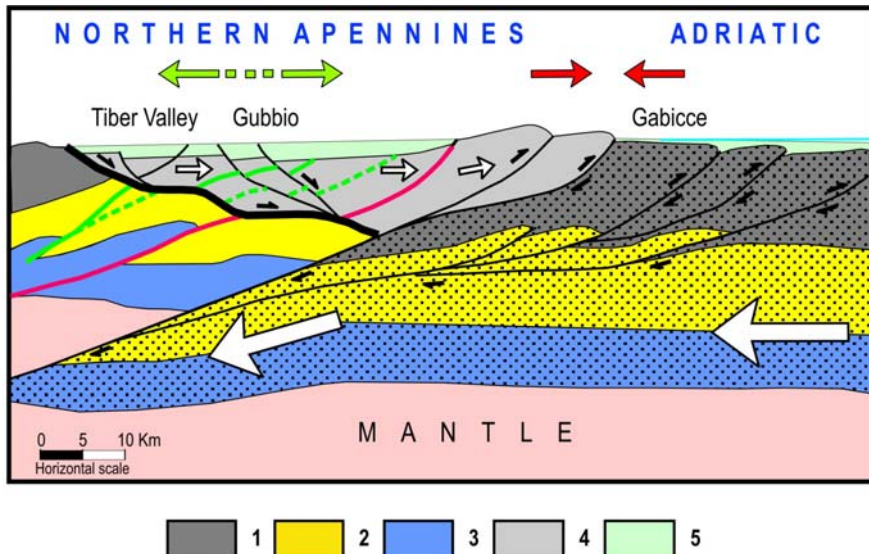


Figure 6 - Particular of the CROP-03 cross section (after Finetti et al., 2005) illustrating the eastward escape of the Tiber upper crustal wedge (light grey). The migration of this wedge (little empty arrows) causes extension (green diverging arrows above the section) at its western margin (where the wedge diverges from the internal zones) and thrustings (converging red arrows above the section) at the eastern front of the wedge, where it collides with the underthrusting Adriatic lithosphere (dotted). Green and pink lines cut by the main Tiber normal fault (thick black line) indicate older thrust faults which have been laterally shifted by the eastward motion of the extruding wedge. 1) Pre-Pliocene sedimentary cover 2) Upper crust 3) Lower crust 4) Tiber crustal wedge 5) Pliocene-Quaternary filling of the Tiber and Gubbio basins and Adriatic foredeep.

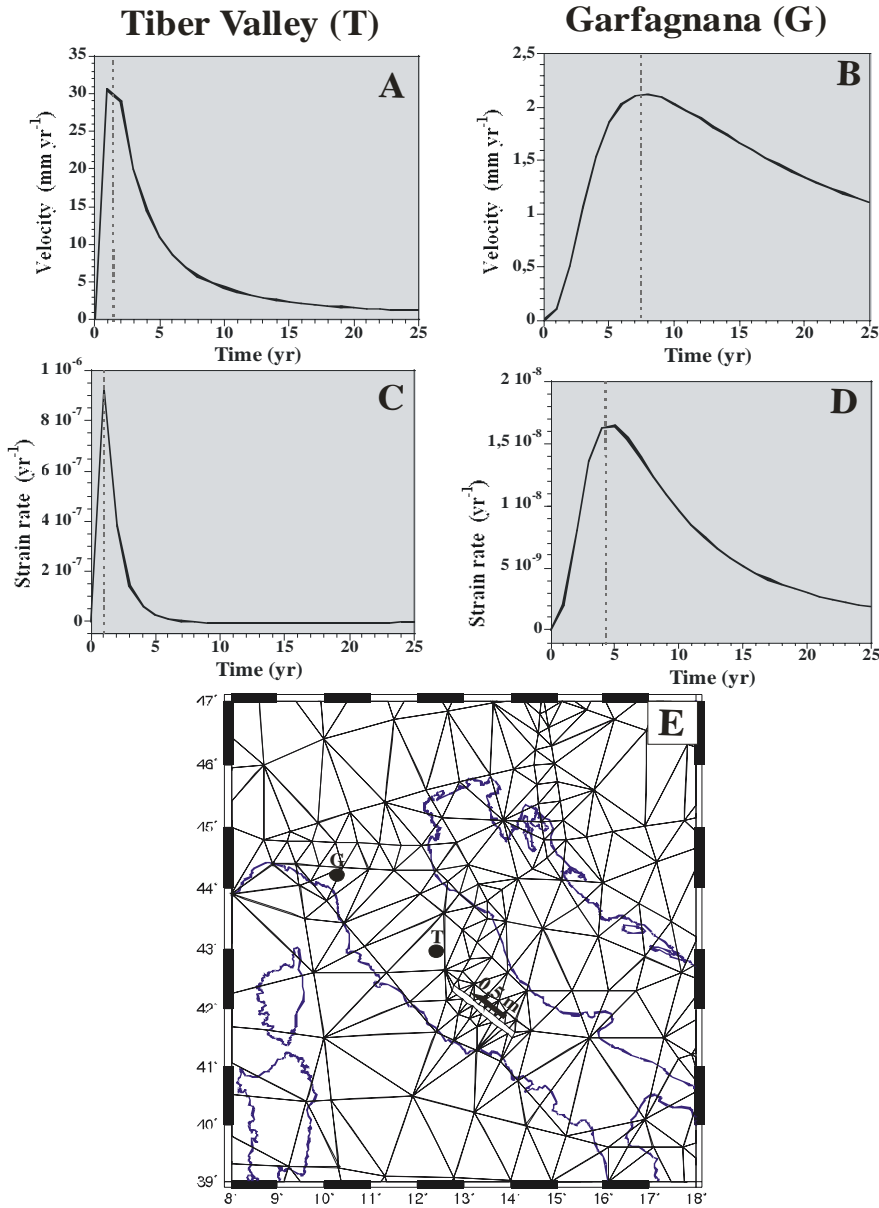


Figure 7 - Quantification of post-seismic relaxation effects in the Northern Apennines, induced by a seismic dislocation in the Central Apennines compatible with that determined by the 1915 Avezzano earthquake. After Cenni et al. (submitted). Numerical simulation of post seismic relaxation in a elastic-viscous model has been carried out following the procedure described by Viti et al. (2003). See text for more details. Velocity (a) and strain rate (c) time patterns in a site located in the Tiber Valley (T in (e), 42.9°N, 12.5°E). Velocity (b) and strain rate (d) time patterns in a site located in the Garfagnana zone (G in (e), 44.2°N, 10.3°E). Dashed vertical lines identify peaks in time patterns (see text for interpretation). e) Finite element grid adopted in experiments. The thin elongated box in the Central Apennines indicates the modelled fault zone (length $L = 120$ km), whose northeastern side is displaced by 0.5 m with respect to the southeastern one. A diffusivity value $D = 150 \text{ m}^2\text{s}^{-1}$ is adopted for the whole elastic-viscous sheet shown in (c). This last parameter, which actually controls the time evolution of strain diffusion, is related to the structural and mechanical properties of the elastic-viscous model here adopted: $D = HhE/\eta$, where H and E are thickness and Young modulus of the upper elastic layer, h and η are thickness and viscosity of the lower viscous layer (e.g., Wang, 1995; Viti et al., 2003).

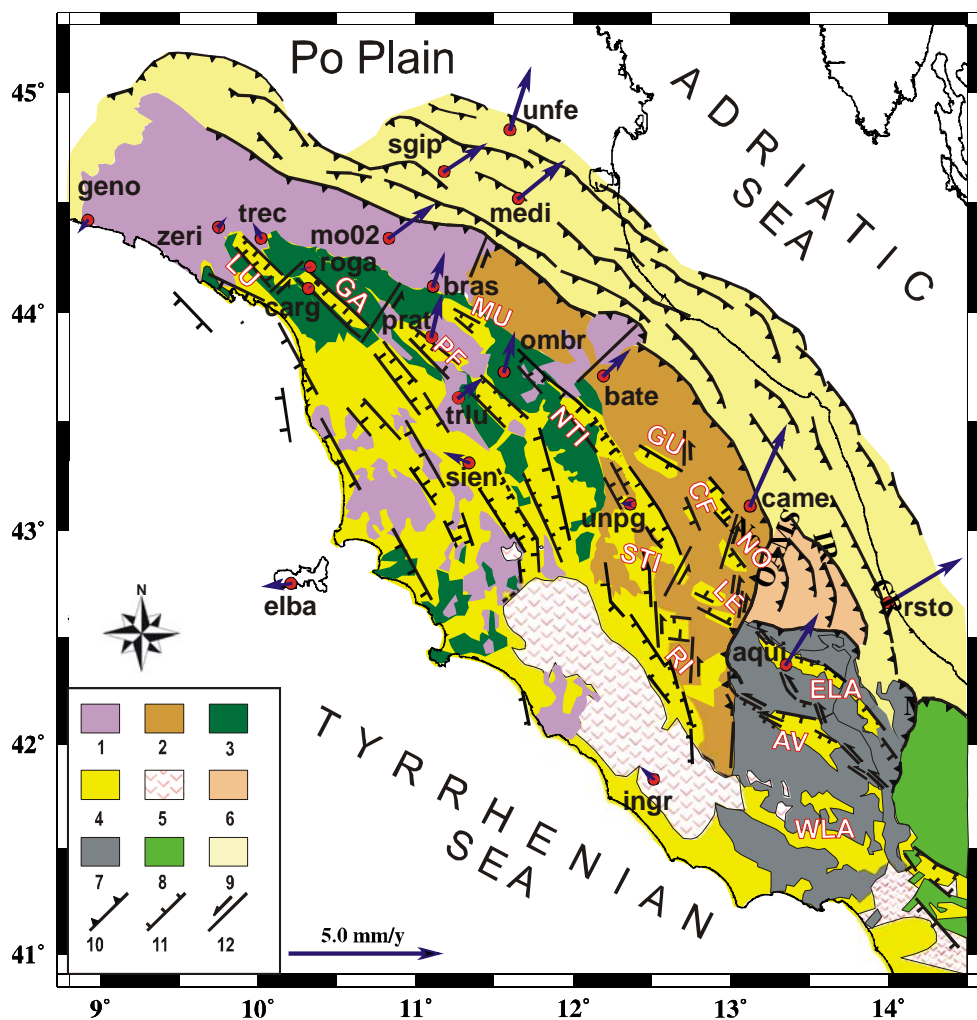


Figure 8 - Residual velocities (arrows) of the GPS regional network shown in Fig.1 (red dots) with respect to a fixed Eurasia Euler pole at 53.8 °N, -105.5 °E with rotation velocity $\omega = 0.249$ °/Myr (Serpelloni *et al.*, 2005). Tectonic sketch and main structural units of the Central-Northern Apennines: 1) Ligurian Units 2) Romagna-Marche-Umbria (RMU) Units 3) Tuscan Units 4) Zones affected by Plio-Quaternary extension 5) Magmatic products 6) Laga Units 7) Latium-Abruzzi platform 8) Molise-Sannio units 9) Zones affected by Plio-Quaternary thrusting and folding 10,11,12) Compressional, tensional and transcurrent features. AV = Avezzano fault zone, ELA, WLA = Eastern and Western parts of Latium-Abruzzi platform. Pliocene-Quaternary basins: CF = Colfiorito, GA = Garfagnana, GU = Gubbio, LE = Leonessa, LU = Lunigiana, MU = Mugello, NO = Norcia, NTI = Northern Tiber, PF = Pistoia-Firenze, RI = Rieti; STI = Southern Tiber.



UR 4.7 - Coordinatore: Maura Murru (INGV-Sezione di Roma1)

The topics dealt with by UR 4.7, are very vast and articulated, and so have been subdivided, by the Supervisors of S2 in December 2005, in two themes.

Theme 1 - Occurrence probability of a major earthquake, by the use of physical models

Introduction

This study aims at the assessment of the occurrence probability of future earthquakes on the whole Italian territory, conditional to the time elapsed after the latest characteristic earthquake and to the history of the following events on the neighbouring active sources. The methodology adopted here is based on the fusion of the statistical renewal model called *BPT* (*Brownian Passage Time*, Matthews *et al.*, 2002) with a physical model. This latter computes the instantaneous change of the static Coulomb stress ($\square CFF$) for the computation of both the permanent and the transient effects of the earthquakes occurred on the surrounding sources. The transient effects derived from the *rate-and-state* model for earthquake nucleation (Dieterich, 1994). The whole procedure arises from the studies of Stein and his collaborators (Stein *et al.*, 1997; Toda *et al.*, 1998; Parsons, 2004).

The analysis, in the first year, has been carried out on four seismogenetic sources (DISS 3.0.1 database) of the Central Italy region (41° - 43° N; 12° - 14° E), in agreement with the coordinators of the project. In the second year, the analysis has been extended to a larger area of Central and Southern Italy (40° - 43° N; 12° - 17° E), containing 37 seismogenetic sources reported in the DISS 3.0.2 database.

1 - Outline of the earthquake occurrence probability model adopted

A standard procedure for seismic hazard assessment assumes that all relevant earthquakes occur on well recognized faults with characteristic mechanism and size. The procedure needs the adoption of a probability density function $f(t)$ (pdf) for the inter-event time between consecutive events on each fault, together with some basic parameters of the model. One can adopt either a time independent Poisson model or a renewal model, based on a non-stationary seismogenetic process. For the former model, the expected recurrence time T_r is the only necessary piece of information. For the latter, also a parameter as the coefficient of variation (also known as aperiodicity) α of the inter-event times is required.

In lack of observational evidence, in this study we adopt the *BPT* distribution (Matthews *et al.*, 2002) to represent the inter-event time probability distribution for earthquakes on single sources in Italy. This distribution is expressed as

$$f(t; T_r, \alpha) = \left(\frac{T_r}{2\pi\alpha^2 t^3} \right)^{1/2} \exp \left\{ -\frac{(t - T_r)^2}{2T_r \alpha^2 t} \right\}. \quad (1)$$

In this study we adopt a method of numerical integration by discretization.

By manipulating the pdf we may obtain the probability that an event occurs between time t and $t + \Delta t$, under the condition that no other event has occurred after time $t=0$ (i.e. the occurrence time of the last characteristic event). Of course, this model assumes that the renewal process for the characteristic event is independent of any other circumstance that could perturb it.

As stated in the introduction, it is supposed that in real circumstances earthquake sources may interact, so that earthquake probability may be either increased or decreased with respect to what would be expected by a simple renewal model. The interaction is taken into consideration by the computation of the Coulomb static stress change or the Coulomb Failure Function (ΔCFF) caused by previous earthquakes on the concerned fault (*King et al.*, 1994):

$$\Delta CFF = \Delta\tau + \mu'\Delta\sigma_n , \quad (2)$$

where $\Delta\tau$ is the shear stress change on a given fault plane (positive in the direction of fault slip), $\Delta\sigma_n$ is the fault-normal stress change (positive when unclamped), and μ' is the effective coefficient of friction.

For this computation, the knowledge of the fault parameters (strike, dip, rake, dimensions, and average slip) is necessary for all the triggering earthquakes. A guess for the earthquake mechanism of the triggered source is also needed. Dealing with old events, for which details as fault shape and slip heterogeneity are not known, we assume rectangular faults with uniform slip distribution. The algorithm for ΔCFF computation assumes an Earth model such as a half space characterized by uniform elastic parameters. As ΔCFF is strongly variable in space, we consider its value in the point of the triggered fault where it may have the largest effect.

As recalled in the introduction, the effect of ΔCFF on the probability for the future characteristic event can be considered from two view points (*Stein et al.*, 1997). The first view point assumes that the time elapsed since the previous earthquake is modified from t to t' by a shift proportional to ΔCFF , that is

$$t' = t + \frac{\Delta CFF}{\alpha} \quad (3)$$

where α is the tectonic stressing rate.

The second view point works on the idea that the stress change can be equivalent to a modification of the expected recurrence time, T_r :

$$T_r' = T_r - \frac{\Delta CFF}{\alpha} . \quad (4)$$

According to *Stein et al.* (1997) both methods yield similar results. However, in our experience, they lead to different results, in particular when the elapsed time t is significantly smaller or larger than the recurrence time T_r , and also when the time interval Δt is not negligible respect to T_r . In our applications, the choice between the first and the second view has been decided according to practical considerations, as explained in the following sections.

Equations (3) and (4) express what has been called “permanent effect” of the stress change by *Stein et al.* (1997). We then need to consider the so called “transient effect”, due to rheological properties of the slipping faults. The application of the *Dieterich* (1994) constitutive friction law to an infinite population of faults (imagined as characterized by a complete distribution of states) leads to the expression of the seismicity rate as a function of time after a sudden stress change:

$$R(t) = \frac{R_0}{\left[\exp\left(\frac{-\Delta CFF}{A\sigma}\right) - 1 \right] \exp\left(\frac{t}{t_a}\right) + 1} \quad (5)$$

where R_0 is the seismicity rate before the stress change, A is a fault constitutive parameter, σ is the normal stress acting on the fault, t_a is a time constant equal to $A\sigma/\alpha$, and α is the tectonic stressing rate (supposed unchanged by the stress step). In all our applications of equation (5) $A\sigma$ works as a single parameter. Its value can be determined by experimental observations on real seismicity, rather than being derived from guesses on A and σ separately. It can be easily recognized that the time dependent rate $R(t)$ goes to zero when time goes to infinity.

We apply equation (5) to individual faults, with the substitution of the appropriate value for the hazard rate in place of the background rate R_0 . For this computation we assume a constant hazard rate, although the conditional probability obtained for the *BPT* increases with elapsed time, in consideration of the fact that the time constant T_r (typically hundreds to thousands of years) is much larger than t_a (typically few years) (Stein *et al.*, 1997).

Once the time dependent rate $R(t)$ is estimated by equation (5), the expected number of events N over a given time interval $(t, t+\Delta t)$ is computed by integration:

$$N = \int_t^{t+\Delta t} R(t) dt . \quad (6)$$

Under the hypothesis of a generalized Poisson process, we may finally estimate the probability of occurrence for the earthquake in the given time interval:

$$P = 1 - \exp(-N) . \quad (7)$$

2 - Short Summary of the first year of activity

The computation of the occurrence conditional probability of future earthquakes requires the knowledge of the recurrence time of characteristic earthquakes, based on historical or paleoseismological data.

In lack of historical data spanning a time interval significantly longer than the recurrence times on the analyzed sources, and given also the paucity of paleoseismological data for most of the same sources, as a first instance we have used the results obtained by L. Peruzza in the frame of the "GNNDT" project coordinated by Amato and Selvaggi, on the basis of the above mentioned *BPT* renewal model.

These results concerned the conditional probability of occurrence of a characteristic earthquake on every individual source reported in the DISS 2.0.516, 2001 database. Our UR has computed the variation of this probability by the perturbation produced on the specific individual source by the stress change due to the earthquakes following the latest characteristic earthquake. The stress change was computed for each of the four sources selected in Central Italy (Ovindoli-Pezza, Sulmona Basin, Fucino Basin e Aremogna-Cinquemiglia), using the parameters reported in the DISS 3.0.1 database (origin time of the latest event, hypocentral coordinates, focal mechanism, fault size and average slip).

In order to estimate the permanent effect of the stress change, we have computed an equivalent Poisson mean recurrence time by substitution of the equivalent probability,

provided by L. Peruzza, in equation (7). Then we have computed the *clock change*, Δt , by the ratio between ΔCFF and $\dot{\sigma}$ (tectonic stress change rate). The values of $\dot{\sigma}$ has been computed for each source by means of the geodetic data reported by Hunstad *et al.* (GRL, 2003). Equation (4) has allowed the computation of a modified mean inter-event time. Doing so, we have chosen the second of the above mentioned view points. In these first applications, such choice did not appear too dramatic, because of the relatively small time changes, in comparison with the recurrence times.

These so modified equivalent recurrence times have been then used for computing new probabilities of an earthquake exceeding the threshold magnitude for the next 30 years, and the corresponding instantaneous occurrence rates have been used in the application of the rate-and-state model by equation (5) for the estimate of the transient effect.

The results of the first year of study have lead to the conclusion that, for the four analysed sources, the permanent effects of the stress change on the occurrence probabilities were moderate, and the transient effects were even negligible.

3 - Second year of activity

We were aiming to extend our analysis to a wider region, including 37 individual sources recognized in the DISS 3.0.2 database (Figure 1 and Table 1). We were initially intentioned to follow the same procedure developed in the first year of activity. However, few circumstances have leaded us to modify some steps of this procedure. In light of the fact that for some of the 37 sources the clock advance was larger than the recurrence time of the source itself, we modified our choice, passing to the first of the previously views, by the use of equation (3), that affects positively the elapsed time, rather than the equivalent recurrence time.

Following this decision, we had to make directly use of the *BPT* model described by equation (1). In order to proceed on this way, we needed both the mean recurrence time T_r , the *aperiodicity* parameter α , and the time elapsed since the latest event for each of the 37 seismogenetic sources. Rather than carrying out specific investigations that were outside of the tasks of our UR we decided to use the existing information from UR 4.8 of this same project (L. Peruzza). This choice must be considered as subject to revision on the basis of new and more reliable information, but still useful at the present time in connection with the methodological character of our work.

The computation of the *hazard function* conditional to the time elapsed since the latest characteristic earthquake has allowed the estimate of the probability of occurrence of the next possible event in a future time interval (in our case assumed 30 years long starting on 2005).

The above mentioned methodology has been applied to each of the 37 seismogenetic sources, using the hypocentral parameters reported in the DISS 3.0.2 database (origin time of the latest event, hypocentral coordinates, focal mechanism, fault size and average slip).

Among the events that could have potentially changed the stress conditions on the 37 studied faults, we have considered:

- The characteristic events associated to the same seismogenetic sources (reported in DISS 3.0.2);
- The events reported in the CPTI04 catalog associated to the Areal Sources (120 events with $Mw \geq 5.0$) (results of Task 1 of this project, Feb. 2007)
- The events reported in the catalog CSI (1986-2002) + those reported in the more recent bulletins (2003-2006), ($Ml \geq 5.0$).

Obviously, all these events have been considered only once in case that they were reported by more than one information source.

In the application of this second year the *clock changes* have been estimated through the *tectonic stress rates*, coming themselves from the tectonic strain changes provided by the UR 3.2a of this project (A. Caporali). The strain tensor has been projected on the specific source taking into account the mechanism of its characteristic earthquakes. The *time change* is positive (the fault becomes closer to failure) if the Coulomb stress change is positive. In the opposite case (negative change) the fault become farther from failure, being possible, in extreme situations, that the elapsed time is reset to zero.

As example, the computation of the ΔCFF on Sulmona basin is shown in Figure 2.

It is possible to note how the subsequent events the December 3, 1315 caused on the different parts of this structure both an increase and decrease of stress. The values ranges between -0.2 and 0.04MPa.

Failure is encouraged in the source parts where the ΔCFF is positive and discouraged if negative. The zones with a positive change will have an advance in the expected occurrence time (*clock change*) of next large earthquake on the examined source.

Table 1 shows, for the 37 sources examined in this study, the code, name, the latest earthquake date (unknown for three of them), the expected magnitude and the focal mechanism, as reported in the DISS 3.0.2 database.

Table 2 contains, for the 37 seismogenetic sources, the physical parameters relevant for the computation of the *clock advance*: the *strain* and the *stress rate* obtained from geodetic observations, the *stress change* caused by the subsequent earthquakes, and the *time change*.

In Table 3 are reported, for each of the 37 sources: the time elapsed since the latest earthquake (including the *clock change*), the mean recurrence time, the conditional occurrence probability in the next 30 years, the probability modified by the permanent effect of the subsequent earthquakes, and the probability affected by the transient effect. These probabilities are not reported for the sources whose latest earthquake is unknown.

It can be noted that for most of the sources, the renewal model forecasts a negligible probability of occurrence for the next 30 years, due to the relatively short elapsed time, compared with the mean recurrence time.

It is interesting to note also that for two sources the stress change due to the subsequent events has affected the probability of occurrence, increasing significantly its value. This happened in particular, for Norcia Basin (12.7%), Sulmona Basin (15.6%), San Marco in Lamis (9.2%), San Severo (4.1 %), Foligno (1.1 %), and Ariano Irpino (2.9%).

The probabilities obtained from the transient effect are generally smaller than the conditional probabilities obtained from the permanent effect only. This is due to the assumption of constant background rate made for the application of the rate-and-state model. Anyway the transient effect decays as the supply of nucleation sites is consumed; the duration of the transient is inversely proportional to the fault stressing rate.

In Figure 3 the expected probability values in the next 30 years, starting on January 1, 2006, have been also plotted in map on the respective seismogenetic sources. The higher probability is related to Norcia Basin (10.9 %) and Sulmona Basin (12.8 %). The last characteristic events are occurred on these two sources on January 14, 1703 and December 3, 1315, respectively (Table 1).

Theme 2 – Occurrence probability of moderate and large events, using dataset of instrumental and historical events

Introduction

We apply “a purely stochastic” epidemic model, based on earthquake clustering, to the (undeclustered) instrumental database of shallow seismicity (July 1987-December 2006) in a forward-retrospective way for short-term moderate and large earthquakes forecasted in Italy, based on smoothed seismicity. This database, collected by the Istituto Nazionale di Geofisica e Vulcanologia, contains 9 307 earthquakes of magnitude equal to or larger than 2.6. The largest recorded magnitude is $M_{max} = 5.9$.

1 - Brief outline of the earthquake occurrence probability model adopted

The software is based on algorithms, published by the team on international reviews, pertaining to the category of the *ETAS* (*Epidemic Type Aftershock Sequence*) models. These models offer a quantification of earthquake interactions (*Console et al.*, 2001, 2003, 2006a, 2006b, 2007, *Papadimitriou et al.*, 2006). They have been used in many studies to describe or predict the spatio-temporal distribution of seismicity and reproduce many properties of real seismicity.

This forecast uses earthquake data only, with no explicit use of tectonic, geologic, or geodetic information. In this model all earthquakes have identical roles in the triggering process. In fact every earthquake can be regarded at the same time as triggered by previous events and triggering future earthquakes. The expected occurrence rate density of earthquakes, at any instant of time and geographical point, is modeled as the sum of the independent, or time-invariant “spontaneous”, activity and the contribution of every previous event using a kernel function that takes in proper account: (a) the magnitude of the triggering earthquake, (b) the spatial distance from the triggering event, and (c) the time interval between the triggering event and the instant considered for the computation. The magnitude distribution adopted here is the *Gutenberg-Richter* (G-R) law. All the tests are carried out on a different and independent data set. In this way the requirement that the test is carried out on an independent dataset on which the hypothesis is formulated is fulfilled.

2 - Short Summary of the first year

Our tests showed that the CSI catalog from 1986 to 2002, used in the first year of activity, is homogeneous and complete, as a function of time and space, for magnitude equal to 2.1 and larger starting from July 1, 1987 (n.ev. 18 623). Moreover analysis on spatial variations of a and b parameters of G-R relationship were carried out.

All free parameters of the algorithm were determined beforehand in the learning phase, for the whole period covered by the CSI catalog, through a procedure of best fit based on the maximum likelihood criterion. The predictive capability of such a model was verified, using just the parameters obtained from the learning phase, for various sequence (September 1997- April 1998 Umbria-Marche; October-November 2002 Molise and Val Topino, December 2005).

3 - Second year of activity

The shallow database (CSI +Bulletin) used in the second year of activity, spans from July 1987 to December 2006.

The second year activity focused on the occurrence probability analysis of 26 shocks ($M \geq 5.0$) which occurred in Italy (not far off the coast) from 1987 to 2006, just some hours before they occurred (Figure 4 and Table 5).

In order to quantify the expected occurrence rate density, $M \geq 5.0$, (events/day/km²) the earthquake clustering forecasting model has been fitted to 10 different learning periods. The minimum magnitude considered for the triggering and target events is 3.0 and 5.0, respectively. The maximum log-likelihood best fit of the free parameters characterizing the model, run on each period, has provided the results shown in Table 2.

The capability of the model has been tested in a retrospective way for each (26) target shock, considering in this phase the parameters obtained in the previous learning phases, whose periods extend until the year before the considered shocks (i.e. for Potenza shock occurred on May 5, 1990, the learning period considered is reported in the second column of Table 4).

The background seismicity is that obtained from the respective learning periods.

The results of occurrence probability for $M \geq 5.0$ events, in the following 24 hours, inside a radius of 100 km centred on the same shock area are shown in Table 5.

In Figure 5(a) and (b) we show 2 examples of how the ETAS model could be applied in real cases to display the spatial changes of the expected occurrence rate density, $M \geq 5.0$, before the two largest shocks of 2002 Molise sequence. The values of all free parameters considered in this test phase are reported in column 7 of Table 4, for the learning period July 1987-December 2001.

Figure 5(a) and Figure 6(a) show the situation of the rate on October 31, 2002 at 08:00 UTC, just (2 hours) before the largest shock of October 31 ($5.4 M_I$, 10:32 UTC), the epicenter of which is indicated by a black star. The occurrence rate density before this event, ranging from 1E-005 and 2E-005, is affected by the largest foreshock ($3.2 M_I$) activity at 02:27 UTC on October 31, 2002. Figure 5(b) and Figure 6(b) show at 08:00 on November 1, 2002 the changes in the expected occurrence rate after the shock of October 31, 2002 (($5.4 M_I$, 10:32 UTC) but before the November 1, 2002 Molise main shock ($5.3 M_I$, 15:08 UTC). They change from 0.001 and 0.003, reflecting the increase of the rate density which occurred in that area after the beginning of the sequence. These two maps can then be considered real forecasts of the subsequent seismicity.

The occurrence probability of an $M_I \geq 5.0$ shock, inside a radius of 100 km centred on the Molise ($5.4 M_I$) event of October 31, 2002, in the next 24 hours starting from 08:00 UTC is 0.038 %. The increase in the occurrence probability of future shock ($M \geq 5.0$) caused by the stress changes associated with the previous events at 08:00 on November 1, 2002 before the $5.3 M_I$ earthquake (15:08 UTC) is rather high, raising up to 1.24 % (Figure 5b and Table 5)

Selected References

- Console, R. and M. Murru (2001), A simple and testable model for earthquake clustering, *J. Geophys. Res.*, 106, 8699-8711.
- Console, R., M. Murru, and A.M. Lombardi (2003), Refining earthquake clustering models, *J. Geophys. Res.*, 108, 2468, doi: 10.1029/2002JB002130.
- Console, R., M. Murru, and F. Catalli (2006a), Physical and stochastic models of earthquake clustering, *Tectonophysics*, 417, 141-153.
- Console, R., D.A. Rhoades, M. Murru, F.F. Evison, E.E. Papadimitriou and V.G. Karakostas (2006b), Comparative performance of time-invariant, long-range and short-range forecasting models on the earthquake catalogue of Greece, *J. Geophys. Res.*, 111, B09304, doi:10.1029/2005JB004113.
- Console, R., M. Murru, F. Catalli, and G. Falcone (2007), Real time forecasts through an earthquake clustering model constrained by the rate-and-state constitutive law: Comparison with a purely stochastic ETAS model, *Seismological Research Letters*, 78, 49-56.
- Dieterich, J. H. (1994), A constitutive law for rate of earthquake production and its application to earthquake clustering, *J. Geophys. Res.*, 99, 2601-2618.
- Hunstad, I., G. Selvaggi, N. D. Agostino, P. England, P. Clarke, and M. Pierozzi (2003), Geodetic strain in peninsular Italy between 1875 and 2001, *Geophys. Res. Lett.*, 30 (4), 1181, doi:10.1029/2002GL016447.
- King, G. C. P., R. S. Stein, and J. Lin, Static stress changes and the triggering of earthquakes, *Bull. Seismol. Soc. Am.*, 84, 935-953, 1994.
- Matthews, M.V., W.L. Ellsworth, and P.A. Reasenberg (2002), A Brownian model for recurrent earthquakes, *Bull. Seism. Soc. Am.*, 92, 2233-2250.
- Papadimitriou, E.E., F.F. Evison, D.A. Rhoades, V. Karakostos, R. Console and M. Murru (2006), Long-term seismogenesis in Greece: Comparison of the evolving stress field and precursory scale increase approaches, *J. Geophys. Res.*, 111, B05318, doi:10.1029/2005JB003805.
- Parsons, T. (2004), Recalculated probability of $M \geq 7$ earthquakes beneath the Sea of Marmara, Turkey, *J. Geophys. Res.*, 109, B05304, doi:10.1029/2003JB002667
- Stein, R., A. Barka, and J. Dieterich (1997), Progressive failure on the North Anatolian fault since 1939 by earthquake stress triggering, *Geophys. J. Int.*, 128, 594-604
- Toda, S., R. Stein, P. Reasenberg, J. Dieterich, and A. Yoshida (1998), Stress transferred by the 1995 $Mw=6.9$ Kobe, Japan, shock: Effect on aftershocks and future earthquake probabilities, *J. Geophys. Res.*, 103 (B10), 24,543-24,565.

Table 1. Parameters of the seismogenetic sources considered in this study

GG	GG Name	last event	M	strike	dip	rake
ITGG001	O vindoli-Pezza		6.6	151	60	270
ITGG002	Fucino Basin	13/1/1915	6.7	145	60	270
ITGG003	Aremogna-Cinque Miglia		6.4	144	60	270
ITGG004	Boiano Basin	26/7/1805	6.6	304	55	270
ITGG005	Tammaro Basin	6/5/1688	6.6	311	60	270
ITGG006	Ufita Valley	29/11/1732	6.6	308	60	270
ITGG008	Agri Valley	16/12/1857	6.5	316	60	270
ITGG010	Melandro-Pergola	16/12/1857	6.5	317	60	270
ITGG015	Montereale Basin	2/2/1703	6.5	147	60	270
ITGG016	Norcia Basin	14/1/1703	6.5	157	60	270
ITGG019	Sellano	14/10/1997	5.6	144	40	260
ITGG020	Monte Sant'Angelo		6.4	280	80	215
ITGG022	San Marco Lamis	6/12/1875	6.1	95	80	215
ITGG026	Amatrice	7/10/1639	6.1	150	65	270
ITGG027	Sulmona Basin	3/12/1315	6.4	135	60	270
ITGG028	Barrea	7/5/1984	5.8	152	50	264
ITGG052	San Giuliano di Puglia	31/10/2002	5.8	267	82	203
ITGG053	Ripabottoni	1/11/2002	5.7	261	86	195
ITGG054	San Severo	30/7/1627	6.8	266	80	215
ITGG059	Velletri	26/8/1806	5.6	225	70	270
ITGG061	Foligno	13/1/1832	5.8	330	30	270
ITGG062	Trevi	15/9/1878	5.5	330	30	270
ITGG068	Casamicciola	26/7/1883	5.6	233	85	270
ITGG070	Offida	3/10/1943	5.9	150	35	90
ITGG077	Colliano	23/11/1980	6.8	310	60	270
ITGG078	San Gregorio Magno	23/11/1980	6.2	300	60	270
ITGG079	Pescopagano	23/11/1980	6.2	124	70	270
ITGG080	Cerignola	20/3/1731	6.3	269	80	180
ITGG081	Melfi	14/8/1851	6.3	269	80	180
ITGG082	Ascoli Satriano	17/7/1361	6.0	269	80	180
ITGG083	Bisceglie	11/5/1560	5.7	269	80	180
ITGG084	Potenza	5/5/1990	5.7	95	88	175
ITGG088	Bisaccia	23/7/1930	6.7	280	64	237
ITGG092	Ariano Irpino	5/12/1456	6.9	85	70	230
ITGG094	Tocco da Casauria	30/12/1456	6.0	89	70	230
ITGG095	Frosolone	30/12/1457	7.0	83	70	230
ITGG096	Isola del Gran Sasso	5/9/1950	5.7	95	75	225

Table 2. Physical parameters used for computing the time change

GG	GG Name	Strain rate (nanostrain/y r)	Tau_dot (Pa/yr)	ΔCFF (MPa)	Δt=ΔCFF/tau_d ot (year)
ITGG001	O vindoli-Pezza	17.0	412.3	0.7497	1818.3
ITGG002	Fucino Basin	17.0	412.3	-0.4300	-1042.9
ITGG003	Aremogna-Cinque Miglia	14.9	361.4	0.0650	179.9
ITGG004	Boiano Basin	22.7	597.3	0.0036	6.0
ITGG005	Tammaro Basin	22.7	597.3	0.2300	385.0
ITGG006	Ufita Valley	22.7	597.3	0.2900	485.5
ITGG008	Agri Valley	16.4	397.8	0.0102	25.6
ITGG010	Melandro-Pergola	16.4	397.8	0.0203	51.0
ITGG015	Montereale Basin	16.4	397.8	0.2046	514.2
ITGG016	Norcia Basin	17.0	412.3	0.6107	1481.1
ITGG019	Sellano	42.8	1180.1	0.0001	0.1
ITGG020	Monte Sant'Angelo	1.2	33.6	0.0320	952.5
ITGG022	San Marco Lamis	1.2	33.6	0.0143	426.2
ITGG026	Amatrice	14.9	319.7	0.0761	238.1
ITGG027	Sulmona Basin	14.9	361.4	0.0461	127.5
ITGG028	Barrea	17.0	468.8	0.0003	0.7
ITGG052	San Giuliano di Puglia	0.9	25.2	0.0000	1.0
ITGG053	Ripabottoni	0.9	25.2	0.0000	1.1
ITGG054	San Severo	0.9	25.2	0.0261	1037.6
ITGG059	Velletri			-0.0009	
ITGG061	Foligno	9.3	225.5	0.0423	187.4
ITGG062	Trevi	9.3	225.5	-0.0168	-74.4
ITGG068	Casamicciola			-0.0009	
ITGG070	Offida	11.5	302.5	0.0031	10.3
ITGG077	Colliano	16.4	397.8	0.0007	1.7
ITGG078	San Gregorio Magno	16.4	397.8	0.0017	4.2
ITGG079	Pescopagano	35.3	635.7	0.0001	0.2
ITGG080	Cerignola	1.0	28.0	-0.0797	-2845.4
ITGG081	Melfi	1.2	33.6	-0.3104	-9237.7
ITGG082	Ascoli Satriano	1.0	28.0	-0.0359	-1283.2
ITGG083	Bisceglie	1.0	28.0	-0.0087	-309.3
ITGG084	Potenza	6.9	193.2	-0.0545	-282.1
ITGG088	Bisaccia	5.2	145.6	-0.2529	-1737.1
ITGG092	Ariano Irpino	3.6	100.8	0.4055	4022.8
ITGG094	Tocco da Casauria	1.4	25.2	0.1044	4143.8
ITGG095	Frosolone	24.8	694.4	0.1197	172.4
ITGG096	Isola del Gran Sasso	3.8	53.3	0.0003	5.0

Table 3. Results of the statistical analysis

GG	GG Name	Elapsed time+ Δt (year)	Mean recurrence time (year)	P(30)	P_mod(30)	P_trans(30)
ITGG00 1	Ovindoli-Pezza	11810.3	756.4	9999.0	9999.0	9999.0
ITGG00 2	Fucino Basin	-950.9	562.5	0.00E+0 0	0.00E+00	0.00E+00
ITGG00 3	Aremogna-Cinque Miglia	10171.9	1649.4	9999.0	9999.0	9999.0
ITGG00 4	Boiano Basin	208.0	1332.5	0.00E+0 0	0.00E+00	0.00E+00
ITGG00 5	Tammaro Basin	704.0	1317.1	0.00E+0 0	1.97E-04	1.28E-04
ITGG00 6	Ufita Valley	760.5	1307.7	0.00E+0 0	4.19E-05	2.19E-05
ITGG00 8	Agri Valley	175.6	1171.6	0.00E+0 0	0.00E+00	0.00E+00
ITGG01 0	Melandro-Pergola	201.0	940.4	0.00E+0 0	0.00E+00	0.00E+00
ITGG01 5	Montereale Basin	818.2	1170.3	0.00E+0 0	5.28E-04	1.20E-04
ITGG01 6	Norcia Basin	1785.1	1830.3	0.00E+0 0	1.27E-01	1.09E-01
ITGG01 9	Sellano	10.1	410.2	0.00E+0 0	0.00E+00	0.00E+00
ITGG02 0	Monte Sant'Angelo	10944.5	687.5	9999.0	9999.0	9999.0
ITGG02 2	San Marco Lamis	558.2	665.1	0.00E+0 0	9.17E-02	1.30E-02
ITGG02 6	Amatrice	606.1	1318.5	0.00E+0 0	0.00E+00	0.00E+00
ITGG02 7	Sulmona Basin	819.5	888.1	1.40E-02	1.56E-01	1.28E-01
ITGG02 8	Barrea	23.7	523.2	0.00E+0 0	0.00E+00	0.00E+00
ITGG05 2	San Giuliano di Puglia	6.0	498.3	0.00E+0 0	0.00E+00	0.00E+00
ITGG05 3	Ripabottoni	6.1	442	0.00E+0 0	0.00E+00	0.00E+00
ITGG05 4	San Severo	1417.6	1687.1	0.00E+0 0	4.14E-02	1.34E-02
ITGG05 9	Velletri		442.7	0.00E+0 0		
ITGG06 1	Foligno	362.4	598.1	0.00E+0 0	1.09E-02	6.59E-03
ITGG06 2	Trevi	54.6	435.7	0.00E+0 0	0.00E+00	0.00E+00
ITGG06 8	Casamicciola		442.7	0.00E+0 0		
ITGG07 0	Offida	74.3	701.1	0.00E+0 0	0.00E+00	0.00E+00
ITGG07 7	Colliano	28.7	1970.9	0.00E+0 0	0.00E+00	0.00E+00
ITGG07 8	San Gregorio Magno	31.2	824.6	0.00E+0 0	0.00E+00	0.00E+00
ITGG07	Pescopagano	27.2	914.3	0.00E+0	0.00E+00	0.00E+00

9				0		
ITGG08 0	Cerignola	-2569.4	958.6	0.00E+0 0	0.00E+00	0.00E+00
ITGG08 1	Melfi	-9081.7	964.3	0.00E+0 0	0.00E+00	0.00E+00
ITGG08 2	Ascoli Satriano	-637.2	684.5	2.30E-01	0.00E+00	0.00E+00
ITGG08 3	Bisceglie	137.7	489.9	2.96E-01	0.00E+00	0.00E+00
ITGG08 4	Potenza	-265.1	507.8	0.00E+0 0	0.00E+00	0.00E+00
ITGG08 8	Bisaccia	-1660.1	1459.8	0.00E+0 0	0.00E+00	0.00E+00
ITGG09 2	Ariano Irpino	4573.8	2081.8	3.00E-03	2.87E-02	2.87E-02
ITGG09 4	Tocco da Casauria	4694.8	698.8	4.10E-02	0.00E+00	0.00E+00
ITGG09 5	Frosolone	723.4	2468.5	0.00E+0 0	0.00E+00	0.00E+00
ITGG09 6	Isola del Gran Sasso	62.0	523.7	0.00E+0 0	0.00E+00	0.00E+00

Table 4
Maximum log-likelihood parameters of the Purely Stochastic Model (ETAS)
(Learning phases)

The Lower magnitude threshold of triggering and target events is 2.6 and 3.0, respectively.

The exponent of the spatial distribution (q) is 1.5 (fixed)

Table 5

Events, $M \geq 5.0$, occurred on the Italian territory from 1987 to 2006. The shocks indicated in red are not considered in the probability analysis because not relevant for civil purposes.

Locality	Lon	Lat	year	month	day	Time	M_I	P (%) ($M \geq 5.0$)
Porto S. Giorgio	13.95	43.21	1987	7	3	10:21	5.0	-----
Potenza	15.86	40.64	1990	5	5	7:21	5.2	0.011
Siracusa	15.24	37.33	1990	12	13	0:24	5.4	0.047
Southern Tyrrhenian.	15.21	39.40	1994	1	5	13:24	5.8	-----
Gargano	15.91	41.81	1995	9	30	10:14	5.4	0.023
Northern Apennines.	10.60	44.76	1996	10	15	9:56	5.1	-----
Southern Tyrrhenian.	13.27	40.40	1996	12	21	8:46	5.1	-----
Umbria-Marche Region	12.89	43.02	1997	9	26	0:33	5.6	0.020
Umbria-Marche Region	12.85	43.01	1997	9	26	9:40	5.8	0.75
Umbria-Marche Region	12.82	43.04	1997	10	3	8:55	5.0	0.17
Umbria-Marche Region	12.85	43.03	1997	10	6	23:24	5.4	0.11
Umbria-Marche Region	12.92	42.91	1997	10	12	11:08	5.1	0.080
Umbria-Marche Region	12.90	42.90	1997	10	14	15:23	5.5	0.25
Umbria-Marche Region	12.81	43.15	1998	3	26	16:26	5.4	0.070
Umbria-Marche Region	12.76	43.19	1998	4	3	7:26	5.3	0.072
Southern Tyrrhenian	15.02	39.06	1998	5	18	17:19	5.4	-----
Lucano Apennines	15.95	40.06	1998	9	9	11:28	5.6	0.10
Southern Tyrrhenian	15.59	38.89	2001	5	17	11:43	5.0	-----
N-E Italy (border)	11.07	46.7	2001	7	17	15:06	5.3	-----
Palermo off-shore	13.65	38.38	2002	9	6	1:21	5.6	0.026
Molise	14.89	41.72	2002	10	31	10:32	5.4	0.038
Molise	14.84	41.74	2002	11	1	15:09	5.3	1.24
Centr. Adriatic	15.42	43.10	2003	3	27	16:10	5.2	0.0067
Centr. Adriatic	15.46	43.11	2003	3	29	17:42	5.9	0.63
Centr. Adriatic	15.53	43.17	2003	3	30	11:09	5.1	6.54
Western. Apennines	8.87	44.76	2003	4	11	9:26	5.2	0.012
Northern Apennines	11.38	44.26	2003	9	14	21:42	5.5	0.037
Southern Tyrrhenian.	15.20	39.83	2004	3	3	2:13	5.1	-----
App. bresciano	10.52	45.69	2004	11	24	22:59	5.7	0.0050
Centr. Adriatic	15.44	43.13	2004	11	25	6:21	5.4	0.024
Anzio	12.50	41.44	2005	8	22	12:02	5.2	0.0048
Eastern Sicily	14.11	37.6	2005	11	21	10:57	5.2	0.0098
Gargano	15.90	41.80	2006	5	29	2:20	5.3	0.021
Gargano	16.28	42.01	2006	12	10	11:03	5.0	0.021

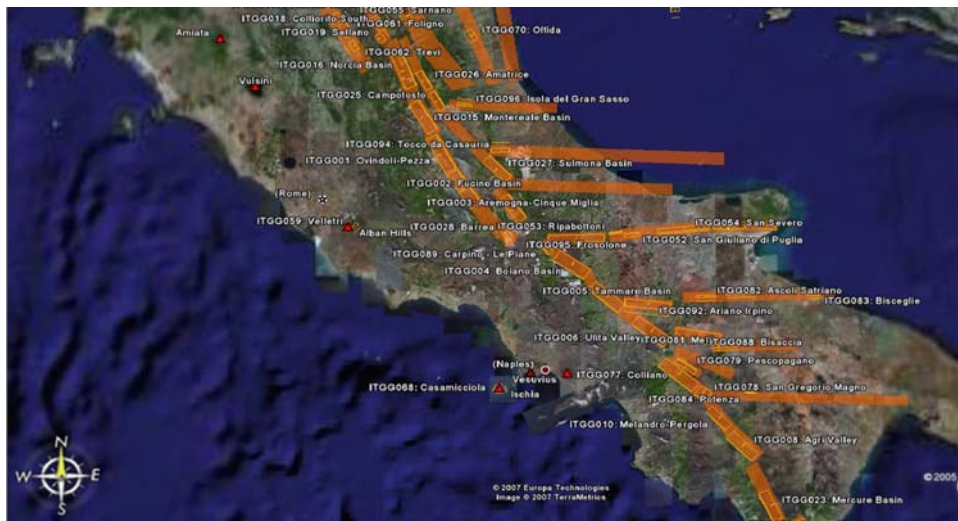


Figure 1 -Map of the area in analysis, including 37 seismogenetic sources (database DISS 3.0.2, September 2006).

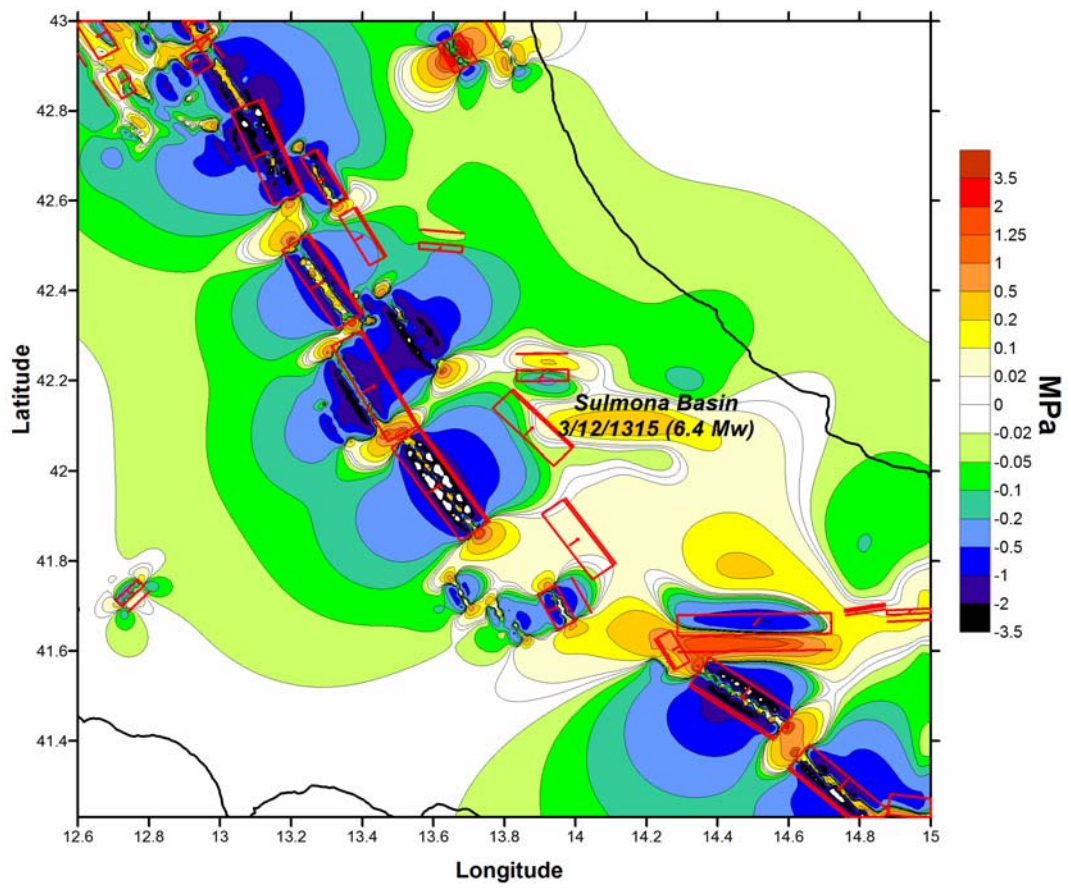


Figure 2 - Coulomb failure change at a depth of 6.8 km caused by all earthquake after December 3, 1315. The induced focal mechanism is the same of "Sulmona Basin" earthquake.

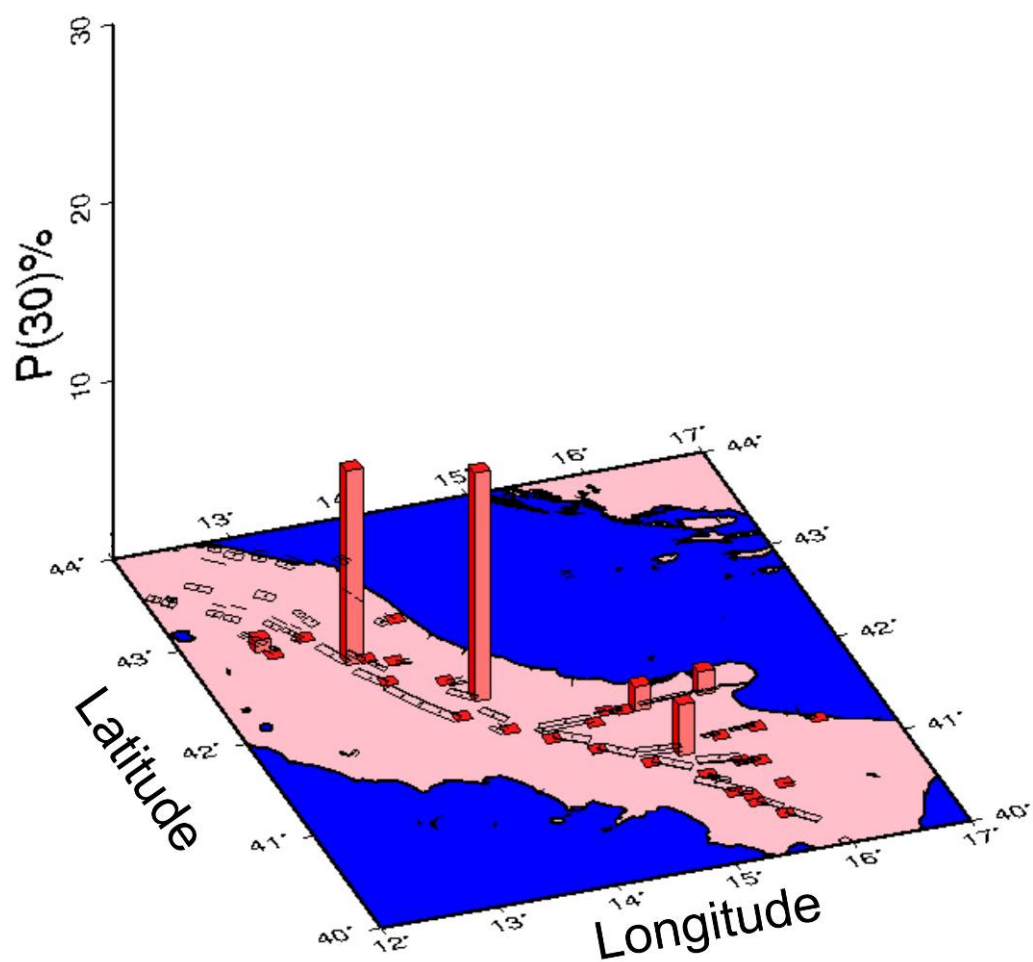


Figure 3 - Map showing the conditional probabilities of occurrence probabilities obtained from the transient effect for a characteristic earthquake in the next 30 years starting in January 1, 2006 for the 37 seismogenic sources considered in this study.

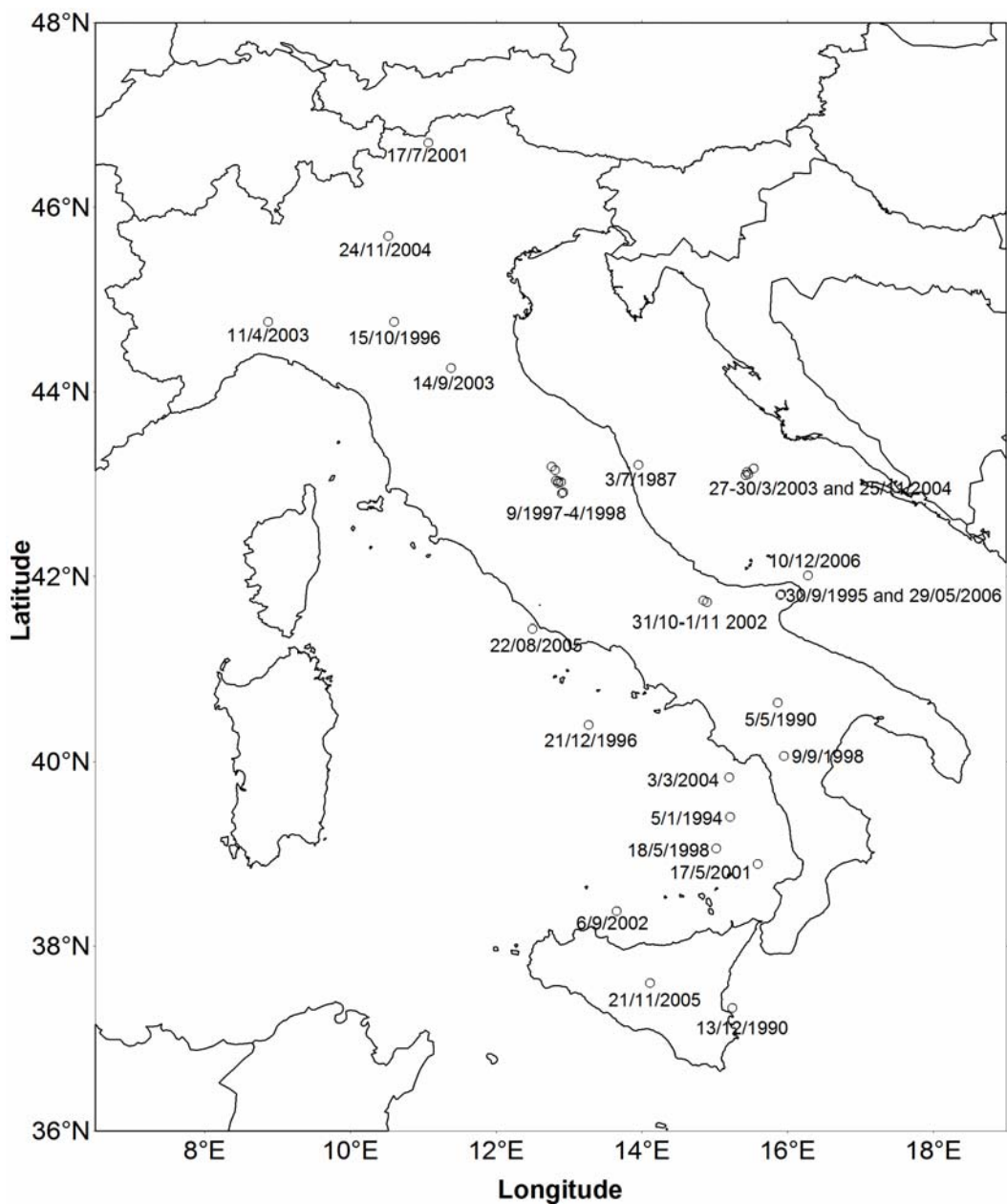


Figure 4 - Epicentral map of earthquakes ($M \geq 5.0$) which occurred in Italy from July 1987 to December 2006.

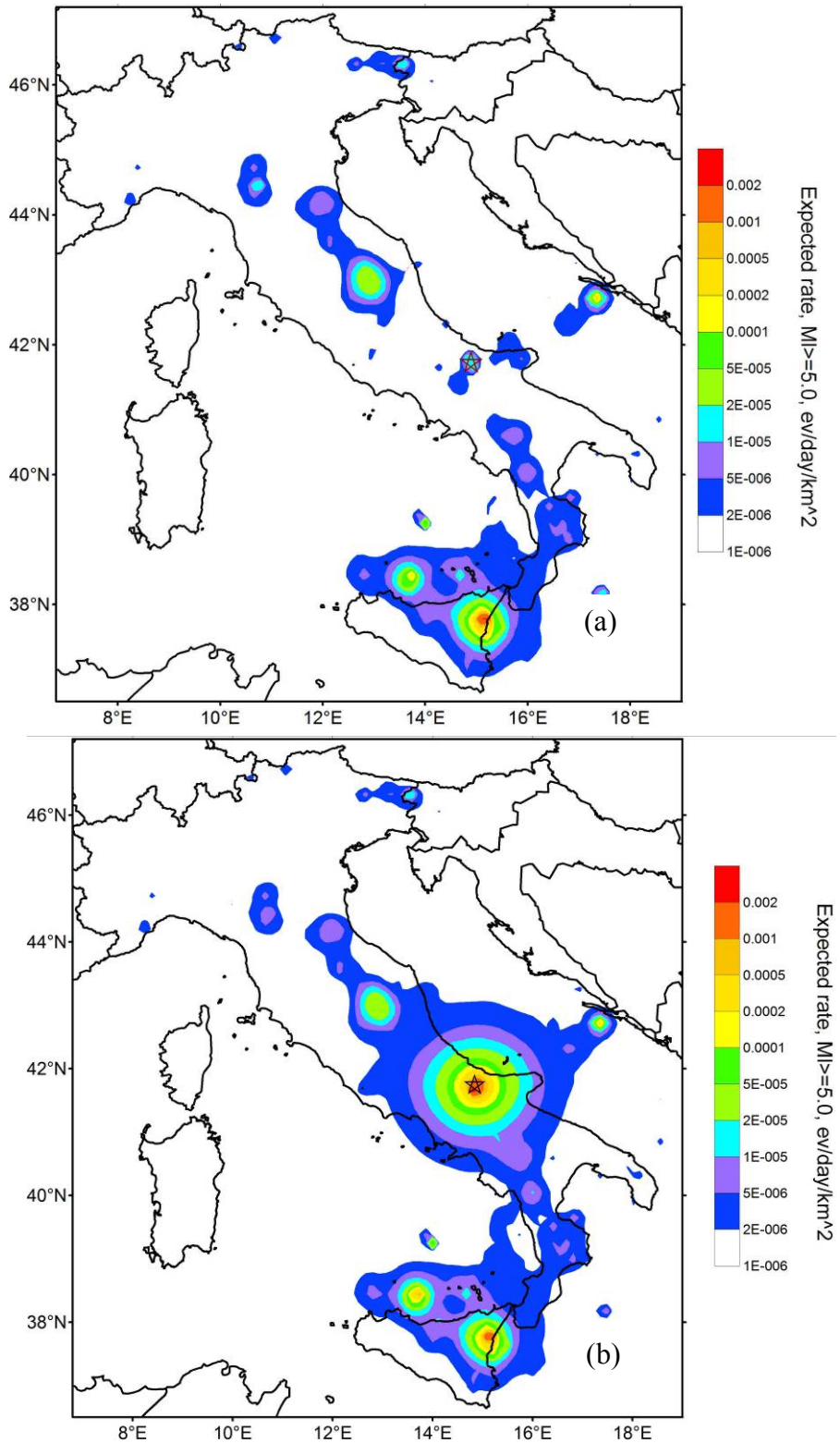


Figure 5 - The maps represent the modeled expected occurrence rate density, $M \geq 5.0$, (events/day/km 2) for the whole Italian territory. (a) On October 31, 2002 at 08:00 UTC, just (2 hours) before the strongest Molise event ($5.4 M_l$, 10:32 UTC). A black star shows the epicenter (lat 41.72°N -lon 14.89°E) of the Molise shock. (b) On November 1, 2002 at 08:00 UTC, before $5.3 M_l$ shock (15:09 UTC). A black star shows the epicenter (lat 41.74°N -lon 14.84°E) of the Molise shock. The occurrence probability of an $M \geq 5.0$ shock on October 31, 2002 and on November 1, 2002, inside a radius of 100 km centred on the Molise event, in the next 24 hour starting from 08:00 UTC is 0.0038 % and 1.24%, respectively. The stochastic model of earthquake clustering (ETAS) has been applied for the computation of the occurrence rate density, from the earthquakes ($M \geq 2.6$) recorded by the Italian Seismological Network, using the maximum likelihood parameters shown in the seventh column of Table 4.

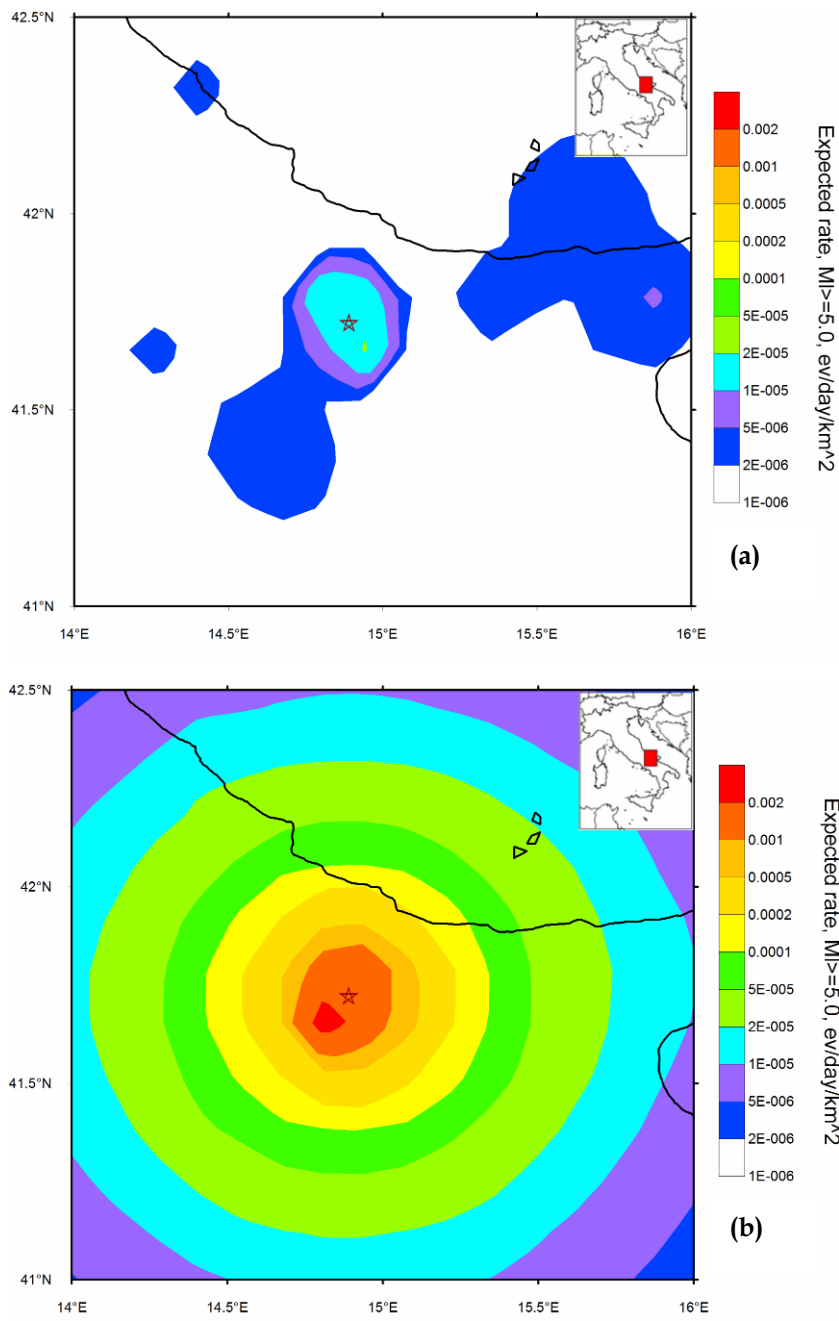


Figure 6 - Enlargement corresponding to the Molise zone related to the expected rate in Figure 5. **(a)** On October 31, 2002. **(b)** On November 1, 2002.



UR 4.8 - Coordinatore: Laura Peruzza (OGS - Istituto Nazionale di Oceanografia e di Geofisica Sperimentale)

This report synthesizes the activities and results obtained by the OGS research team, including M. Stirling, visiting researcher in Feb-Mar 2007. The UR is involved in computing the occurrence probabilities of characteristic earthquakes on DISS seismogenic sources, in a time-dependent perspective; moreover, Slejko is one of the two project leader, and Peruzza coordinates the research units (9 UR's) working on Task 4 (Characterizing the behaviour of seismogenic sources and assigning probabilities of activation) by facilitating the use of the most updated results released by Task 1 and Task 3. The critical analysis of the Task's activities is described in chapter 2.4, while in Tab. 1 an agenda of the facts organized in this framework is given. All the Task's reports and documents are stored and available on restricted access at ftp web site [ftp.ogs.trieste.it](ftp://ogs.trieste.it).

In the time period of the Project, the UR performed analyses with the aim at:

- 1) using the information stored in DISS to quantify the probability of occurrences of the next event in a mid-long term perspective (30 years);
- 2) checking the influence of uncertainties of source characterization in the earthquake probabilities;
- 3) balancing the seismic moment rate derived from earthquake catalogue with the geodetic moment rate obtained from observation or models;
- 4) constraining the most sensitive and uncertain data (e.g. slip rate on a fault) using points 1-3, to obtain more robust estimates of the probabilities of activation.

These are very recent topics in the international literature, and only countries with a big amount of repeated events data on fault segments have been facing the problem of time-dependent analyses (Japan, California). Nevertheless, Italy plays its role in this context, for the originality in the approaches used in compiling and using source models that derive from a mixture of geological and seismological observations (e.g. [1-3]); not least, time-dependent issues may play a critical role in seismic risk reduction strategies, by giving higher priority to earthquake-prone areas (e.g. [4]).

The UR worked on the seismogenic sources identified by DISS.

By applying a similar technique to the one proposed in a previous project [3, 5], we computed expected magnitudes, mean recurrence time and a statistical proxy of aperiodicity for a characteristic earthquake on the individual geologic sources (GG); the computations combine empirical relationships based on geometric parameters of the fault, with the uncertainty given in kinematics (e.g. slip rate). In Fig. 1 the histograms of the analyzed datasets, including DISS2, demonstrate the increase of sources recognised to have a geological signature in the last few years, and their distribution in magnitude. The DISS v. 3.02 released in Sep 2006 is used for the final elaboration and it contains 115 GG sources; 95 faults report the date of the last event.

The statistical analysis proposed at the end of the first year [6] suggested to subdivide the variability in characterizing the individual geologic sources into two main components, that can be linked to the widely used terminology of aleatoric and epistemic uncertainties. Belongs to the first type the variability associated to the size (magnitude) of the characteristic event; epistemic is the one related to the deformation process itself (slip rate on the fault). The tests done demonstrated that the uncertainties on magnitude introduced by the proposed statistical proxy are small, comparable and often smaller than the experimental data; the recurrence times derived by using a mean slip rate values span usually in a factor of ten, and their central tendency is near to the minimum recurrence time (MinRecInt) given in DISS; the aperiodicity alfa (standard deviation over mean

recurrence time) is usually below 0.5, and compatible with periodic or quasi-periodic processes. The combination in the renewal application of the Brownian-Passage-Time model of relatively short mean recurrence times, small alfa values, and, for some sources, fictitious elapsed times (in the first phase of the project, the elapsed time of a fault, if not available, is a priori imposed equal to its mean recurrence time) enhances the conditional probabilities of having an event in the next 30 years (from 2006), like shown by the results reported in the 1st year report. Conversely, the range of slip rate assigned to the fault (mostly given as 0.1-1 mm/yr) causes a longer and distinct central moment (mean recurrence time nearest to MaxRecInt, in DISS), and an higher aperiodicity, now compatible with Poisson more than quasi-periodic processes (alfa tends to 1); very low values of probabilities are expected in this case in the time period of interest. For sake of simplicity, the 1st year results reported in the annual report of UR4.8 and described in detail in [6] are now synthesized in Fig. 2.

This initial phase of the work forced the following efforts in the direction of using the geodetic observations to reduce the uncertainties on slip rates given to the faults, and in introducing a formal error propagation in mean recurrence time and aperiodicity obtained by different relationships. Both are innovative topics, and no common practice "recipe" is available to solve these problems.

We put also efforts to export these techniques to the second kind of seismogenic sources mapped in DISS, i.e. the seismogenic areas (SA), described later on.

Becoming available in July 2006 the first preliminary results of Task 3, we tried to apply the strain rate values directly to the faults, for limiting the range of expected slip rate. Accepting that, as reported in the following simple formulas, the strain rate is the variation of strain in time, and that the seismic strain is the displacement over an effective length, in a first approximation equal to the square root of the rupture area LW, or the length of the rupture for strike slip faults:

$$\dot{\epsilon} = \frac{1}{l} \frac{dl}{dt} = \frac{v}{l} \quad \Delta\epsilon = \frac{D}{L^*} \quad L^*_{normal/reverse} \approx \sqrt{A} = \sqrt{LW} \\ L^*_{strike-slip} \approx L$$

the first rough boundary condition from geodesy to slip rate values on the fault is:

$$V_{horizontal} = \& L^*$$

and can be resolved along the fault plane using trigonometry.

Using these simple rules we accept controversial issues like: a) no matter how the area to compute the strain rate from some velocity points is shaped, the strain rate is a property that equally belongs to all the points of that area; b) all the strain is transformed into seismic - not reasonable - defining an upper limit to slip rate, and possible overestimates of the seismic activity; c) the short term deformation of geodetic observation is representative of the long term behaviour of the fault - controversial -. This methodological approach has been applied to several strain rate elaborations, released during the project; they derive both from GPS observations (Caporali UR) and numerical modelling (Barba UR). Some promising results have been obtained using the values of 27-47 Nstrain given in 2006 by Braitenberg for the Friuli area, but except this special case, the other elaborations lead to very low slip rates assigned to the faults, often smaller than the minimum values given in DISS: Fig. 3 summarizes two tests done in 2006 and 2007 for GG sources in NE Italy. In addition, the community does not fully accept the methodology

proposed, and to overcome this problem other procedures have been used on SA instead of GG sources, described later on.

For these reasons, the results for GG sources obtained in 2007 by the UR 4.8 do not introduce geodetic constraints in the computation. A first set of results released for the benefit of other participant to S2 Project (in the followings referred as Spring07 results [7]), and the final ones (Summer07 results [8]) are here briefly described.

The Spring07 earthquake probabilities of having a characteristic earthquake on DISS 3.02 GG sources in the next 30 years (from 2007) have been computed in a very similar way to the ones graphed in Fig. 2a. The differences are due to: a) the changes in parameters of GG sources given in the last DISS (v. 3.02) released; b) the choice of using a very long elapsed time (~ 10000 years, to avoid fake effects of periodicity) for those 20 sources not having the date of the last event. The probabilities graphed in Fig. 4 uses the time-dependent BPT distribution function, and also the results of exponential formulation of the stationary Poisson process are given. Only five sources exhibit a significant conditional probability, higher than the one associated to traditional stationary application; from N to S they are Ferrara (090), Zola Pedrosa (091), Ascoli Satriano (082), Bisceglie (083) and Aspromonte Nord (040). Notable the fact that for Japanese colleagues (Tab. 2, taken from [9]) probabilities higher than 3% in 30 years have to be considered highly probable sources; most of the GG sources, if represented by a Poisson process, should therefore be taken as highly probable earthquakes.

The Summer07 results represent an innovative part of the work, as formal error propagation enters into the calculation. Instead of using the means of values obtained by different relationships (e.g. magnitude from length, area, or seismic moment), the general formulation of error propagation:

$$F(x, y, z, \dots) \approx F(\bar{x}, \bar{y}, \bar{z}, \dots) + \frac{\partial F}{\partial x}(x - \bar{x}) + \frac{\partial F}{\partial y}(y - \bar{y}) + \frac{\partial F}{\partial z}(z - \bar{z}) + \dots$$

is applied to the recurrence time obtained by the technique of conservation the seismic moment rate on the fault segment [10], by using partial derivatives on magnitude and slip rate. Then the maximum likely value of recurrence time and associated error is retained, instead of using the simple mean and standard deviation of a small set of computed recurrence times. This technique, that may be subjected to revision and implementation according to the choices adopted to perform propagation of errors, is formally correct to represent the dispersion derived from the use of different relationships and it also considers the intrinsic errors of empirical regression relationships (e.g. [11, 12]). The results are somehow different from the Spring07 ones, but the general behaviour remains similar. We consider now of highest priority to define a reasonable time interval to date the last event for those sources not having it.

The research performed on SAs aimed at defining the seismic potential of all faults in the SAs on the basis of the information about the present strain rate in Italy and using the data of the earthquake catalogue for characterizing the regional seismicity pattern.

As not all existing faults are known in the SAs, a statistical procedure was developed [13] to fill the empty space of the SAs with fictitious faults (FFs), of rupture length in agreement with the regional rupture length pattern. For each rupture length of these FFs a probability remains associated (appearance probability: AP). At the end we have a suite of rupture lengths for each SA with an appearance frequency (AF) associated: it comes from the AP for the FFs and from the actual number for the GGs.

The basic idea of the approach followed is that the regional moment rate will be transformed with the time into earthquakes: it constrains, consequently, the seismicity

pattern. More precisely, a Gutenberg-Richter (GR) distribution is assumed to hold at a regional scale, and the regional b -value is computed by the earthquake catalogue while the a -value is obtained by the regional moment rate:

$$\log N = a - b \log M_0$$

where N is the number of earthquakes with seismic moment larger than, or equal to, M_0 and

$$a' = a + \frac{9.1}{1.5} b \quad \text{and} \quad b' = \frac{1}{1.5} b$$

considering the relation between magnitude M_w and seismic moment, in Nm [14]:

$$\log M_0 = 9.1 + 1.5 M_w$$

The main problem was represented by the computation of the moment rate. Two approaches were followed. In the first approach (developed by the Caporali UR), the moment rate was computed at a regional scale from the national strain rate map applying the Kostrov relation [15], considering the area covered by the GPS stations used for the strain rate computation and a seismogenic layer of 10 km (see [16]). In the second approach (developed by the Barba UR), the moment rate was computed for the SAs using a geodynamic modelling. As working hypothesis it is assumed that only earthquakes with $M_w \geq 5.5$ occur in the SAs, and while in the first case the moment rate represents the regional total value (earthquakes in the SAs + background seismicity + aseismic creep), in the second case it refers to the SA seismicity only (it is assumed that it amounts to 60% of the total considering an average SA maximum M_w of 6.5).

The regional-scale approach was applied considering 4 macro-regions covering Italy and for which the regional moment rate can be computed. The number of events for each seismic moment class was determined according to the total regional AF and it was then scaled in the SAs according to the SA AF. The cumulative rate was obtained and from it the exceedence probability of different magnitude classes inside each SA. The SA-scale approach was applied directly considering the SAs. In both cases a general b -value equal to 1 was used (tests done assure the low influence of this parameter in the results) and only the Poisson distribution was consider for the intercurrence times.

The results obtained, in terms of exceedence probability for Mw 6.0 and 6.5 is shown in Fig. 6. It can be seen that the results with the SA-scale approach are lower than those with the regional-scale approach and this is due to the fact that the sum of the individual SA moment rate is by far lower than that associated to the region where the SAs insist.

As final comment, we consider the S2 Project an important step forward in earthquake probabilities estimate, and very fruitful, and promising techniques have been developed in its framework.

References

- Mucciarelli, M., *A test for checking earthquake aperiodicity estimates from small samples.* Natural Hazards and Earth System Sciences, 2007. 7: p. 399-404.
- Peruzza, L., *Ideas and tests for earthquake probability estimates in Italy, in Earthquake and shaking probabilities: helping society to make the right choice.* 2006, EMCSC: Erice, Sicily.
- Pace, B., et al., *Layered Seismogenic Source Model and Probabilistic Seismic-Hazard Analyses in Central Italy.* Bulletin of the Seismological Society of America, 2006. 96(1): p. 107-132.
- Grant, D.N., et al., *Defining Priorities and Timescales for Seismic Intervention in School Buildings in Italy, in ROSE Report,* I. Press, Editor. 2006, ROSE: Pavia. p. 2006/03.
- Peruzza, L., *Earthquake probabilities and probabilistic shaking in Italy in 50 years since 2003: trials and ideas for the 3rd generation of Italian seismic hazard maps.* Bollettino di Geofisica Teorica ed Applicata, 2006. 47(4): p. 515-548.
- Peruzza, L., *Extended report of the researches developed by UR 4.8 during the first phase of the project S2- Valutazione del potenziale sismogenetico e probabilità dei forti terremoti in Italia.* 2006, OGS. p. 25.
- Peruzza, L., *Note descrittive sui tempi di ricorrenza e probabilità di terremoto caratteristico nei prossimi 30 anni (dal 2007) associata alle GGsources del DISS v. 3.0.2.* 2007, OGS. p. 14.
- Peruzza, L., *Error propagation in earthquake probabilities of Italian geological sources (DISS 3.02).* Bollettino di Geofisica Teorica ed Applicata, 2007. Special Issue S2-T4(in prep.).
- Shimazaki, K., *Long-term earthquake forecasts of Japanese earthquakes, in Earthquake and shaking probabilities: helping society to make the right choice.* 2006, EMCSC: Erice, Sicily.
- Field, E.H., D.D. Johnson, and J.F. Dolan, *A mutually consistent seismic-hazard source model for Southern California.* Bulletin of the Seismological Society of America, 1999. 89(3): p. 559-578.
- Wells, D.L. and K.J. Coppersmith, *New empirical relationships among magnitude, rupture length, rupture width, rupture area, and surface displacement.* Bulletin of the Seismological Society of America, 1994. 84(4): p. 974-1002.
- Peruzza, L. and B. Pace, *Sensitivity analysis for seismic source characteristics to probabilistic seismic hazard assessment in Central Apennines (Abruzzo area).* Bollettino di Geofisica Teorica ed Applicata, 2002. 43(1): p. 79-100.
- Stirling, M.W., et al., *Seismotectonic Modelling in Northeastern Italy, in Consultancy Report,* G. Science, Editor. 2007: Trieste, Wellington. p. 22.
- Hanks, T.C. and H. Kanamori, *A moment magnitude scale.* Journal of Geophysical Research, 1979. 84: p. 2348-2350.
- Kostrov, V.V., *Seismic moment and energy of earthquakes, and seismic flow of rock.* Izv. Acad. Sci. USSR Phys. Solid Earth, 1974. Eng. Transl.(1): p. 23-44.

Ward, S.N., *On the consistency of earthquake moment rates, geological fault data, and space geodetic strain: the United States*. Geophysical Journal International, 1998. **134**: p. 172-186.

Tabella 1 - Agenda delle riunioni relative al Task 4 di S2

Table 1 - Facts and meetings in the frame of Task4 of S2 Project

When, Where	Who	What
2005/06/24, Padova	Steering Committee	Avvio progetto S2
2005/07/11	Lettera1, tutte UR	Richiesta piano lavoro dettagliato e desiderata
2005/09/14-26	Lettera2-3, tutte UR	Convocazioni, predisposizione web scambio dati
2005/09/27, Roma	Meeting tutte le UR + coordinatori tasks	Riunione di start-up, presentazione proposte progettuali, identificazione ingredienti da usare
2005/09/28	Lettera4, tutte UR	Verbale riunione
2005/11/16, Roma	Convegno GNGTS	Presentazione attività del task4
2005/12/15, Trieste	Riunione coordinamento	Ristrutturazione task4
2005/12/19	Lettera5, tutte UR	Convocazione, rilascio DISS 3.01
2006/01/25, Roma	Meeting, coordinatori tasks + UR 4.1, 4.2, 4.5, 4.7	Presentazione della ristrutturazione del task4 in tre filoni di ricerca/prodotti in maggior accordo con le proposte progettuali, presentazione dati/risultati preliminari disponibili
2006/02/02-28	Lettera6-7, tutte UR	Convocazioni, verbale riunione
2006/03/03, Roma	Meeting, coordinatori tasks + UR 4.3, 4.6, 4.7	Presentazione della ristrutturazione del task4 in tre filoni di ricerca/prodotti in maggior accordo con le proposte progettuali, presentazione dati preliminari disponibili
2006/07/18, Padova	Meeting Task3, coordinatori	Armonizzazione prodotti geodesia per task4
2006/10/18-24, Erice	International School	Presentazione avanzamenti italiani nel settore
2006/10/25	Lettera8, tutte UR	Richiesta materiale per relazione a GNGTS
2006/11/16, Roma	Convegno GNGTS	Presentazione attività del task4
2007/01/31	Lettera9, tutte UR	Trasmissione ppt GNGTS, ipotesi workshop
2007/03/16, Roma	Seminario	Stirling, stato di avanzamento in analisi S2
2007/05/09	Lettera10, tutte UR	Convocazione riunioni di chiusura progetto
2007/06/15, Roma	Meeting, coordinatori tasks + UR 4.1, 4.2, 4.3, 4.6, 4.7	Presentazione risultati finali per filone 1 e 2
2007/03/20, Roma	Meeting, coordinatori tasks + UR 4.1, 4.4, 4.7, 4.8, 4.9	Presentazione risultati finali per filone 3

Tabella 2 - From Shimazaki, 2006

Table 2 - Taken from Shimazaki, 2006

Summary of 30-yr probability (BPT model)	
■ High probability relative to other active fault zones: 3% or higher (30yr probability) 29 faults
■ Slightly high probability: 0.1-3% 22 faults
■ No comments: less than 0.1% 45 faults
The largest probability is used when the range of probability is estimated.	

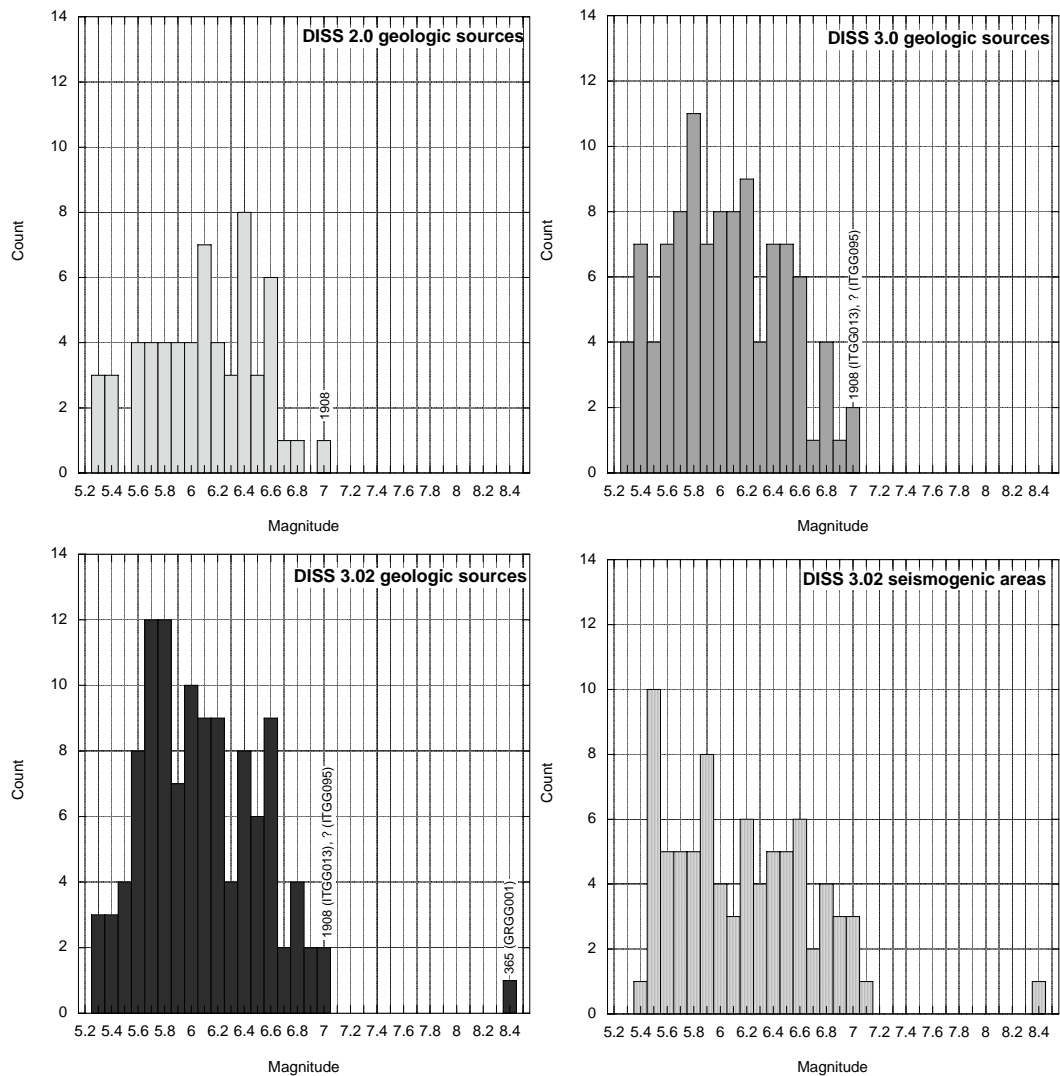


Figura 1- Istogramma delle magnitudo massime delle sorgenti parametrizzate in DISS; a) geologiche versione 2.0 del 2001; b) idem v. 3.0 del 2005; c) idem v. 3.02 del 2006; d) sorgenti areali v.3.02.

Figure 1-Histogram of the maximum magnitude represented by DISS seismogenic sources: a) GG sources v. 2.0 (2001); b) GG sources v.3.0 (2005, start of the S2 Project); c) GG and d) SA sources, version 3.02 released in Sept. 2006, in use for the final results of the project.

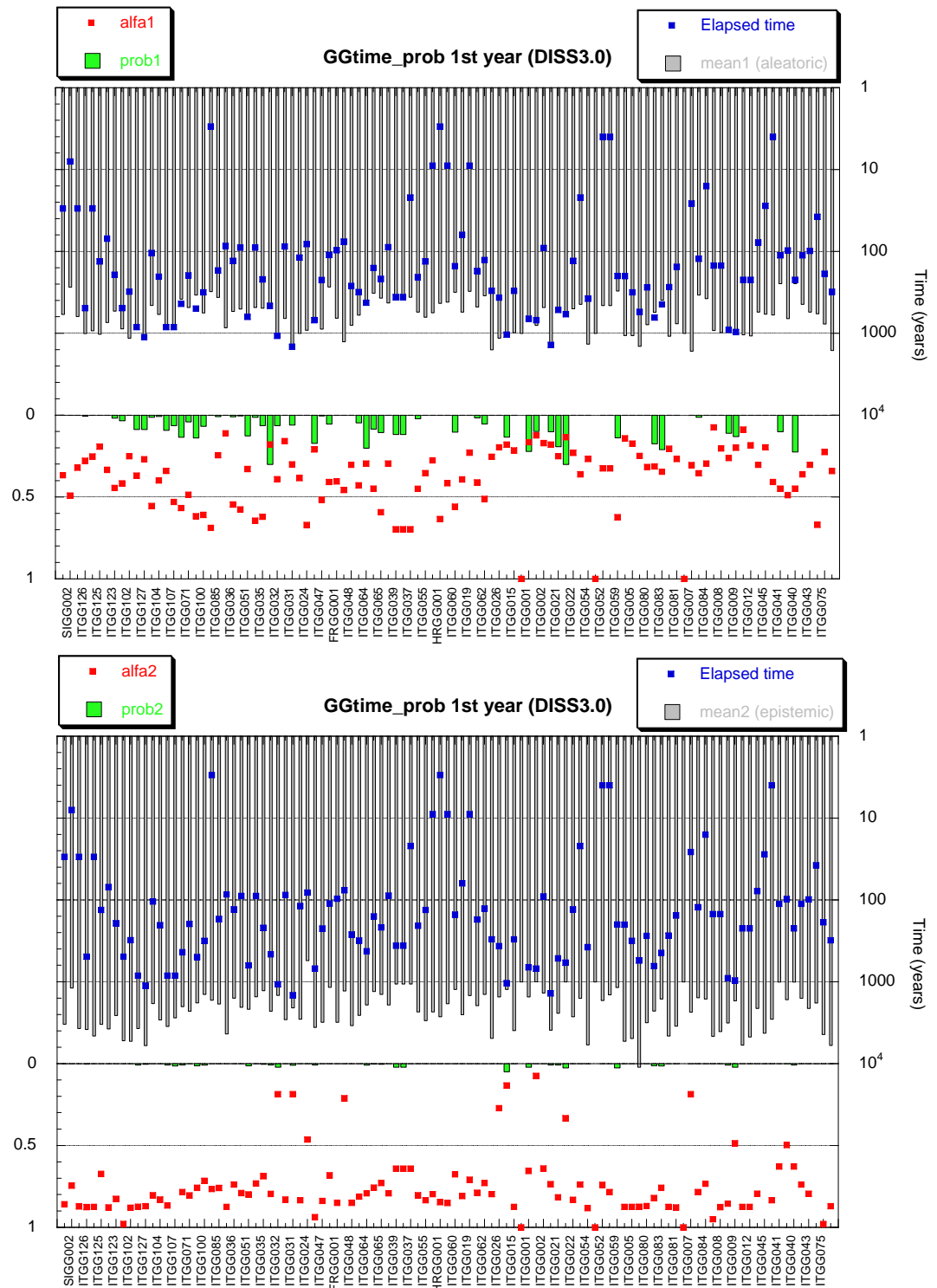


Figura 2 - Sintesi dei risultati ottenuti il primo anno; tempo medio di ricorrenza e tempo trascorso dall'ultimo evento (asse y di destra), aperiodicità alfa e probabilità associata ai prossimi 30 anni (2006); a) valori rappresentativi dell'incertezza aleatoria (magnitudo dell'evento); b) valori rappresentativi l'incertezza epistemica (slip rate della faglia). Le sorgenti sono ordinate per latitudine decrescente.

Figure 2 - Results of the 1st phase. Mean recurrence time, elapsed time (right y-axis), alfa and probability in the next 30 years from 2006 for GG sources (decreasing sorted in latitude). They are representative of a) aleatoric uncertainty on magnitude; b) epistemic uncertainty on the deformation process (slip rate).

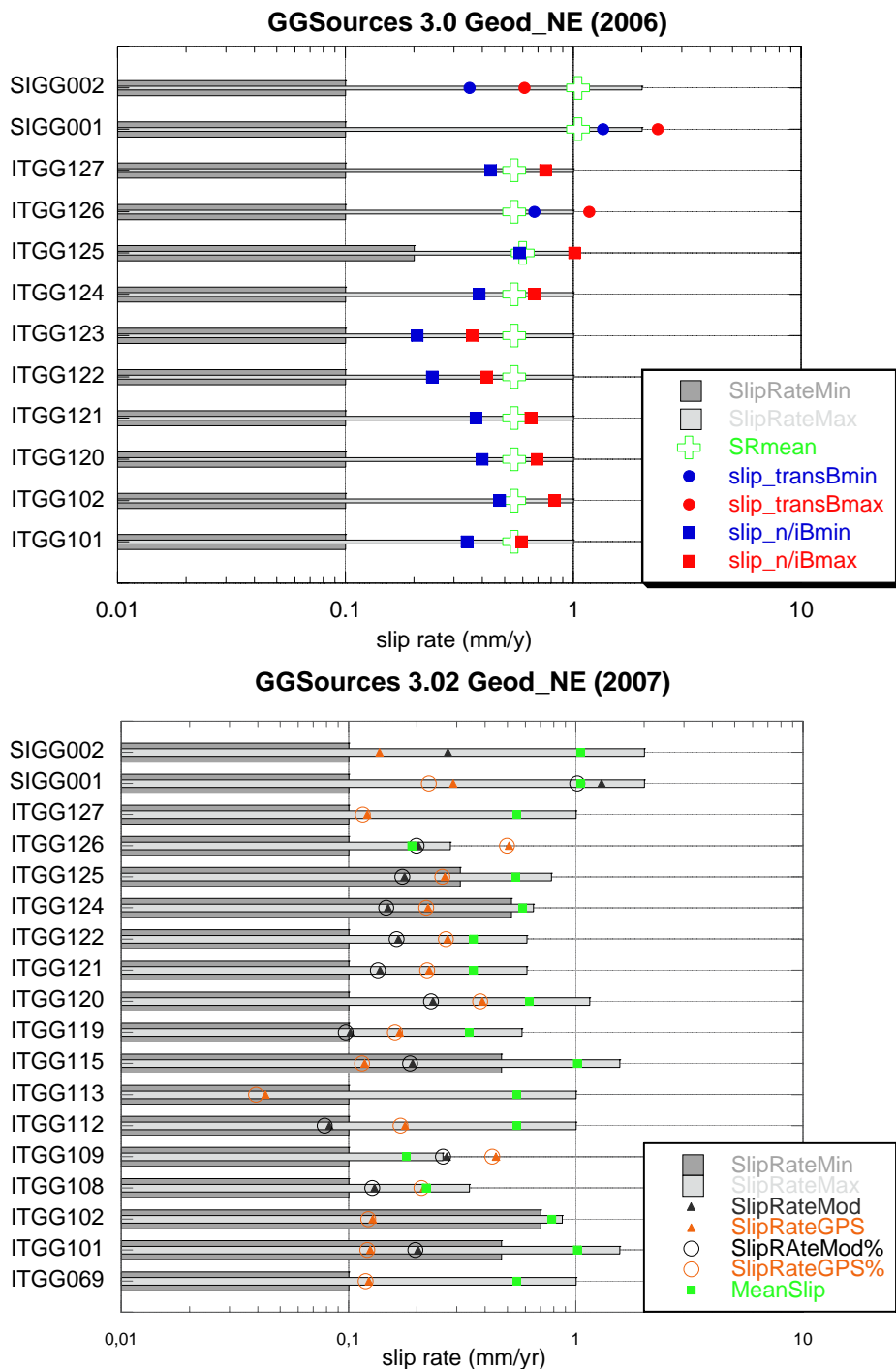


Figura 3 - Confronto fra i valori di slip rate attribuiti alle sorgenti in Italia nord-orientale in DISS (barre grigie), e ottenuti tramite lo strain rate da osservazioni geodetiche o modellazioni numeriche; in verde il valore medio usate nella stima di probabilità. a) risultati di Braitenberg, 2006 relativi a due ipotesi regionali (27-47 Nstrain); risultati osservativi (GPS) o modellati (Mod) ottenuti rispettivamente da Caporali e Barba e riferiti alle sorgenti areali (pers. Comm. 2007).

Figure 3 - Slip rates for GG sources in NE Italy. The grey bars are the values reported in DISS, the green symbols are the mean values used in earthquake probability, other symbols are slip rates derived via strain rate (see the text); a) using Braitenberg regional results of 2006 (27-47 Nstrain); b) using GPS or modelled strain rate assigned to the seismogenic areas by Caporali and Barba in 2007 (pers. Comm.).

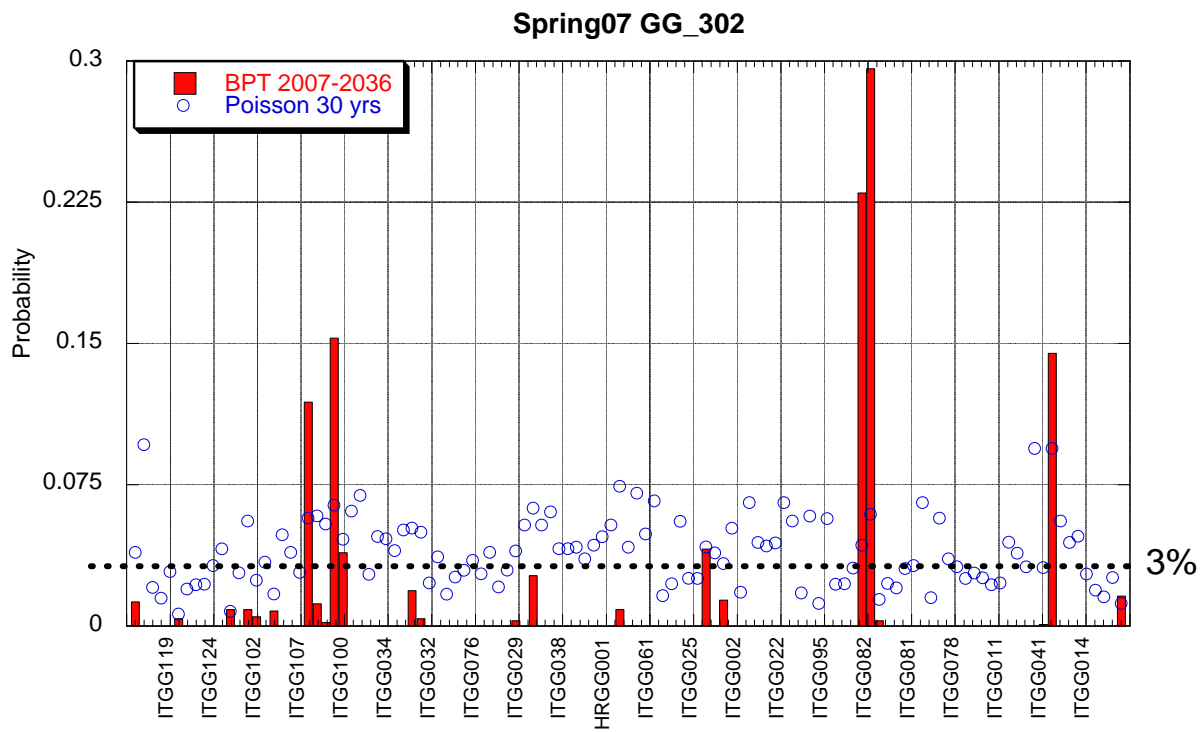


Figura 4 - Sintesi dei risultati rilasciati a metà del secondo anno (Spring07); probabilità associata ai prossimi 30 anni (2007) con modello time-dependent (BPT) e stazionario. La linea a tratteggio indica la soglia internazionalmente considerata sui 30 anni come probabilità elevata. La maggior parte delle sorgenti, trattate con Poisson superano il 3%. Le sorgenti sono ordinate per latitudine decrescente.

Figure 4 -Results released for the project purposes in Spring07; conditional probability for having a characteristic earthquake on GG sources in the next 30 years using BPT model, and stationary estimates following Poisson. The dashed line shows the threshold used to consider highly probable a source by Japanese colleagues.



Figura 5 - Sintesi dei risultati rilasciati a fine progetto (SUMMER07); probabilità in 30 anni con modello stazionario e time-dependent (BPT, prossimi 30 anni dal 2006). In nero sono indicate le sorgenti DISS prive della datazione dell'ultimo evento.

Figure 5 -Final results (SUMMER07) obtained by formal propagation of errors in mean recurrence time; probability in 30 years using Poisson and time-dependent models (BPT, conditional probability in the next 30 years from 2006). In black DISS GG sources without date of the last event; high priority has to be given to define it.

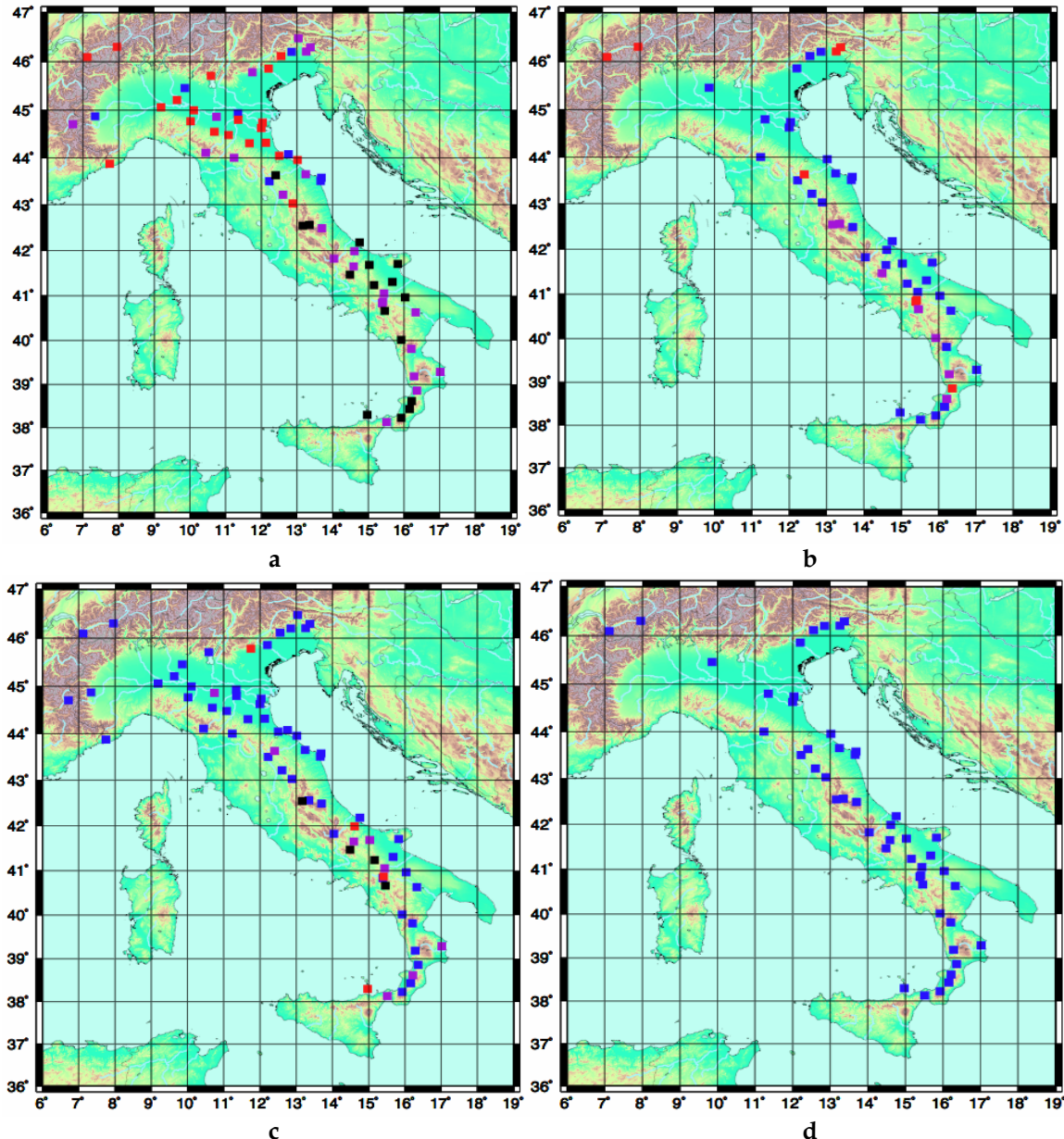


Figura 6 - Probabilità di superamento in 30 anni con modello Poissoniano: **a)** per $M_w \geq 6.0$ con approccio alla scala regionale; **b)** per $M_w \geq 6.0$ con approccio alla scala delle SA; **c)** per $M_w \geq 6.5$ alla scala regionale; **d)** per $M_w \geq 6.5$ alla scala delle SA. I simboli rappresentano: blu $P < 5\%$; rosso $5\% \leq P < 10\%$; viola $10\% \leq P < 25\%$, nero $P \geq 25\%$.

Figure 6 - Exceedence probability in 30 years according to a Poisson model: **a)** regional-scale approach for $M_w \geq 6.0$; **b)** SA-scale approach for $M_w \geq 6.0$; **c)** regional-scale approach for $M_w \geq 6.5$; **d)** SA-scale approach for $M_w \geq 6.5$. Blu squares for $P < 5\%$; red $5\% \leq P < 10\%$; purple $10\% \leq P < 25\%$, black $P \geq 25\%$.



UR 4.9 - Coordinatore: Renata Rotondi (C.N.R. – I.M.A.T.I.)

The aim of the researches performed by RU 4.9 was the analysis of stochastic nonstationary models of occurrence of strong earthquakes on long/middle time scale in order to get hazard assessments for different forecasting horizons. The models adopted were chosen on the basis of the available data sets, in particular of the recent development of the discoveries on the Italian seismogenic areas (SA) stored in the database DISS. The theory of the point processes provides a sufficiently extensive and flexible framework to describe phenomena occurring irregularly in time and space like the earthquakes; in particular we have considered versions of the stress release model based on Reid's theory of the elastic rebound and renewal models for which the hazard depends on the time elapsed since the last event.

■ First year

- data sets and seismogenic region: catalogue CPTI04, events with $M_S \geq 4.8$ in the zone 927 of the zonation ZS9, subdivided into four subunits, each characterized by the presence of a fault segment which generated at least an earthquake with $M_S \geq 6$ in the past (Fig. 1);
- aim: analyse how the contribution of recent studies on the fault segmentation model of Sannio-Matese-Ofanto-Irpinia region can improve the performance of stochastic models for hazard assessment;
- stochastic models: the original version of the stress release (SR) model fitted to the entire zone and the version, called *independent*, in which a different model is associated with each subunit, having equal or different loading rate;
- results: the probability of occurrence in $(t, t + dt)$ in sample areas.

Like every point process the stress release is characterized by the conditional intensity function $\lambda(\cdot)$; in this case we have $\lambda(t | H_t)$ – the probability of occurrence in $(t, t + dt)$, given the stress level at time t - where H_t is the history of the process up to t , that is the sequence of occurrence time and magnitude of all the events recorded in the interval under study. In the *independent* SR model the function $\lambda(\cdot)$ is the sum of as many $\lambda_i(\cdot)$ as the tectonic subunits; a variant of this model with interesting physical interpretation was obtained by assuming that the tectonic input is the same in all the subunits. Following the Bayesian paradigm we inserted information from previous studies by assigning the prior distributions of the model parameters. In this way we took into account the uncertainty in the evaluation of the conditional intensity function. Various SR and Poisson models were compared each other on the basis of the Bayes factor. The *independent* SR model came out to be the best; Fig. 2 shows the estimates of its conditional intensity function and the shortest 90% interval obtained by generating sufficiently large samples from the posterior distributions of the parameters through Markov chain Monte Carlo (MCMC) methods. Moreover we forecast the next step in the time evolution of the process, that is the date of the next earthquake in the region; a stochastic simulation method, the timescale transformation method, was adopted and the forecasts were given in terms of mean and quantiles of the distribution of the date of the next event (Rotondi and Varini (2006b)). A preliminary backward test was performed consisting in using as learning set the data from 1650 to 1992 and as test set the events that occurred in the period 1993-2002, end of the catalogue. A unique earthquake exceeding the threshold magnitude was recorded on September 9, 1998; here we just report the quantiles produced by the *independent* SR models:

$$- t_{10} = 1993.70 \quad t_{50} = 1999.74 \quad t_{90} = 2021.01 \text{ for equal loading rate}$$

- $t_{10} = 1994.11$ $t_{50} = 2000.39$ $t_{90} = 2018.12$ for different loading rates.

It was impossible to repeat the analysis using the seismogenic sources of the database DISS released in 2005 since only 13 earthquakes were associated with the six sources included in the zone 927, and enlarged through an external buffer of km 5.

■ Second year

- data bases: seismogenic areas of the database DISS3.0.2 related to the entire Italian territory, subdivided into eight tectonically homogeneous macro-regions, and associated earthquakes from the CPTI04 catalogue with magnitude $M_w \geq 5.3$;
- aim: time-dependent maps of occurrence probability at national scale making use of the more structured information provided by the new data bases;
- stochastic models and methods: nonparametric analysis of renewal processes, that is, models in which the occurrence probability depends on the time elapsed from the previous event. They are hence characterized by the probability distribution of the interevent time; starting from the not completely satisfactory results provided by the parametric distributions presented in the literature, we followed a general approach in which the distribution of Δt is considered as a random probability measure; in other words, under mild conditions it is some continuous function with a certain probability, assigned according to a stochastic process, called Polya tree, defined on a space of functions.
- results: for each seismogenic area, probability of having an earthquake in the next 5, 10, 20, 30, 50, 100 years from 2002/12/31, end of the CPTI04, given that no events have occurred from the date of the latest record in catalogue for each area.

The most recent version DISS3.0.2 of the database of the Italian seismogenic sources also includes seismogenic areas (SA), that is, crustal bodies drawn on the basis of large set of available evidence (known large-scale tectonic structures, earthquakes not ascribable to specific tectonic structures, and so on) and which contain an unspecified number of aligned seismogenic sources that cannot singled out. In November 2006 the Research Unit 1.1 of this project subdivided those areas into eight groups, we call macro-regions (MR), which are independent and tectonically coherent with a prevalent fault mechanism (Fig. 3). Of course every macro-region has a larger number of events than each member seismogenic area, and its events can, in same way, be studied jointly because they share the tectonic process; so we assumed that the times between the consecutive events occurred in each of the areas SA_{ji} belonging to the same macro-region MR_i follow the same probability distribution $F_i(\Delta t)$. In January 2007, RU1.1 has also provided the earthquakes of the catalogue CPTI04 with $M_w \geq 5.3$ that can be associated with each seismogenic area; being strong earthquakes we can assume that the interevent times are independent. Hence, given MR_i , $i=1,\dots,8$, we first computed the interevent times in each area SA_{ji} , $j=1, \dots, n_i$ (n_i = number of SA's in MR_i), and then we collected all those data in a unique set D_i , one for each macro-region. In practice we obtained eight data sets that, being formed by realizations of independent and identically distributed random variables, satisfy the conditions underlying a renewal process.

This model is completely defined by the probability distribution of $u=\Delta t$; in fact the conditional intensity function of this point process, also denoted as *hazard function*, is given by $\lambda(u) = f(u)/[1 - F(u)]$ where $f(u)$ and $F(u)$ are the density and the distribution of Δt respectively.

Standard parametric distributions proposed in the literature - exponential, gamma, Weibull, lognormal - have turned out to be not completely successful; so we tried to solve

the estimation problem of $f(\cdot)$ making the least requirements: it has to be a continuous function that agrees with what we expect it is, according to our past experience, for instance, a function similar to a generalized gamma (GG) distribution $G(u; \eta, \xi, \rho)$ where ‘similar’ means that we use such a distribution only as expected value of F . We remind that the GG family properly includes all the distributions we have above-mentioned.

More formally $F(\cdot)$ is a random measure following a Polya tree distribution defined through an iterative binary partition of its domain R^+ : at the first level let (B_0, B_1) be a measurable partition of the domain, at the second let (B_{00}, B_{01}) be a partition of B_0 and (B_{10}, B_{11}) a partition of B_1 and so on. Let us consider an observed interevent time and let us find to which element of the partition that time belongs at every level. Initially it will be in B_0 or in B_1 with probability C_0 or $C_1 = 1 - C_0$ respectively; then, supposing that it stays in B_0 , it will belong to B_{00} or B_{01} with probability C_{00} or $C_{01} = 1 - C_{00}$ and so going on. In general the probabilities $C_{\varepsilon 0}$ and $C_{\varepsilon 1}$ are conditional probabilities that the observation is in the left or right subdivision of the component B_ε of the partition at the $\dim(\varepsilon)$ -th level. According to a Polya tree these probabilities are random and have a Beta distribution $Beta(a_{\varepsilon 0}, a_{\varepsilon 1})$ with non-negative parameters $a_{\varepsilon 0}$ and $a_{\varepsilon 1}$. A Polya tree is hence characterized by the partition and by the set of a 's parameters. The nodes of our partition are given by the quantiles of the generalized gamma distribution that expresses our prior knowledge on the phenomenon; in practice, in estimating the density for the i -th macro-region such a knowledge is provided by the data belonging to the other macro-regions. The choice of the a 's parameters expresses our belief on the sample distribution rather than on G , expectation of F ; to analyse the sensitivity of the model to these parameters we have considered four cases: a) small values, $a=20$; b) large values, $a=10^6$, and c) values varying with the level j of the partition, $a=j^2$ and $a=2^j$. Some theorems guarantee that the latest two choices for a yield F that is continuous with probability 1. For this reason later on we just refer to results obtained by using $a=j^2$. When new interevent times are observed, the parameters a 's are updated as usually in the Bayesian framework.

To reconcile model complexity with computational difficulties of the inferential procedure we resorted to stochastic simulation methods based on the generation of Markov chains, the so-called Markov chain Monte Carlo methods (MCMC). In particular we have applied the Metropolis-Hastings within Gibbs sampling algorithm generating, for each parameter, a Markov chain whose equilibrium distribution is the posterior distribution of the parameter itself. In this way we have estimated not only some summaries of the parameters, like mean, variance, etc., but their complete probability distribution.

Summarizing we have implemented an iterative algorithm with 500000 sweeps, deleting the initial 20% of scans from each chain to allow for the burn-in, recording the output every 10th iteration, and computing the running sample means on the remaining 40000 values. The outline is the following:

- at each iteration we generate values for the variates C_ε 's and hence obtain a sequence of probabilities $\{p_1^{(n)}, p_2^{(n)}, \dots, p_{2^j}^{(n)}\}$ of belonging to the 2^j sets at the level j ;
- each 50 iterations we draw a sample of 50 interevent times according to those probabilities and we use them to get a nonparametric kernel density estimate.

Fig. 4 shows the estimated density functions of the interevent time for each of the eight macro-regions depicted in Fig. 3; the dots indicate the N times forming the data set of the macro-region whereas the bars constitute the normalized histogram of the sampled values. We point out the multimodality of the estimates. As side-result we have obtained the posterior means of the parameters η, ξ, ρ of the generalized gamma distribution that,

substituted into that function, give the plug-in estimates of the generalized gamma densities. In Fig. 5 these estimates (blue) are compared with the nonparametric (red) estimates of the interevent time densities; the green curves denote the hazard function of the corresponding generalized gamma density.

For each seismogenic area SA_{ji} of the macro-region MR_i , $i=1, \dots, 8$, we have approximated the probability that an event occurs in the interval (t_0, t_0+u) through the expression $\{F(t_0+u-t_{last}) - F(t_0-t_{last})\}/\{1 - F(t_0-t_{last})\}$ where t_{last} is the date of the last event recorded in SA_{ji} and $t_0=2003.0$ is the end of CPTI catalogue. Probability maps have been obtained for different values of the forecasting horizon: $u=5, 10, 20, 30, 50, 100$ years; Figs. 6-7 correspond to the cases $u=5$ and $u=30$ years respectively.

References

- Rotondi R., Varini, E. (2007); Bayesian inference of stress release models applied to some Italian seismogenic zones, *Geophysical Journal International*, 169, 1, 301-314.
- Rotondi R. (2007); Time-dependent hazard through nonparametric Bayesian estimation of the interevent time probability density", 5th International Workshop on: "*Statistical Seismology: Physical and Stochastic Modelling of Earthquake Occurrence and Forecasting*", Erice, 31 May - 6 June 2007 (poster)
- Rotondi R., Varini, E. (2006a); Bayesian analysis of marked stress release models for time-dependent hazard assessment in the western Gulf of Corinth, *Tectonophysics*, 423, 107-113.
- Rotondi R., Gospodinov D. (2006); Statistical analysis of triggered seismicity in the Kresna region of SW Bulgaria (1904) and the Umbria-Marche region of central Italy (1997), *Pure and Applied Geophysics*, 163, 1597-1615.
- Rotondi R., Varini E. (2006b); Reconciling short- and long-term seismic modelling, International School of Geophysics, 26th Workshop on "*Earthquake and Shaking Probabilities: Helping Society to Make the Right Choice*", 18-24 October 2006, Erice (Sicily)
- Rotondi R., Varini E. (2005); Stochastic simulation of point process models for forecasting seismic events, Atti del Convegno S.Co.2005: "*Modelli Complessi e Metodi Computazionali Intensivi per la Stima e la Previsione*", Bressanone, 15-17 September 2005, 485-490.

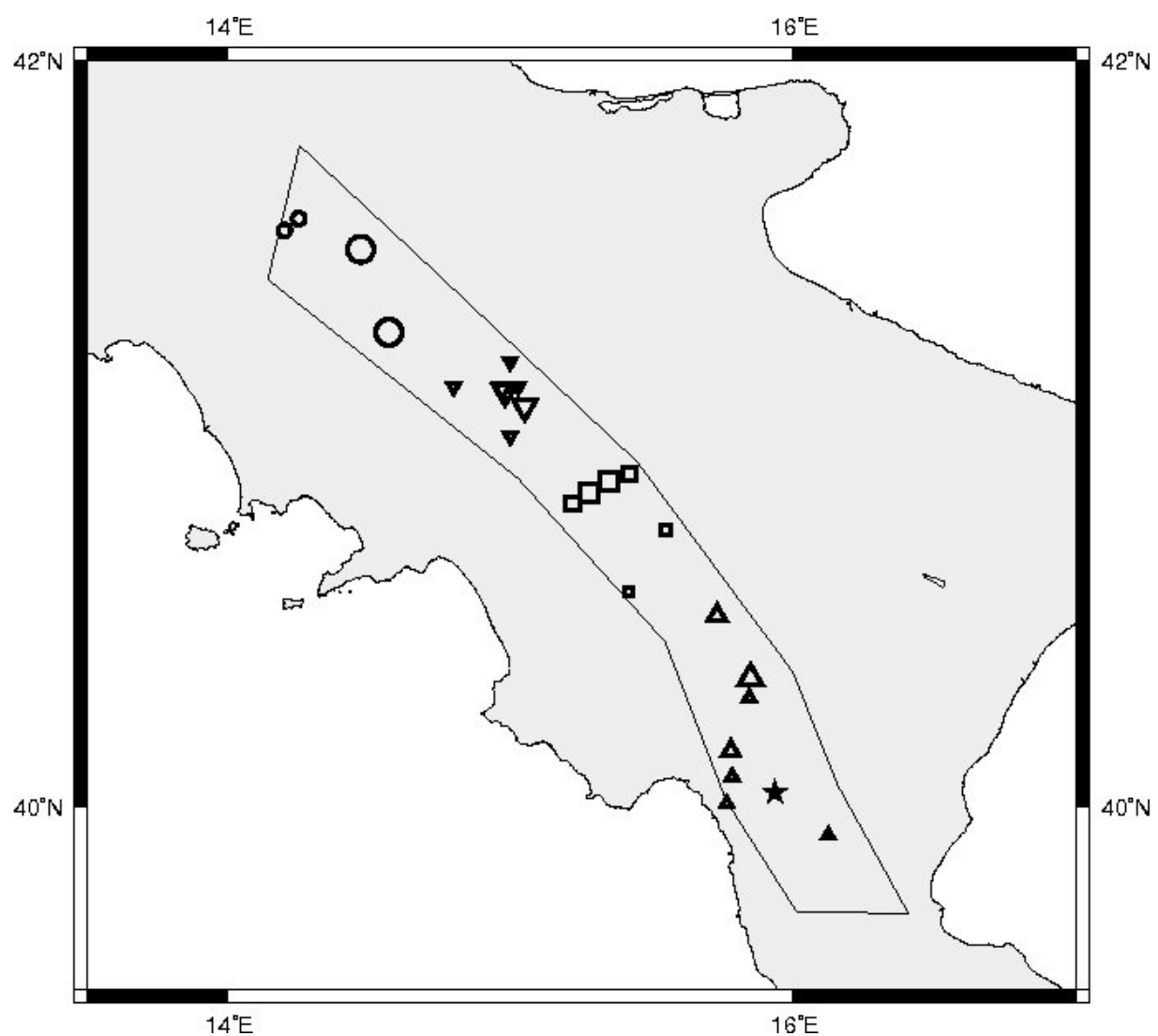


Figure 1 - Seismogenic zone 927 of the Italian zonation ZS9 and epicenter of the shocks with magnitude $M_S \geq 4.8$ in the time interval 1650-2002. The symbols mark the events belonging to different subunits (Rotondi R, Varini E. (2007)).

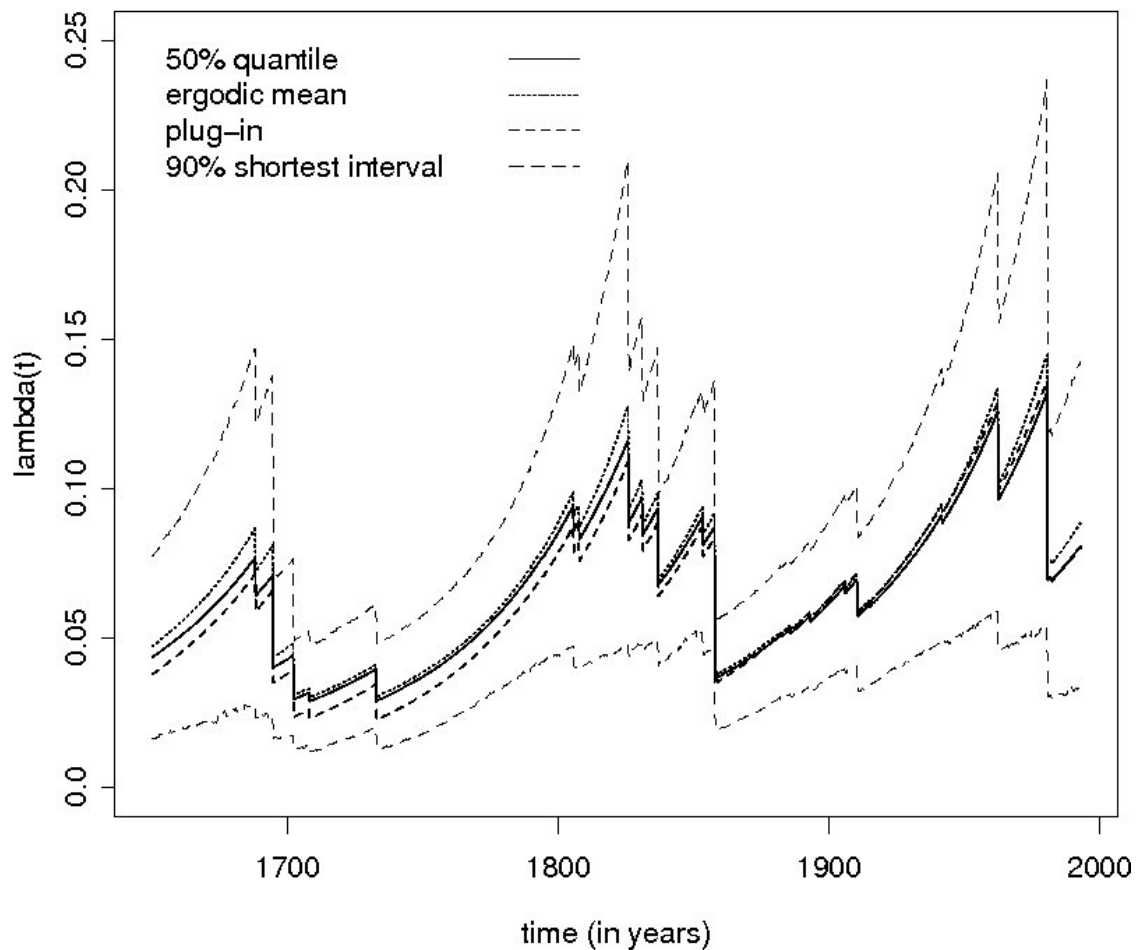


Figure 2 - Plug-in estimate (short dashed line) and ergodic mean (dotted line) of the conditional intensity of the independent SR model with common loading rate, and the shortest interval including 90% of the values calculated through the MCMC method (Rotondi R, Varini E. (2007)).

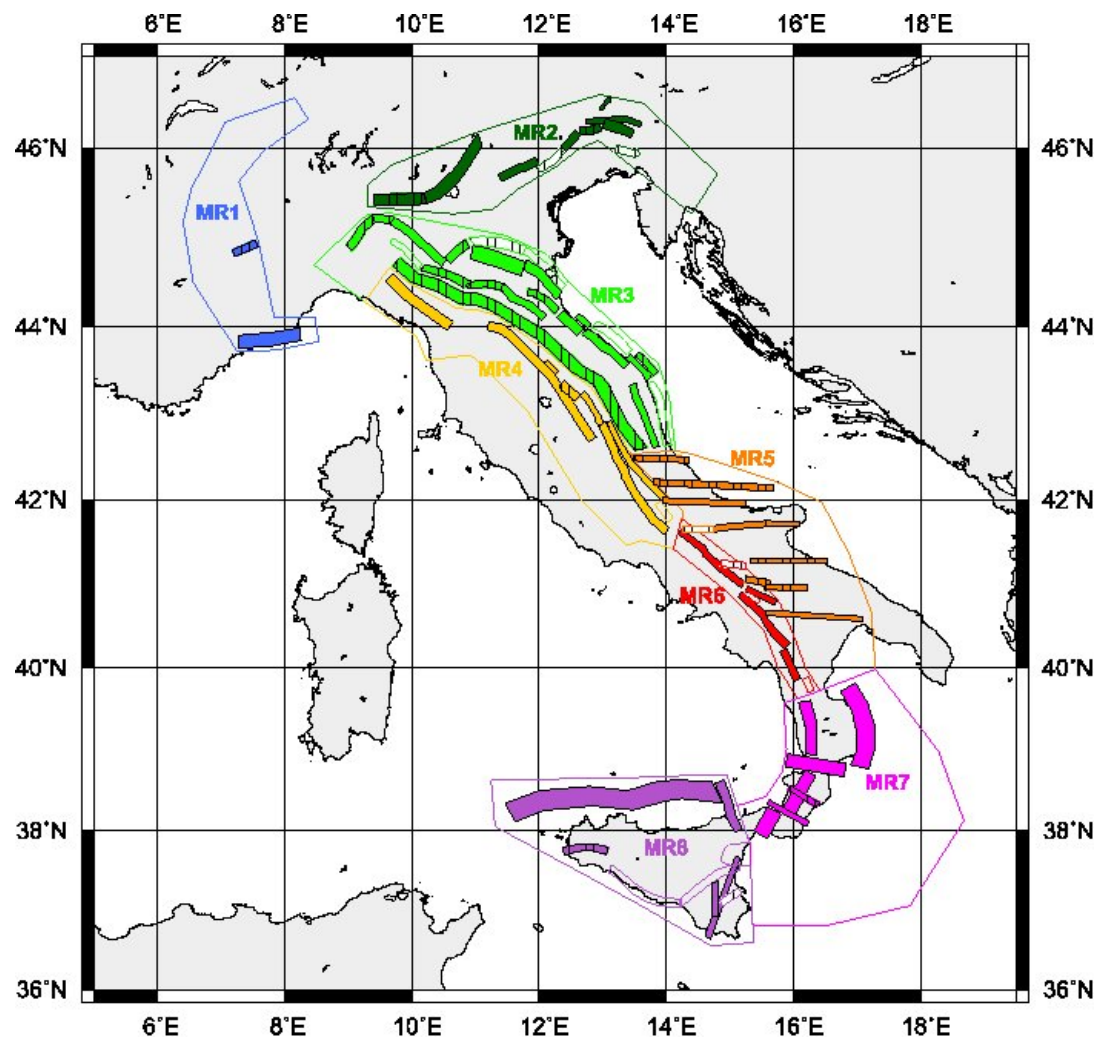


Figure 3 - Seismogenic areas of DISS3.0.2 subdivided into eight tectonically homogeneous macro-regions.

nonparametric estimate of density functions

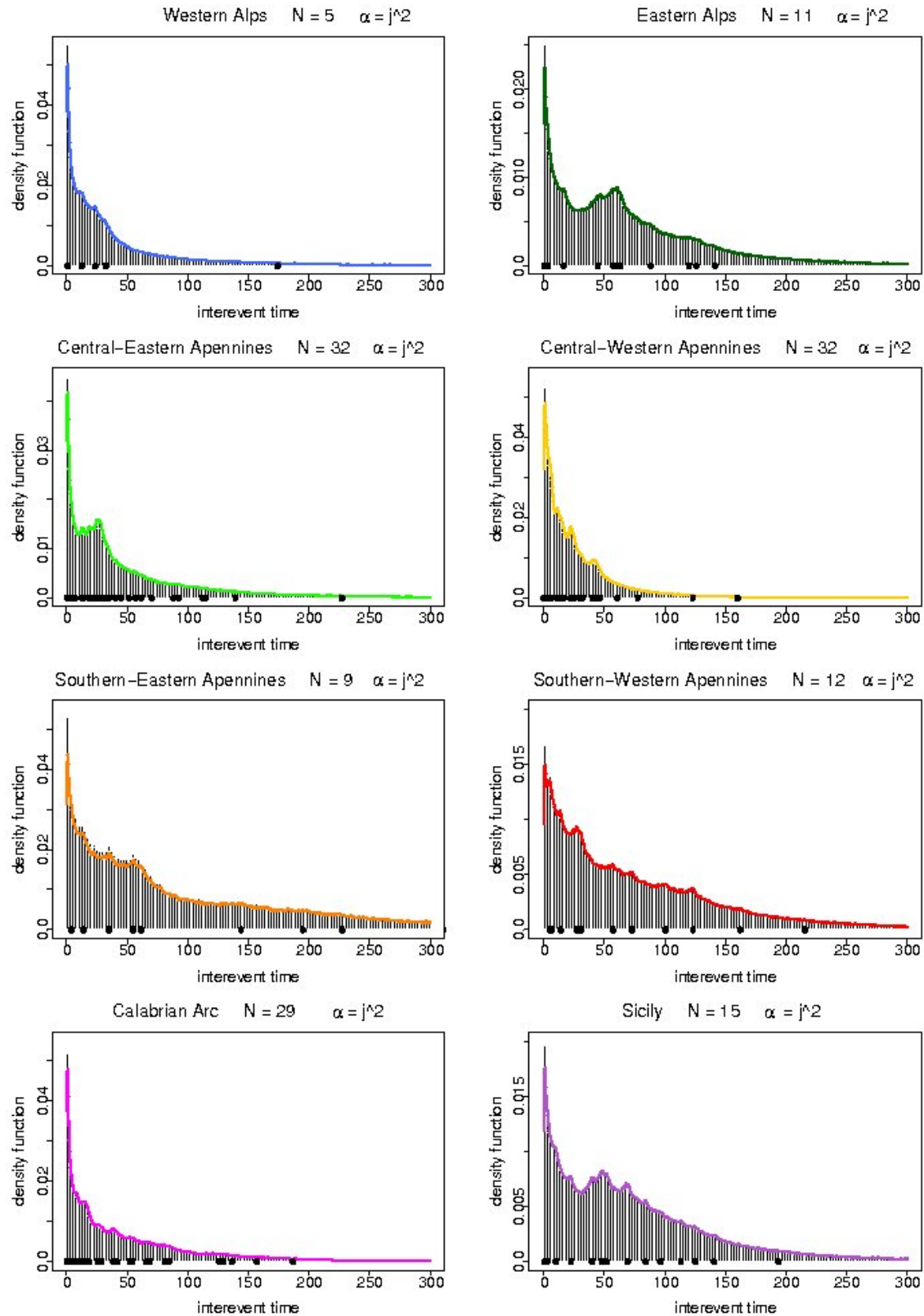


Figure 4 - Nonparametric estimate of the density function for the interevent time in each of the eight macro-regions.

nonpar-density (red) gen.gamma-density (blue) gen.gamma-hazard (green)

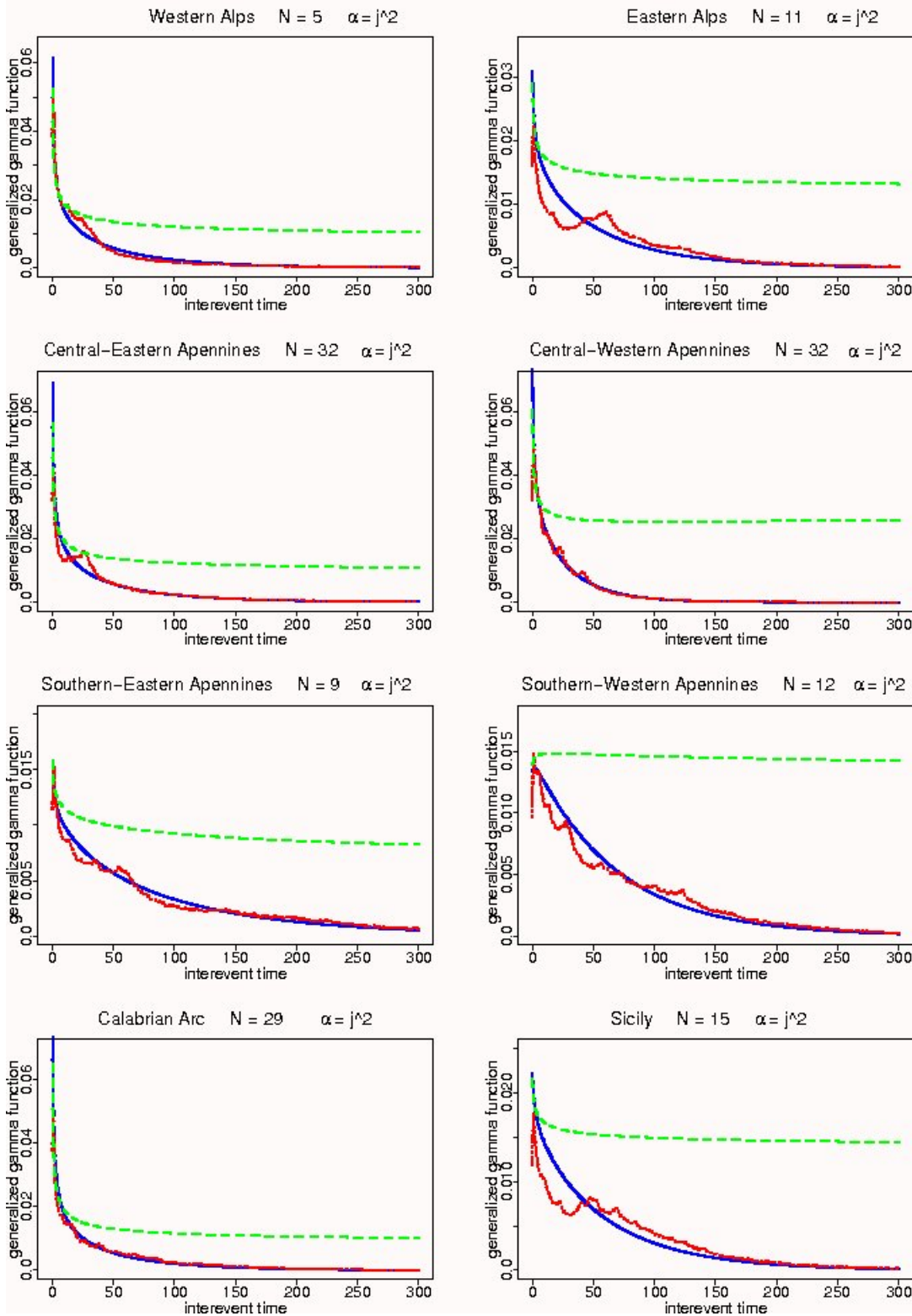


Figure 5 - Comparison between nonparametric (red) and parametric (blue) estimates of the density functions for the interevent time in the eight macro-regions; the parametric model is given by a generalized gamma distribution and in green we report the corresponding hazard function.

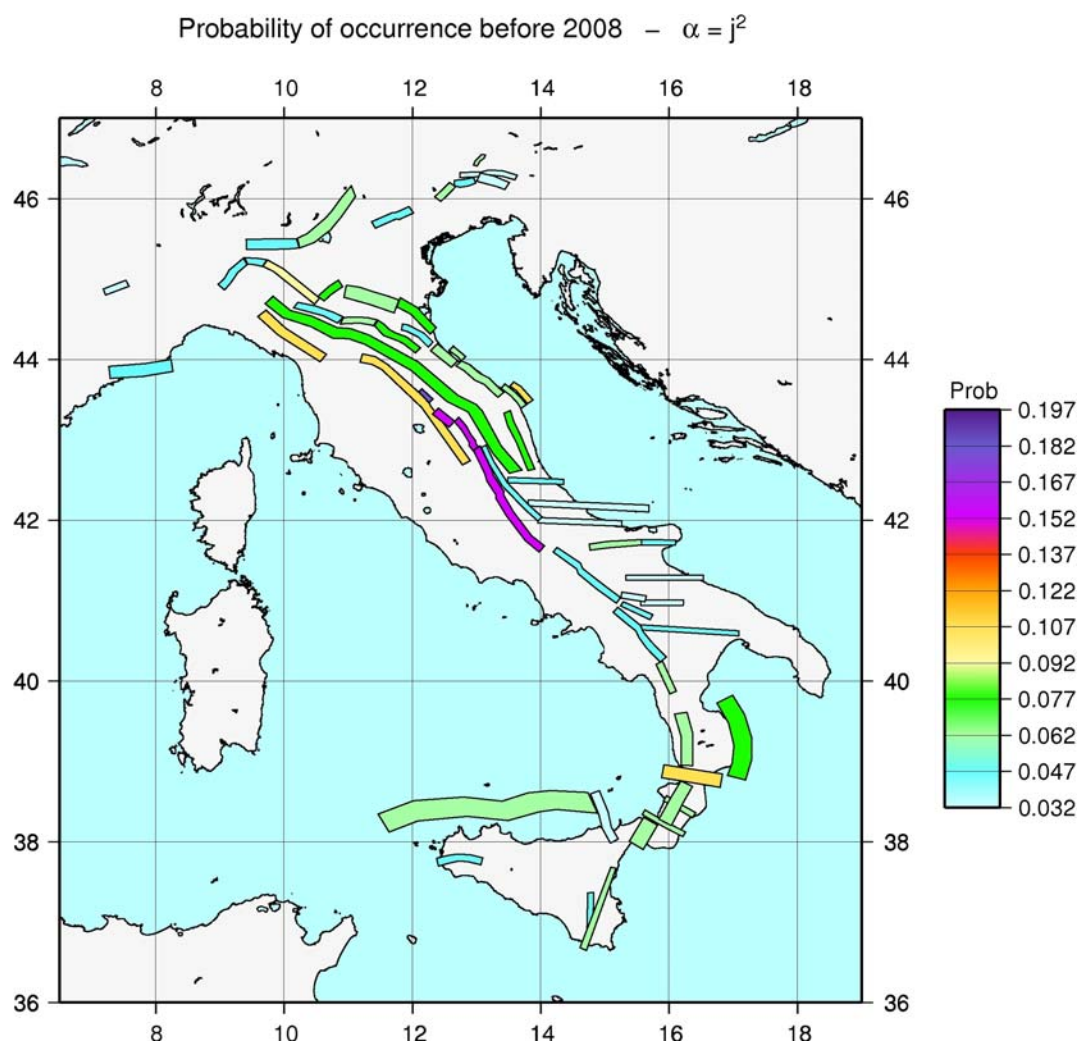


Figure 6 - Probability of occurrence in each seismogenic areas SA before $t=2008.0$ given by

$$\text{Prob} = [F(t+t_0-t_{\text{last}})-F(t_0-t_{\text{last}})]/[1 - F(t_0-t_{\text{last}})]$$
 where $t_0 = 2003.0$ and t_{last} is the date of the last event recorded in the area.

Probability of occurrence before 2033 – $\alpha = j^2$

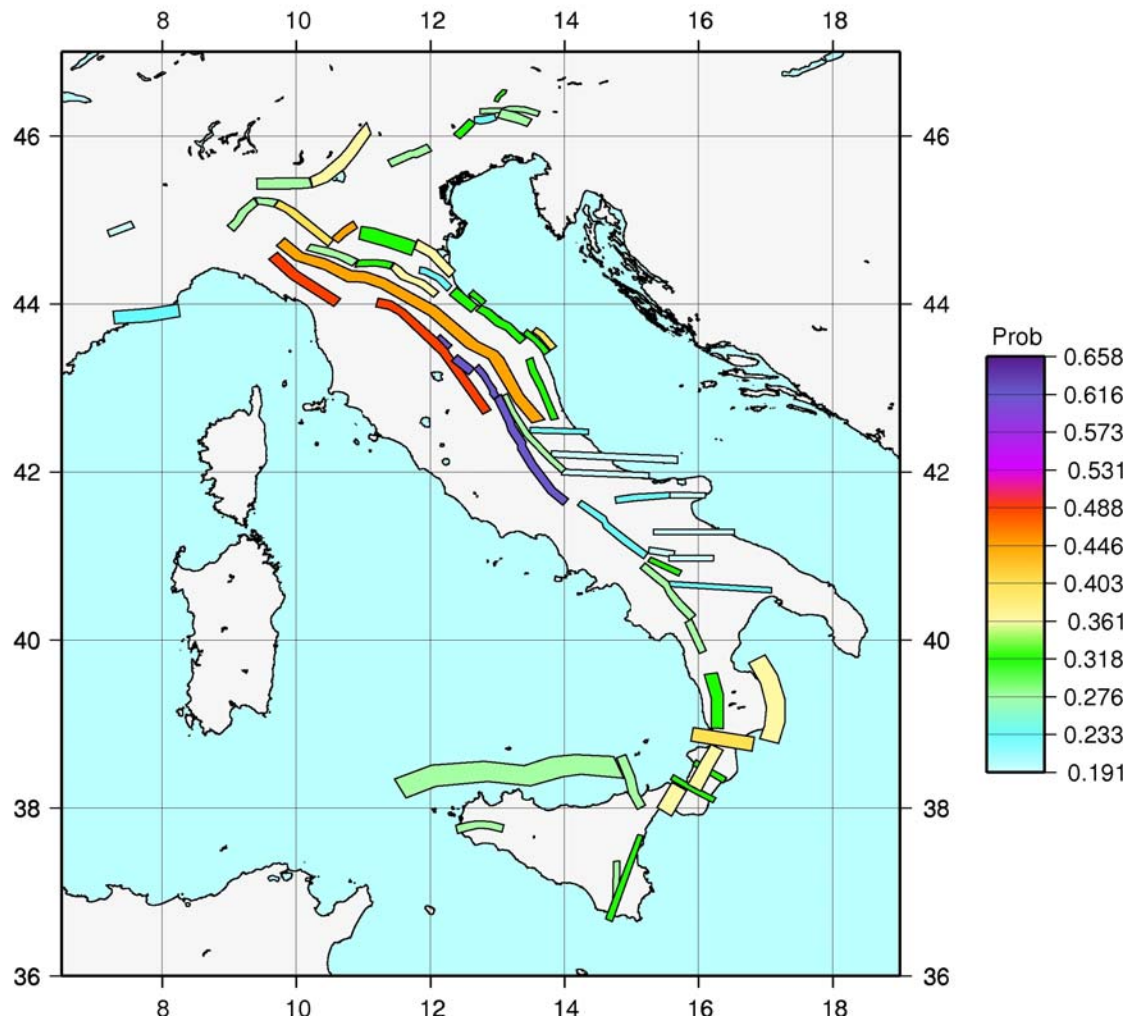


Figure 7 - as Figure 6. with $t = 2033.0$